Distribution Agreement

In presenting this thesis or dissertation as a partial fulfillment of the requirements for an advanced degree from Emory University, I hereby grant to Emory University and its agents the non-exclusive license to archive, make accessible, and display my thesis or dissertation in whole or in part in all forms of media, now or hereafter known, including display on the world wide web. I understand that I may select some access restrictions as part of the online submission of this thesis or dissertation. I retain all ownership rights to the copyright of this thesis or dissertation. I also retain the right to use in future works (such as articles or books) all or part of this thesis or dissertation.

Signature:

_____	_____
Lauren Byrd-Leotis	Date

Influenza A Virus Hemagglutinin: An Examination of Divergent Subtypes with Respect to Stability and Receptor Binding Properties

By

Lauren Byrd-Leotis
Doctor of Philosophy

Graduate Division of Biological and Biomedical Sciences
Microbiology and Molecular Genetics

_____
David Steinhauer, Ph.D.
Advisor

_____
Richard Cummings, Ph.D.
Committee Member

_____
Jackie Katz, Ph.D.
Committee Member

_____
Anice Lowen, Ph.D.
Committee Member

_____
Martin Moore, Ph.D.
Committee Member

Accepted:

_____
Lisa A. Tedesco, Ph.D.
Dean of the James T. Laney School of Graduate Studies

_____
Date

Influenza A Virus Hemagglutinin: An Examination of Divergent Subtypes with Respect to Stability and Receptor Binding Properties

By

Lauren Byrd-Leotis
B.S., University of Georgia, 2009
A.B., University of Georgia, 2009

Advisor: David Steinhauer, Ph.D.

An abstract of
A dissertation submitted to the Faculty of the
James T. Laney School of Graduate Studies of Emory University
in partial fulfillment of the requirements for the degree of
Doctor of Philosophy
in Microbiology and Molecular Genetics
2016

ABSTRACT

Influenza A Virus Hemagglutinin: An Examination of Divergent Subtypes with Respect to Stability and Receptor Binding Properties

By Lauren Byrd-Leotis

The hemagglutinin (HA) of influenza A viruses mediates the processes associated with viral entry: binding to cell surface receptors and facilitating fusion of the virion membrane with the host endosomal membrane. The HA structure incorporates two functional domains related to these activities, the receptor binding site in the globular head and the fusion peptide and pocket in the stem region. These sites have specific characteristics associated with subtype and host, and the differences often define species barriers. In this work, we have characterized the effects of mutations in the stem region of HA for strains representing each structural group, as well as avian and human hosts. We found that for the conserved residue 58, a lysine to isoleucine change increased the acid stability of most HAs, lowering the pH of fusion. A mutation at conserved residue 112, from aspartic acid to glycine, decreased the acid stability, raising the pH of fusion for all HA subtypes. The effects of both mutations were consistent across structural and host classifications, correlating with the conserved nature of both residues. Future studies are planned to examine the effects of mutations at group specific positions. We began our study of receptor binding by characterizing the broad receptor specificity of a range of influenza viruses again differing in subtype and host. The receptor specificity is linked to residues within the receptor binding pocket of HA, though their positions are altered between group 1 and group 2 subtypes. Avian viruses preferentially recognize α2,3-Sialic acid terminating glycans and mammalian viruses recognize α2,6-Sialic acid. Our results using the Consortium for Functional Glycomics glycan microarray corroborate these statements, though they reveal a general over-simplification in that other structural determinants beyond the terminating sialic acid moiety are important for Influenza A virus binding. To identify the receptors used in natural infection, we developed the Pig Lung Shotgun Microarray incorporating N-glycans isolated from swine lung tissue. Eight endogenous receptors were identified and characterized. Continuation of this work involves expanding our repertoire of natural arrays to include human lung glycans and examining the role of neuraminidase in entry as the substrate specificity overlaps with that of HA.

Influenza A Virus Hemagglutinin: An Examination of Divergent Subtypes with Respect to Stability and Receptor Binding Properties

By

Lauren Byrd-Leotis
B.S., University of Georgia, 2009
A.B., University of Georgia, 2009

Advisor: David Steinhauer, Ph.D.

A dissertation submitted to the Faculty of the
James T. Laney School of Graduate Studies of Emory University
in partial fulfillment of the requirements for the degree of
Doctor of Philosophy
in Microbiology and Molecular Genetics
2016

ACKNOWLEDGMENTS

The work presented here would not have been possible without of the generous support of many people. I would like to acknowledge and thank Dr. David Steinhauer for everything from allowing me to join his lab when he wasn't planning to take students to encouraging me to pursue the projects I was excited about even when the pursuit required a temporary move to Boston. Dave is truly an excellent advisor and I am grateful for the opportunity to study with him and learn from his examples, the most important of which being the absolute joy he derives from scientific discovery. Dave reinforced the idea that science is fun and I thoroughly enjoyed working on my projects under his guidance. I would like to thank Dr. Richard Cummings for allowing me to work in his lab, both at Emory University and at Harvard Medical School, and for his support as I embraced the field of glycobiology. I would also like to thank Dr. Jackie Katz, Dr. Anice Lowen and Dr. Marty Moore for serving on my committee and providing valuable advice and support along the way.

The members of both the Steinhauer lab and the Cummings lab have become a second family and I am grateful for our shared experiences. In particular, I'd like to thank Dr. Summer Galloway for being a fantastic mentor and a wonderful friend. I learned so much from Summer, both scientifically and professionally and I continue to be inspired by her confidence and many successes. I'd also like to thank Dr. Jamie Heimburg-Molinaro and Sandra Cummings for always being so kind and patient and for making me feel welcome in the Cummings lab.

My family is the foundation of my success. My mother and father have always supported and encouraged me and taught me the value of hard work and creativity. I would not be where I am today without their influence. I would like to thank my father for exemplifying integrity and perfectionism and reminding me to be the best scientist I can be. I would like to thank my mother, for though I am fortunate to have so many truly inspiring women in my life, she is the foremost. I want to thank her for her example, her determination, and her love, all things that drive me to be better. To my sister, Kelsey, thank you for being a constant best friend, for supporting me through the good times and fighting for me through the bad. Finally, I have to acknowledge my husband, Stephen, who has always expressed unwavering confidence and belief in me. His love and support has been invaluable to me through this whole process. To Stephen, thank you for listening and for believing in me even when I didn't believe in myself, for making me laugh, for sharing adventures with me, and for reminding me of what is important in life.

TABLE OF CONTENTS

TABLE OF CONTENTS

TABLE OF CONTENTS

LIST OF FIGURES AND TABLES

LIST OF FIGURES AND TABLES (continued)

INTRODUCTION

Influenza A viruses, common respiratory pathogens, have been the subject of much examination since they were discovered as the etiological agents behind Influenza disease in 1933. Despite the early origins of influenza A viruses (IAV), the frequency and persistence of Influenza respiratory illness still have a significant impact upon the collective health worldwide. The study of influenza viruses is consistently expanding and adapting, often providing foundational model systems for other aspects of infectious disease and even biological research, as well as encouraging the exploration of new technologies that enhance our understanding of virus-host interactions. This work explores the role of the IAV surface protein hemagglutinin in the processes of entry: receptor binding and fusion. Novel techniques to identify natural IAV receptors are described that provide an unprecedented level of biological significance, allowing for the exploration of the functional balance of HA and NA within the context of virus-host interactions prior to initiation of infection.

Influenza viruses, the causative agents of Influenza, are members of the Orthomyxoviridae family and all share the genomic make-up of single stranded, negative sense RNA. The genomes are segmented with the number of segments varying between genera. Influenza A and B viruses each contain 8 segments, while Influenza C viruses contain 7. A newly identified influenza C-like virus, with a reservoir in cattle, has been characterized and denoted Influenza D [1]. There are other members of the Orthomyxoviridae family including thogotavirus, isavirus, quaranfilvirus each with a segmented negative sense genome, though the number of segments varies. The RNA

basis and segmented nature of the genome are aspects of influenza biology that allow for persistence of circulation within human and animal hosts. The virus is able to incorporate changes both in site mutations and in switching of entire genome segments that allow for genetically distinct progeny virions to continue the evolution of the virus in response to environmental conditions, transmission prerequisites, and host immune pressure. Influenza A viruses specifically have a wide host range, branching out from the natural reservoir of waterfowl to domestic poultry and to mammalian species, including but not limited to swine [2], seals [3], horses [4], and finally humans.

These viruses are estimated by the World Health Organization to infect 5-10% of the adult population annually with a morbidity rate of 3 to 5 million and a mortality rate of 250,000-500,000 deaths [5]. These statistics are attributed to seasonal influenza, a more frequent epidemic form of the disease than that caused by influenza virus pandemics. While seasonal influenza infects during predictable periods within the calendar year based on temperature and humidity [6, 7], influenza pandemics can occur outside those constraints and can also infect subgroups outside the typical population of the elderly, very young, and immunocompromised. Pandemic Influenza is often characterized by increased pathogenicity with drastic changes in the rate of morbidity and mortality compared to epidemic strains. In both seasonal and pandemic influenza, the disease is established in the upper respiratory tract and can involve the lower respiratory tract and lungs. The course of infection starts with a brief incubation period, during which time virus shedding can already begin, followed by the onset of symptoms. Viral titer and shedding peak, on average, 2 days after infection, with clinical symptoms being most severe at day 2 or 3. For infections mediated by highly pathogenic viruses, the disease is

much more severe, resulting in increased sickness and often death. Currently, highly pathogenic viruses are found primarily in birds, though avian to human transmission has occurred in cases of direct contact [8-11]. Of great concern to researchers and health officials is the possibility of a highly pathogenic virus adapting to circulation within the human population and causing an unprecedented pandemic event.

The Virus Life Cycle and Management of Infection

The genome of influenza A virus consists of 8 gene segments PB1, PB2, PA, HA, NP, NA, M, and NS that encode at least 10 proteins PB1, PB1-F2, PB2, PA, HA, NP, NA, M1, M2, NS1 and NS2. Various strategies have been developed to combat Influenza and they focus primarily on three proteins, HA, NA, and M2, and the roles they play in the virus life cycle which is described in the section below.

Receptor binding and Entry

Influenza A viruses express hemagglutinin (HA) on the surface of the virion in order to facilitate entry via receptor binding and fusion of the virion membrane with the endosomal membrane. The HA is composed of two domains, a stalk containing the transmembrane domain and fusion peptide and a globular head containing the receptor binding pocket. The 550 amino acid homotrimeric protein extends as a 130 angstrom spike from the virion surface. HA is a type 1 transmembrane protein and is often cited as an example of such classification. The globular head domain contains the receptor binding pocket which can be broken down into 4 critical regions, the 190-alpha helix, 130-loop, 220-loop and the base of the site, all of which contain residues known to make

contacts with the receptor [12]. Residues at positions 98, 153, 183, and 195 are critical for the hydrogen bond network at the base of the site [13]. The 130 loop contains residues 135, 136, and 137 which directly interact with the sialic acid motif of the receptor. The 220 loop contains residues that appear to define host specificity by altering the shape of the site to accommodate the different conformations associated with the linkage type [14-16]. Position 226 is such an example with a leucine in mammalian strains binding to α2,6-linked Sia and a glutamine found in avian strains binding to α2,3-linked Sia. The impact of these individual amino acids has been described for both H2 and H3 subtypes: the L226 widens the site changing the hydrogen bond network that would make contacts with the sialic acid whereas the Q226 does not [14, 17, 18]. The final domain is the 190-helix which contains residues that have also been implicated in determining specificity. Residues 190 and 193 have been shown to have importance for group 1 viruses, namely H1 and H5 strains [19-22]. 'Second-site" residues have also been shown to be important for binding and specificity including but not limited to: 189, 193, 194, 216, 198, 211, and 222 [21, 23-25]. The virus typically infects cells in the upper respiratory tract of humans, where the HA recognizes glycan structures terminating in N-acetylneuraminic acid (Neu5Ac), generally known as sialic acid, linked to galactose (Gal) in a beta1-4 linkage to glucosamine (GlcNAc) [26]. The linkage of the sialic acid to the penultimate galactose is a determinant of species specificity. Avian viruses bind α2,3-Sia mediated by the specific residues described above, while mammalian viruses bind to α2,6-Sia [14, 18, 20, 21, 27-39]. This linkage preference, directed by the shape of the receptor binding pocket correlates with receptor availability in the host [40, 41].

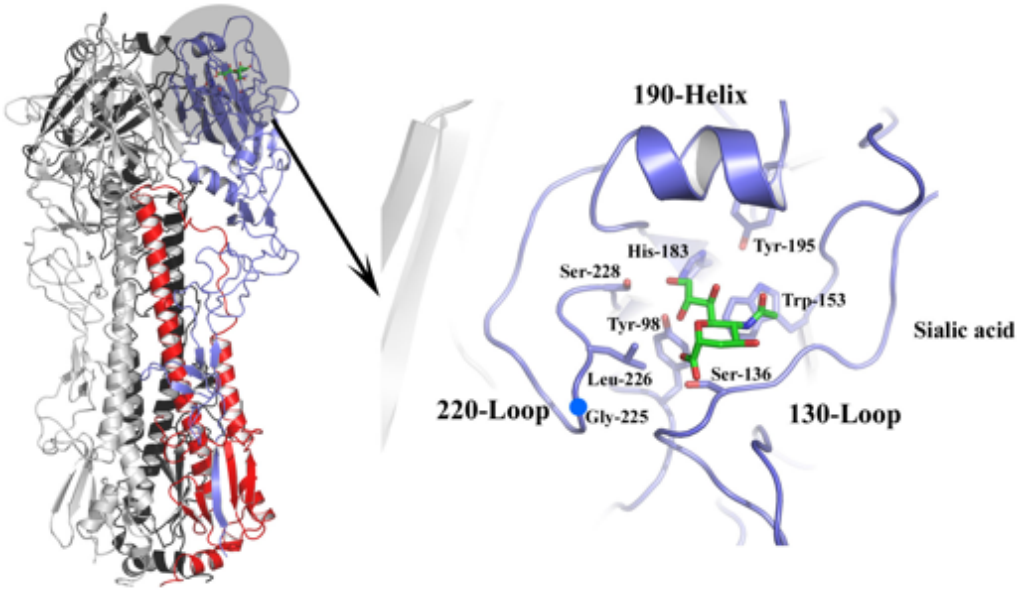

Figure 1. Trimeric HA with receptor binding pocket highlighted in gray. Features of the receptor binding site are highlighted and shown in complex with a sialic acid structure in green. Figure from Steinhauer 2010.

Once contact has been made, the virion is thought to be endocytosed via a clathrin mediated process, though there is also evidence for macropinocytosis [42-46]. The second function of HA is needed once the virus is located within the endosome. The HA has been crystallized in three structural conformations, precursor HA0, cleaved pre-fusion intermediate, and post-fusion HA [12, 47, 48]. Cleavage of the HA occurs before receptor binding and resolves the precursor into two domains, HA1 and HA2. Cleavage is mediated by host proteases: trypsin, furin, TMPRSS2, HAT, and Tryptase Clara found in the upper respiratory tract [49-52]. Protease availability and specificity may have an impact on transmission as a new virus must be able to be activated prior to entry to sustain fusion and initiate the virus life cycle. Cleavage of HA0 results in rearrangement of the molecule, enclosing the hydrophobic N-terminus of HA2 in the interior of the trimer. This domain will ultimately be the fusion peptide. A covalent bond links HA1 and

HA2 post-cleavage. This conformational state is considered high energy and can readily undergo the structural change need to reorganize the protein for fusion [53].

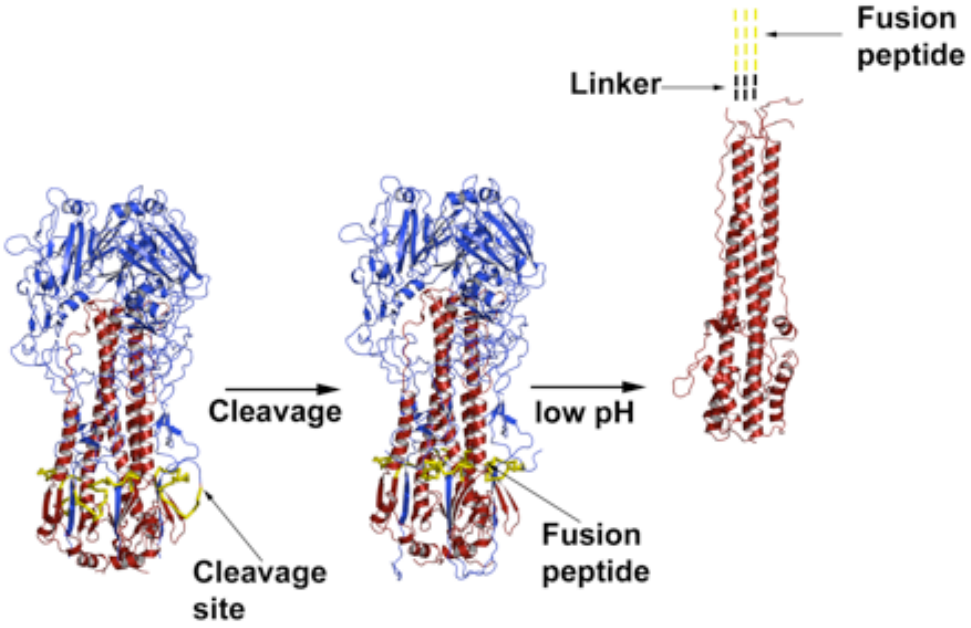

Figure 2. Structural conformations of HA, including the pre-cleavage HA0, post-cleavage metastable HA1 and HA2, and post conformational rearrangement structure with fusion peptide extrusion. Figure from Cross 2009, adapted from Chen 1998, Wilson 1981, and Bullough 1994.

As the interior pH starts to drop, the HA undergoes significant conformational changes, with the globular head domains shifting away from each other and the stalk reorienting, such that the long alpha helix of HA2 is extended, inserting the fusion peptide into the target membrane of the endosome. The structure then flips back on itself opening a fusion pore [48, 54-58]. Much work has been done isolating specific residues and characterizing their effects on the acid stability of the protein. They have not only been localized to the fusion peptide pocket and the fusion peptide itself, but also appear in various distal sites, highlighting the extensive structural changes involved in the reorganization of the protein [59-68]. As the protons have been pumped into the

endosome, the M2 proton channel embedded in the virion membrane allows for proton transfer to and acidification of the interior of the virion [69]. The M2 proton channel, encoded by the M gene segment and product of RNA splicing, is tetrameric in nature. There are estimated to be between 4 and 17 M2 tetramers per virion [70]. The drop in pH allows for the genomic units, vRNPs, to dissociate from the M1, the matrix protein also encoded by the M gene, so that they can be released into the cytoplasm of the cell post-fusion [71].

Transcription

The vRNPs are composed of the negative sense viral RNA wrapped in nucleoprotein, NP, [72, 73] and associated with the polymerase complex consisting of PA, PB1 and PB2 [74-81]. These vRNPs are associated with M1 matrix protein in the virion [82] and become released following acidification mediated by the M2 proton channel [69, 83, 84]. The vRNPS are trafficked to the nucleus through the nuclear pore complex (NPC) via nuclear localization signals (NLS) on the NP protein and with the help of host import factors such as Ran and p10 [85, 86]. The reliance on host factors could impact efficient cross-species adaptation as different subsets of proteins within the importin family have been implicated for preferred use with avian vs mammalian viruses [87-89]. Once in the nucleus, the vRNA is transcribed into mRNA, to be translated into viral proteins, and eventually into complementary RNA, cRNA, to be used as a template for the generation of vRNAs [90]. The virus lacks the ability to synthesize the 5' cap of the mRNAs, so in order to begin mRNA transcription, the PB2 protein binds to cellular mRNAs allowing the PA to cleave the 5' terminal 10-12 nucleotides including the cap [91, 92]. PB1 then uses the capped oligomer as a primer and continues the transcription

of the viral mRNA [93-96] creating a poly A tail upon reaching the terminating sequence [95, 97].

Translation

The mRNAs are translated into the nascent proteins in the cytoplasm of the cell. Translation occurs in 2 phases, with NP, PB1, PB2, PA, and NS1 being translated early in the infection cycle, while the remaining proteins are translated later. This switch is thought to be mediated by both the NS1 protein and the accumulation of nascent mRNAs [98]. NS2/NEP and NS1 are products of the NS gene. NS1 acts as an interferon agonist, abrogating the antiviral response of the cell [99-103]. Newly translated NP, PB2, PB1-PA heterodimers, NS2/NEP and M1 are imported into the nucleus via NLS-importin mediated processes [104-106]. NP is required for synthesis of negative sense viral RNA [107]. The vRNA associated with the NP and the newly formed polymerase complexes constitute the new vRNPs. These associate with M1 and NS2/NEP, the nuclear export protein, which work with host export pathway CRM1 via a nuclear export signal on the NS2/NEP [108-114]. Once in the cytosol, the NEP obscures the NLS signal of the M1, preventing nuclear re-entry of the vRNPs [115, 116]. These complexes of vRNP plus M1 utilize the microtubule network and the GTPase Rab11 to transit to the apical membrane in preparation for budding [117-119]. Following translation, HA, NA and M2 are trafficked to the ER and through the Golgi where oligomerization as well as post-translational modifications including glycosylation of HA and NA and palmitoylation of HA and M2 occur [120-122]. The post-structural modifications of HA including the glycosylation of three asparagine residues (Asn12, Asn28, and Asn478) and the palmitoylation of three cysteine residues are important for proper folding and transport

[123-125]. Glycosylation also adds a level of variance that allows for immune evasion of the surface proteins, as the antigenic sites can be altered by the addition or removal of carbohydrate structures [126, 127]. The core proteins composed of NP and PB1, PB2, PA and M1 are folded in the cytoplasm, with the NP and the polymerase units forming new vRNPs with the newly transcribed vRNA.

Assembly and budding

HA, NA and M2 are trafficked to lipid rafts in the membrane at the site of budding in both an independent and assisted fashion [128, 129]. The tails of HA and NA, embedded within the plasma membrane, recruit and interact with M1 which in turn recruits vRNPs to the cell membrane [130]. Virion assembly occurs with the packaging of vRNPs associated with the individual gene segments. Two hypotheses related to the mechanism have been proposed: random packaging, incorporating a random selection of 8 or more vRNPS or ordered packaging, incorporating a vRNP for each gene segment. There is evidence for packaging signals specific to each gene segment and for vRNP specific competition resulting in the incorporation of one segment per gene [131, 132]. While there are electron micrographs showing 8 vRNPs [133], there are also those that reveal virus particles with more or less than 8 segments [134-136]. Together these data suggest that the process is likely more ordered than random, though potentially error-prone, and so a heterogeneous population of virions incorporating an average of 8 segments is produced. Recent work has suggested that semi-infectious particles, or those lacking a segment, can be complemented via reassortment and therefore can contribute to the genetic diversity of the viral population [137, 138].

HA and NA initiate the process of budding [130, 139] while M1 and M2 are necessary but not involved in initiation [140, 141]. Scission is ATP-dependent [142] and may be mediated by M2 [143, 144]. After the virion buds from the membrane, residual proximal sialic acid can be acted on by the HA preventing the dissemination of the virus particles. The neuraminidase, NA, protein is a homotetrameric stalk, approximately 60 angstroms tall [145], though the length has been known to vary by host as a result of adaptation [146-149]. It exhibits sialidase activity [150, 151], cleaving the sialic acid substrates on HA itself and on the membrane that might be bound by HA, and allowing for release of the virions [152, 153]. It is this activity that is ultimately targeted by the class of antivirals developed against influenza virus that are still in use today.

Vaccines and Antivirals

As surface glycoproteins, the HA and NA are immunogenic and will elicit the majority of the host immune response upon infection [154-156]. Antigenic drift, caused by the accumulation of selected mutations maintained by lack of RNA proof reading [157, 158], leads to rapidly changing antibody targets. Vaccine strategies are based on pre-emptively developing an immune response to these proteins so that host antibodies are already established, primed to recognize the invading virion, and able mount an effective immune response before the viral titer is allowed to rapidly increase. Vaccines are developed every year with strain selections predicted to be relevant for the upcoming Influenza season. The current options include a trivalent vaccine with two influenza A subtypes (H1 and H3) and one influenza B and a quadrivalent vaccine which adds an additional influenza B strain. The vaccines can either be inactivated or live attenuated. A vaccine strain is created with a consistent backbone of internal genes (for example, those

of A/Puerto Rico/8/34) with the HA and NA segments of the circulating strains [159-166]. Because the head domain of HA is prone to antigenic drift, a new vaccine is made up every year and there is often little cross-reactivity between groups and subtypes, so two representative IAV subtypes are included. Recently an approach has been proposed to circumvent this need and that is to use a universal vaccine, or one that is directed against the stalk region of HA. This region is fairly conserved between subtypes and would allow for cross-reactivity, eliminating the need to vaccinate against individual subtypes as well as provide protection against those that are found in other hosts but have yet to adapt to humans and enter circulation [Reviewed in 167, 168, 169].

Antivirals have been developed to target the M2 and NA proteins and their respective functions within the life cycle. The M2 proton channel is necessary for vRNP release into the cytoplasm and two drugs have been developed that inhibit that process. Amantadine and rimantadine work by blocking the proton channel and therefore preventing the acidification of the interior of the virus particle [170]. These were the first influenza antivirals developed [170] and after repeated use, circulating viruses have become resistant [171]. Single point mutations in the M2 are enough to garner resistance at no fitness cost to the virus [172, 173]. The study of M2 inhibitor resistant mutants however led to the discovery of the compensatory mutations in other genes, notably HA, that still allow for productive infection to occur [174, 175]. Following the widespread resistance to M2 based drugs, inhibitors targeting the neuraminidase were put into use. These compounds, oseltamivir, peramivir, and zanamivir are sialic acid analogs and bind competitively to the sialidase site on the NA [176, 177], effectively preventing the enzymatic activity. This effect is seen in the inability to release individual virions from

aggregates and from the surface of the cell from which they are budding [178]. As with amantadine and rimantadine, resistance to the NA inhibitors became apparent and manifested not only in the neuraminidase but in other genes as well [178, 179]. This process of adapting to a non-functional NA provided our first clues as to the functional balance of HA and NA as in some cases, it was the HA protein that altered to match the functionality of the now defunct NA.

Subtypes, Reassortment, and Pandemic Events

Influenza pandemics occur when a virus that is antigenically distinct from previously circulating strains is able to transmit to and between human hosts and maintain infection. Antigenically novel viruses have not been recognized by the immune system and therefore, the immune response is not primed against them. The most immunogenic protein of the influenza A virus particle is the hemagglutinin, though antibodies have been found to the other surface glycoprotein, NA, as well as to the NP and M1 proteins [180]. The HA can undergo a process of antigenic drift, slowly evolving away from antibody recognition under immune pressure from the host [126, 181]. Antigenic shift is a more drastic method of becoming antigenically novel and involves the process of reassortment, when an entire viral segment is switched for another of the same type during co-infection with two distinct strains. This process has led to three pandemics in recent history, 1957, 1968, and 2009 [182]. In all three events, a reassortant virus was introduced to the human population.

Influenza A viruses are identified by the subtype of the HA and NA proteins, based on the antigenic reactivity to polyclonal sera [183] and sequence data. Within the common aquatic bird reservoir, there are 16 known HA subtypes and 9 known NA subtypes, with an extra two HA subtypes and NA-like subtypes attributed to bats [184, 185]. The HA subtypes are divided into 5 clades separated into 2 groups. Group 1 consists of subtypes H1, H2, H5, H6, H8, H9, H11, H12, H13 and H16. Group 2 consists of subtypes H3, H4, H14, H7, H15 and H10. The groups are separated by structural characteristics between the members, including the orientation of features about the central helix, the shape and severity of the loop connecting the helices of HA2, and the differential conservation of ionizable residues in the fusion peptide pocket implicated for acid stability [186]. Only 3 of the 16 subtypes in the avian reservoir have been found in human circulation. These are H1, H2 and H3. Other subtypes of note are: H5 and H7 which are associated with highly pathogenic infection in birds and have shown some isolated human transmission [8, 9, 187] and H9 which, though not associated with HPAI viruses, does pose a pandemic threat due to the ability for human adaptation and the novelty of the subtype [188]. For the neuraminidase gene, there are only two subtypes found to circulate in humans: N1 and N2. Establishment of HA and NA subtypes within the human population follows a pandemic event and can proceed to seasonal circulation.

As mentioned, reassortment can be a predictor of pandemic events with the potential antigenic shift of a strain essentially resetting the immune progress. Reassortment can also provide valuable genetic diversity between strains of the same subtype [189-191]. It has been linked to the rapid spread of adamantine resistance [192] and to the circulation of H5N1 in poultry in southeastern Asia [193]. Researchers have

capitalized on reassortment as a way to mix the genetic material of different strains and the greatest example of this is the current strategy for generating vaccines [194]. Reassortment occurs when a cell is co-infected, meaning infected with two virus particles within a certain period of time. Upon co-infection, the genetic material of both particles can be replicated and then packaged together incorporating gene segments from each parental strain so that the progeny strain has a novel genotype. This event was illustrated in the work of Marshall et al. which characterized both the timeline and stochastic nature of reassortment between identical strains. They showed in the guinea pig host that even within 12 hours and up to 18 hours post infection by the original parental strain, superinfection with a co-infecting strain can lead to reassortment. They also noted that incorporation of parental segments of the same gene appears to occur randomly, when controlled for the influence of segment mismatch [132]. The propensity for reassortment has great implications for zoonotic threats. Experimentally, the reassortment of strains has been shown to both create pathogenic progeny [195] and increase the transmissibility so that the species barrier can be overcome [196]. Natural examples of the disastrous potential of reassortment are found in the Influenza pandemics of 1957, 1968 and 2009.

The earliest recorded influenza pandemic occurred in 1918. Dubbed the 'Spanish flu', the H1N1 virus rapidly spread all over the world. This pandemic was the deadliest recorded to date [197]. Clinical presentation was swift with the primary causes of death being related to respiratory failure and secondary bacterial infections. The virus pre-dated periods of modern archival clinical specimen storage, but viral RNA was able to be isolated from formalin-fixed or frozen tissue specimens and used to reconstruct the 1918 pandemic strain [198]. The HA of 1918 H1N1 displayed mammalian receptor binding

characteristics and, while previously thought to have been caused by direct avian to human contact, has been shown to have circulated in mammals prior to acquiring adaptations that led to an increase in virulence [199, 200].

There have been three pandemics following the 1918 pandemic. The pandemic of 1957 was the result of a reassortant virus that incorporated three genes from an avian strain (H2, N2 and Pb1) into the circulating H1N1 strain [201-203]. The resultant virus became an H2N2 subtype and was new to the human population primed against the circulating H1N1. After the initial pandemic status, the virus maintained circulation within the human population, its effects becoming attenuated as population immunity built up against it. The next pandemic, taking place in 1968, was also the result of a reassortment event, this time replacing the H2 and PB1 with those genes of an avian H3 strain [201-204]. The disease severity associated with this pandemic was lessened compared to the one of 1957, potentially due to the incorporation of the existing N2, to which the population had already been exposed [182]. 1977 saw the reintroduction of an H1N1 strain similar to that of the 1957 pandemic [182]. This strain co-circulated with the contemporary H3 until the pandemic of 2009 and the emergence of the novel H1N1 strain. The 2009 H1N1 virus was the result of a reassortment event between two swine viruses: a triple reassortant virus and an avian-origin Eurasian swine strain. The trH1N1 virus donated six segments (PA, PB1, PB2, HA, NP and NS) while the Eurasian swine virus donated 2 (NA and M) [205, 206]. After the pandemic strain became established, it replaced the early 1977 strain and is circulating within our population today. In the cases of the last pandemic outlined here, a switch from a swine host to a human host occurred, though there is evidence for human to swine transmission as well [182, 207]. This

process of interspecies transmission is a determinant of potential pandemics and is rigorously studied in the context of pandemic preparedness.

The Role of the Host: Carbohydrate Interaction, Interspecies Transmission, and Pathogenicity

Carbohydrates recognized by influenza A virus

The receptors utilized by influenza virus terminate in sialic acid (Sia), a monomeric sugar with 9 carbon backbone [208-210]. The term sialic acid broadly refers to this basic structure. This class of monosaccharides is one of the most diverse because of the potential for modifications. Four basic types of sialic acid exist, 2-keto-3-deoxy-D-glycero-D-galacto-nononic acid (KDN) and Neuraminic acid, with N-acteylneuraminic acid (Neu5Ac) and N-glycolylneuraminic acid (Neu5Gc) derivatives, though further modifications are found and expand the Sia repertoire to over 50 types [211]. Sialic acids are added to glycans in the Golgi by linkage specific sialyltransferases and are often found at the terminus of N-glycans, O-glycans, glycoproteins and glycosphingolipids. Sialic acids are important for many biological processes including cellular differentiation, growth, signaling and fertilization [211]. They are known to stabilize protein structures and mask degradation sites [212]. The terminal decoration of glycoproteins makes sialic acid an ideal target receptor for a variety of pathogens, including influenza viruses. When comparing carbohydrates isolated from the swine lung, N-glycans terminating in sialic acid are the preferred receptor for influenza viruses of human, avian and swine host strains [213]. N-glycans, distinguished by the covalent N-glycosidic bond to Asn-X-

Ser/Thr, have a core structure of Manα1-6(Manα1-3)Manβ1-4GlcNAcβ1-4GlcNAc-Asn that can be further modified to generate a wide variety of structures. In general, three types exist: oligomannose, complex, and hybrid. Type 1, or oligomannose, structures contain only mannose. Type 2, or complex- N-glycans have branches attached to the mannose core and Type 3, or hybrid, have mannoses on the Manα1-6 of the core and a branch off of the Manα1-3.

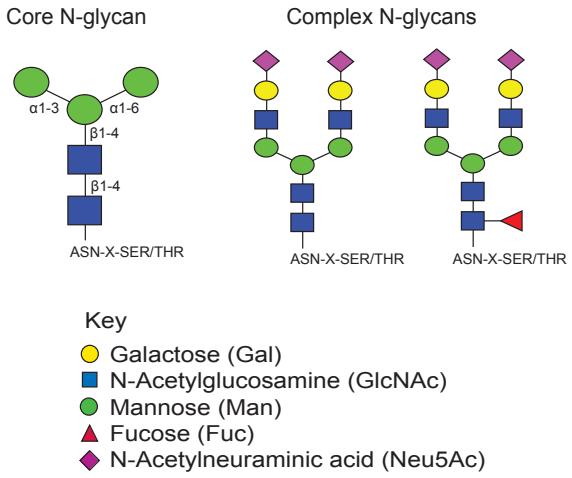

Figure 3. N-glycan core and complex structures. The core N-glycan is modified by the addition of subsequent monosaccharides to differentiate into oligomannose, complex or hybrid structures. Complex N-glycan structures relevant for IAV HA binding are shown.

The synthesis of the N-glycans is mediated by membrane bound glycosidases and glycosyltransferases that are regulated by cellular conditions, such that two different cells may ultimately present a different range of glycans based on the cellular environment. The processing of the N-glycan occurs in the trans-Golgi and involves modifications to the core, elongation of the branches and the addition of terminating sugars such as sialic acid [214]. N-glycans serve many functions both intracellularly and as features of signaling molecules on the cell surface. It is known that N-glycans ensure proper folding of glycoproteins prior to exit from ER [215]. A number of congenital disorders of glycosylation, related to defects in N-glycan synthesis and presentation, have been identified and have developmental, neurological, gastrointestinal and immune effects

indicating the importance of N-glycosylation [216]. Sialic acid is also found linked to O-glycans, a class of carbohydrates designated by the O-glycosidic bond of an N-acetylgalactosamine to a serine or threonine. O-glycans can have one of eight core structures, though core 1- core 4 are the most common, and also can undergo additional elongation and modification processes to generate a wide range of structures. As with N-glycans, O-glycans have many biological roles, from immune recognition to the hydration of mucosal layers in the epithelia [217]. These glycans, though not directly bound by influenza viruses, are a fundamental component in mucins and therefore are significant for the virus interaction with the host environment.

Getting to the surface- Mucins and Virion Morphology

Before the virus can interact with the receptor it must reach the cell surface. Within the host, the environment is not necessarily favorable for viral dissemination and attachment. In fact, in humans there are a number of innate host strategies in place to prevent infection. As an upper respiratory infection, the virus encounters the nasal passages first. Here goblet cells express soluble mucins and ciliated cells serve to move this mucus layer out and away from the surface of the cells [40, 218]. The environment of the respiratory epithelia is complex. Surrounding and above the ciliated cells is a two-layer barrier. The periciliary liquid layer (PCL) is on the bottom and contains tethered mucin structures, while a more viscous gel-like mucus layer is on top. This arrangement has been described as a gel-on-brush model, and allows for the free beating of cilia underneath the mucus [219]. In addition to creating a scaffold in the PCL, mucins are also excreted and are the major components of airway mucus. Mucins, huge macromolecules, are composed of proline, serine, and threonine backbones with

extensive glycosylation mostly with sialylated O-glycans [217]. MUC5ac and MUC5b are the two most abundant secreted mucins within the airway mucus and, while overexpression of MUC5ac appears to inhibit influenza virus infection, MUC5b appears to be essential for mucociliary clearance [220, 221]. The tethered mucins, MUC1, MUC4, MUC16, and MUC20, not only function as a physical support, but also are important immune modulators, have roles in signal sequencing and cell proliferation [reviewed in 222]. The virus must transverse the mucin layer and glycocalyx to reach an internalizable glycoprotein displaying the sialic acid receptor. Though much work has been done in relation to the morphology of the virus and the action of neuraminidase [223, 224], not much is known definitively about the transit to the cell's surface prior to the receptor binding event. Nevertheless, the virus is able to initiate infection and appears to be relatively specific for certain cells types expressing certain sialic acid structures.

Influenza A virus particles are enveloped and as such, lack a rigid outer capsid that creates a defining structure that would be consistent among the virions. The envelope is composed of lipid bilayer and is associated with four proteins, M1, M2, HA and NA. M1, the matrix protein, is thought to have the greatest effect on virion morphology though it is not the sole determinant [223, 225-228]. HA and NA are known to transverse the bilayer and interact with the M1 protein. The matrix protein forms an inner core of the virion, giving structure and shape to an otherwise pleiomorphic lipid bilayer envelope [229]. The virus particles are known to adopt two general shapes, spheres and filaments, dictated at least in part by residues in the M1 protein [230-234]. Typically, spherical strains are found by electron microscopy in lab-adapted cultures, usually 80-100nM in diameter, while most natural isolates are filamentous and vary in

length [117, 231, 235]. It has been speculated that the filamentous shape allows for specific distribution of NA, with the protein clustered near the scission end of the filament to allow for NA cleavage of receptors at the infected cell surface [117]. This spatial arrangement could in theory also benefit transmission, as a cluster of NA at the leading end could be targeted to clearing mucins as the filamentous particle encounters the PCL. Electron micrographs have shown the spatial distribution in spherical particles seems to be a more even for HA and NA around the exterior of the particle [236], perhaps indicating that in an environment intentionally favorable for replication, filamentous shape is not needed and may even be a hindrance. Several groups have noted that changes in M1 that alter the virion morphology also seem to correlate with a change in the neuraminidase activity [223, 234]. The interaction of NA and host mucins has been recognized since the 1940's, however the mechanism in the course of natural infection has yet to be fully elucidated [237, 238]. Matrosovich et al. demonstrated that treatment with NA inhibitor, oseltamivir, diminishes influenza virus infection of differentiated and mucin producing human tracheobronchial cells and nasal epithelial cells indicating a role for NA prior to entry [239]. This result was recapitulated in undifferentiated cell cultures of A549 and MDCK cells [240]. Overlaying MDCK cells with human salivary mucins with mid to high Sia content reduces the rate of influenza infection. However, a porcine mucin overlay did not have the same effect with infection rates staying the same or increasing [241, 242] even in the presence of oseltamivir or with a low activity NA. The inactivation of NA was expected to have an additive effect in combination with the mucus overlay, and so sustained infection may be due to differences beyond the sialidase activity and greater incorporation of Neu5Gc than Neu5Ac in human mucins. These

combined results suggest that the mucin composition may contribute to the species barrier commonly attributed to availability of receptor type.

Presentation of receptors in avian, swine and human hosts

The host range for influenza A virus is diverse, ranging from avian to a number of mammalian species. However, aquatic birds of the orders *Anseriformes* and *Charadriiformes* make up the natural reservoir. The *Anseriformes* include ducks, geese and swans while the *Charadriiformes* include shore bird, gulls and terns. Infection in these animals is gastrointestinal via an oral-fecal route [41, 243, 244] and mostly asymptomatic, indicating an adaptation to the species. Though the virus recognizes the same general structure of receptor, a sialic acid terminating sugar, avian and mammalian viruses have been shown to recognize different sialic acid linkages. It is known that birds, pigs, and humans express sialic acid on cells at the site of influenza virus infection and much work has been done to identify the linkage type present. Most often lectin histochemical studies are done with the plant lectins *Sambucus nigra* and *Maackia amurensis*. *Sambucus nigra*, SNA, derived from elderberry bark, recognizes sugar structures terminating in α2,6-sialic acid (Neu5Acα2-6Galβ1-4GlcNAc). *Maackia amurensis,* MAA, from the legume, contains two isoforms designated MAL (MAA-II) or MAH (MAA-I) that differ in glycan recognition. MAL binds α2,3-sialic acid (Neu5Acα2-3Galβ1-4GlcNAc) and some sulfated structures, while MAH recognizes a different motif (Neu5Acα2-3Galβ1-3) [245-248].

Lectin histochemical studies completed by França et al. have shown that for representative species of the two avian orders, α2,3-sialic acid is present throughout both

the intestinal and respiratory tracts; and while α2,6-sialic acid is found in the respiratory and intestinal tract of *Anseriformes*, it is limited to the respiratory tract of *Charadriiformes* [249]. Wan and Perez found in quail, an example of a farmed terrestrial bird, a similar receptor distribution with the intestinal and respiratory epithelial cells displaying binding by SNA, MAL, and both avian and human viruses [250]. In a direct comparison of terrestrial and aquatic birds, Kuchipudi et al. determined that both chickens and ducks express α2,3-Sia in intestinal epithelial cells and that neither express α2,6-Sia. This finding is contradicted by the aforementioned data that *Anseriformes*, the order encompassing duck species, exhibit 2,6 binding in the intestine and *Charadriiformes* do not [249], but corroborates the results of Gambaryan et al. and Costa et al. [251, 252]. However on the matter of the trachea of the chicken, where Wan found significantly more α2,3- than α2,6- linked sialic acid, both Kuchipudi and Gambaryan found expression of α2,6-Sia denoted by both lectin binding [253] and human virus binding [252]. As these examples show, multiple groups have studied the presentation of sialic acid within the avian respiratory and intestinal tracts with differing results. A comprehensive examination of the literature reveals that instead of firmly understanding the dominating sialic acid linkage present at the sites of infection, we are recognizing the variability and therefore limits of lectin histochemical studies. The two isoforms of MAA are problematic due to the differences in specificity and the fact that they are frequently distributed together or one isoform is not distinguished from the other commercially [254]. Even in more recent studies conducted after the resolution of the ‘MAA problem’ and using both isoforms or just MAL, there are still discrepancies in results for avian

hosts, potentially linked to the method of tissue presentation. In general, though, it appears that both linkage types are present in the tissues harboring virus infection.

Swine have often been implicated in the zoonotic spread of influenza viruses. As discussed, the pandemic event of 2009 occurred when a reassortant swine virus crossed the species barrier to sustain infection in humans. Just as with avian strains, lectin studies have been used to examine the receptor distribution and similar discordant results have been reported. The dogma for some time was that pigs harbor both receptor types and therefore can serve as a mixing vessel allowing for an avian virus to infect via a 2,3 linked receptor and develop the ability to recognize a 2,6 receptor then transmit to humans [243, 255, 256]. Using lung explants, Punyadarsaniya et al. demonstrated both avian and porcine influenza virus infection in swine lung cells. They determined that ciliated and non-ciliated mucus producing cells exhibited α2,6-Sia and were readily infected by the swine virus (H3 subtype). Only ciliated cells stained with MAL, but both cell types were infected with an avian strain (H7 subtype) [257]. Van Poucke et al. report minimal MAL staining of the porcine trachea indicating a lack of α2,3-Sia receptors [258] or perhaps a limit of lectin recognition. Swine viruses typically display a greater 2,6 receptor binding specificity than 2,3 [27, 28, 34, 213, 259-261] which may indicate that, though α2,3-Sia may be present in the porcine respiratory tract, it is not displayed on cells utilized in infection. Interestingly, in swine particularly, influenza viruses recognize the other species of sialic acid, N-glycolyneuraminic acid (Neu5Gc). Neu5Gc is prevalent in swine, but not common in humans [26, 262-265]. Swine viruses that transmit and adapt to humans lose Neu5Gc recognition [27, 266], and though studies show a preference of Neu5Gc binding for swine isolates [266], it is unclear if infection within the

swine host is mediated by both sialic acid species or if a Neu5Ac specific virus, such as a human strain introduced during reverse zoonosis, would require further adaptation to efficiently spread in the porcine respiratory tract. The comparison of recent H3N2 swine isolates to reference human strains reveals distinct similarities between the two, leading to the characterization of the HA gene of the swine isolate as "wholly human" [267] and therefore indicating that modification of the receptor binding pocket to prefer Neu5Gc binding is either unlikely or not associated with residues known to alter linkage specificity.

As with swine viruses, viruses isolated from human infection display a α2,6-Sia receptor preference in receptor binding studies. An attempt to determine the localization of receptors with human respiratory tissue has fallen to the same disparity as avian and swine studies. Couceiro et al. showed a differential expression of Sia linkages with the ciliated cells of the tracheal epithelium expressing α2,6-Sia and the intracellular mucin droplets expressing α2,3-Sia [268]. This finding is directly contradicted by that of Matrosovich et al. who determined that both receptor linkages were present on airway epithelial cells and were differentiated by cell type with ciliated cells expressing α2,3-Sia while non-ciliated cells expressed the α2,6-Sia presumably used for infection [269]. Barkhordari et al. describe similar levels of SNA and MAL staining for alveolar macrophages, type 1 and type 2 pneumocytes, endothelial cells, mast cells, and bronchial epithelial cells [270]. To avoid the issues with lectin binding studies, PVA or pattern of virus attachment experiments were devised. These techniques use viruses as the histochemical agent instead of lectins and provide a direct stain of virus binding [268, 271, 272]. It was shown that human viruses, an H1N1 and an H3N2, bind more to ciliated

cells than non-ciliated and are more localized to the trachea and bronchi than the bronchioles while avian viruses of subtypes H5 and H6 bound more in the alveolar region with less attachment to the trachea [271, 272]. These experiments only tangentially address the classification of the Sia-linkage and perhaps reveal that studies focused solely on the linkage type present at the site of infection have a limit of usefulness in characterizing the initiation of infection.

Two somewhat opposing interpretations of influenza biology in respect to species specificity are generally accepted by the field. The widely accepted explanation for receptor binding specificity has been that the differences in sialic acid linkage type present at the site of infection correlate with the receptor specificity of avian and mammalian viruses. The thought was that avian viruses are specific for α2,3- linked sialic acid because those structures are what predominate the glycosylation at the site of infection in the intestinal tract of birds and that human and swine viruses prefer α2,6-Sia because that is the predominant receptor in the respiratory tract. Though the lectin studies are not the gold standard, it is clear that a more heterogeneous mix of receptors is prevalent in all hosts than was originally thought. In addition to this theory, many groups suggest that certain species of birds and swine could be a mixing vessel for avian and human viruses to intermingle, swapping gene segments and potentially creating a human-adapted virus from the avian host [249, 250, 253, 256]. If, as predicted, there is a prevalence of both receptor types at the site of infection, then what beyond availability leads to the receptor specificity attributed to the different species? To answer this question, a focused investigation into the cellular presentation of the glycans, including

what glycoproteins they modify, and the localization and cellular function of those glycoproteins must be examined.

Interspecies transmission

Interspecies transmission occurs when viruses evolve to cross the species barrier. Though receptor preference might be the most significant and certainly the best known determinant of species specificity, the adaptation required for interspecies transmission is multi-factorial and much is yet to be understood. Starting with the receptor itself, crystal structures have revealed that the position of the sialic acid, both 2,3 and 2,6 linked, within the receptor binding site of an avian or human HA, respectively, is superimposable [273]. It is the glycan adjacent to the terminal sialic acid that is interacting with the residues of the receptor binding site differently. In 2,3 linked receptors, the glycan retains a straighter form interacting with the 220 loop [30]. In 2,6 linked receptors, the glycan twists back on itself, interacting with both the base of the pocket and the 190-helix [36]. This observation has led to the speculation that glycan determinants beyond the terminal sialic acid contribute to binding, and indeed, determinants such as core fucosylation do appear to have an effect [213]. The features of the receptor binding pocket that mediate this receptor preference have been identified as residues 226 and 228 for H3 and H2 viruses and residues 190 and 225 for H1 viruses. A mutation at position 226 from a glutamine to a leucine is associated with a α2,3-Sia to α2,6-Sia binding switch, while at position 228, a glycine to serine switch is necessary [14-17]. For H1 subtypes, a glutamic acid to aspartic acid at residue 190 and an aspartic acid to glycine at residue 225 correlate with the receptor specificity switch [274-276]. Recent avian isolates have been observed with mammalian receptor binding traits. An H5N1 displaying an increase in 2,6 specificity has

been isolated in Egypt and may link to the rise of local direct-contact infections of humans with avian H5 [277]. In China, an H7N9 strain found with the mutation Q226L displays specificity for both receptor types [187, 278]. Though these viruses developed recognition of the mammalian receptor type, avian to human transmission was limited to cases of direct contact. In an experimental setting, both Herfst et al. and Imai et al. described a minimum of 4 mutations in HA, altering receptor specificity and removing a glycosylation site, that contribute to avian-mammalian respiratory droplet transmission, however sustained transmission was not attributed to changes in HA alone [196, 279]. In order for successful interspecies transmission and efficient replication of the virus within the new host, other viral factors in addition to receptor switch must undergo adaptation.

Interspecies transmission is multi-factorial extending beyond the problem of receptor availability. Many host factors such as proteases, nuclear transport pathways, glycosylation pathways, and antiviral responses have been implicated in the process [280, 281]. Even the pH and body temperature of the site of infection can become a barrier to interspecies transmission. PB2 exhibits host restriction in that polymorphisms in the protein specific to avian or mammalian viruses (K627 vs E627, respectively) lead to a change in the replication permissive temperature. A lysine at residue 627 is associated with human isolates and permits replication at 33°C - 37°C [282-284] whereas a glutamic acid at this position found in avian strains necessitates a higher temperature of 37°C - 40°C for efficient replication. These temperature differences reflect the differences in the site of infection of the two host species and have been speculated to be a significant barrier to cross-species transmission [285, 286]. In fact, Herfst et al. noted that one of the mutations critical for aerosol transmission of an avian H5 strain in ferrets is localized to

this residue in PB2 [279]. The pH of fusion can also be a predictor as avian strains have shown tendencies to undergo fusion at higher pH than human strains of the same subtype [49, 68, 287] indicating that an increase of acid-stability of the HA might be required for mammalian replication. Despite these barriers, interspecies transmission is not uncommon with multiple documented instances. Avian to avian transmission between wild waterfowl and domestic poultry has been widely reported and can often lead to huge economic losses either through highly pathogenic infection mortality or culling of the population to control the threat. Transmission from domestic poultry directly to humans has been shown to occur and has been linked with the use of live poultry markets in southeast Asia [288]. Swine hosts frequently play a role in interspecies transmission both as the recipient host of transmitted avian and human viruses and the donor for a human transmission event [reviewed in 289]. Swine are also implicated in reverse zoonosis, as human viruses jump to swine and circulate within the swine host before potentially returning to humans [207, 267]. Though the species barriers are numerous, influenza viruses can overcome them to sustain interspecies transmission in multiple hosts. As of yet, most events have been relatively mild, with the exception of the pandemics, as interspecies transmission and sustained human circulation has been limited to viruses of low pathogenicity. A highly pathogenic virus has not been able to breach the species divide and transmit effectively between humans yet, however, it is likely that eventually this may happen and the effects could be devastating.

Pathogenicity

Influenza A viruses can vary in pathogenicity and while most strains are characterized as low pathogenic avian influenza (LPAI) viruses, highly pathogenic avian

influenza (HPAI) viruses associated with subtypes H5 and H7 have been isolated. The potential of highly pathogenic viruses to transmit to humans is a major public health concern. As mentioned, influenza is typically asymptomatic in birds, however an increase pathogenicity leads to severe morbidity and mortality within the host reservoir [290]. HPAI viruses evolve from multiple passages of LPAI viruses in new avian hosts [291, 292]. For humans, infection with highly pathogenic influenza is severe with up to a 60% case-fatality rate [293]. Similar to transmissibility, the characterization of pathogenicity is multi-factorial. Perhaps the most well-known determinant of pathogenicity of a virus is the sequence of the cleavage loop of HA. Cleavage of this domain is responsible for the transition of HA0 to the fusion primed conformation of HA1 and HA2. In LPAI viruses, the cleavage loop consists of up to two basic amino acids which restricts the recognition of these motifs to select, localized cleavage enzymes. However, HPAI viruses contain a multi-basic cleavage loop, recognized by ubiquitous subtilisin-like proteases leading to more extensive HA activation upon contact with host tissues [294-303]. A substitution at residue 627 in PB2 has implications for increased virulence, potentially linked to its importance for interspecies transmission. The 1918 pandemic virus was reported to include a mutation at this site compared to circulating contemporary avian strains [304] and the residue has been implicated in the increased pathogenicity of both H5 and H7 HPAI strains [305]. Other factors associated with increased virulence include a potential difference in the site of infection, with HPAI viruses infecting the respiratory tract of ducks, in addition to the intestinal tract, and infecting the lower respiratory tract of humans leading to greater severity of disease.

Functional Balance of HA and NA

The two surface glycoproteins of influenza A virus, hemagglutinin and neuraminidase mediate a range of host interactions from receptor binding to viral release. As mentioned previously, the hemagglutinin binds to carbohydrates on the cell surface terminating in sialic acid. Neuraminidase, likewise, acts on sialic acid, cleaving the moiety from both HA and cell surface glycans. Because they share a substrate, it seems obvious then that a functional balance between the two proteins would exist, preventing the work of one from overpowering the role of the other. This functional balance has indeed been established in terms of binding avidity and neuraminidase enzymatic activity. Baum and Paulson recognized a drift in NA specificity to obtain some sialidase activity against α2,6-Sia from 1957 to 1987. Strains circulating prior to 1967 and 1968 had strict α2,3-Sia specificity, but recognition of 2,6 gradually increased until finally, viruses isolated in 1972 exhibited equal sialidase activity against both α2,3-Sia and α2,6-Sia [306]. This time period saw the introduction of the H3 subtype following the 1968 pandemic and might indicate the selective advantage of establishing sialidase activity against potential receptor structures that could lead to a null infection. Data collected identifying the affinities of H3 HAs for 2,3 and 2,6 sialyllactose highlights a general increase in affinity of HA for 2,6-Sia from the time that the strain was introduced in 1968 [276]. Xu et al. compared the HA affinity to 6'-SLNLN, NeuAcα2-6Galβ1-4GlcNAcβ1-3Galβ1-4GlcNAc, to the NA activity against 4-MU-NANA, 2'-(4-Methylumbelliferyl)-a-D-N-acetylneuraminic acid, for pandemic strains from 1957, 1968 and 2009 and found a correlating increase in both [307]. This increase in affinity, if reflected biologically could

explain the rise in 2,6 sialidase activity of human strain NAs and highlights the intrinsic need for functional balance of the two proteins. This concept has been examined in a variety of laboratory studies with a forced imbalance of the two proteins and subsequent adaptation. Studies with oseltamivir produce escape mutants that exhibit resistance, not always by altering the NA, but by sometimes reducing the avidity of HA for its receptor so that it can dissociate without the sialidase activity [308]. Blick et al. even showed that a zanamivir resistant virus incorporating an HA mutation that significantly impaired affinity required the presence of the drug for viral growth, because returning functionality of the NA shifts the balance to overwhelming sialidase activity and HA cannot effectively complete the receptor binding and entry process [309]. Similarly, when NA is inherently defective, growth can be rescued by adaption of HA [310-313]. Baigent et al. combined the study of HA glycosylation and NA stalk length, both characteristics found to change among transmission and adaptation, and illustrated a fine balance of the two modifications needed to sustain infection [146]. As suggested by many, the functional balance of HA and NA has implications for not only the general fitness of the virus, but also interspecies transmission and virulence [314, 315]. Though the need for functional balance has been well established, the timing of these interactions within the course of infection is still unknown. Studies specifically addressing the role of NA at the point of entry have revealed that NA activity could have an impact on the initiation of infection [316]. Novel techniques such as bio-layer interferometry have been developed and allow for measurement in real time of concurrent binding and enzymatic reactions to a sialic acid containing substrate [317]. Characterizing the interplay between the two proteins

during all stages of infection, from prior to entry to release after budding, will facilitate a better understanding of the broad processes of viral host interaction.

Dissertation Overview

This work begins an examination of entry by focusing on the roles of HA in fusion and receptor binding and expanding to a bigger picture of HA and NA balance and interaction with host carbohydrate structures. Starting with the latest stage of the entry process, we looked at the importance of certain HA residues for acid stability of a range of influenza A virus subtypes. Using a qualitative and quantitative assay for cell-cell fusion and expressed HAs, we were able to characterize the contribution of positions 58 and 112 within the fusion peptide pocket to maintaining the structural interactions that dictate the range of fusion pH for the subtypes tested. This aspect of the virus biology is important to ensure that fusion is triggered at the correct stage, in the lysosome and not before, and can be related back to differences in host and sites of infection. Prior to fusion, the HA mediates receptor binding, which as discussed, carries an arguably greater degree of species differentiation. We sought to examine the receptor binding characteristics of a panel of viruses of different hosts and subtypes to provide more detail to the dogma of avian viruses bind α2,3-Sia and human viruses bind α2,6-Sia. We did this using a synthesized glycan array from the Consortium of Functional Glycomics. Our findings revealed that structure beyond the sialic acid could be just as important of a receptor determinant as the sialic acid itself. The limitation to this approach is that though it tells us what can be bound, it provides little biological significance. To address this issue, we developed a natural shotgun array to look at actual natural endogenous

receptors. Using swine lung tissue, we extracted the N-glycans, O-glycan, and glycolipids and printed them to determine virus binding. The shotgun nature of the array relies on positive binding results to direct us to which glycan species to prioritize for sequencing and as such, we determined the structures for 8 ‘high binding’ N-glycans that are potential endogenous receptors for influenza A virus. Future directions we are pursuing rewind the process further, first examining the natural receptors found in human respiratory tract tissue and then characterizing the role that neuraminidase may have in and prior to receptor binding. This information will impart greater understand of the functional balance of HA and NA as well as the processes of entry, interspecies transmission and adaptation that are the prerequisites for a potentially devastating pandemic event.

INFLUENZA HEMAGGLUTININ (HA) STEM REGION MUTATIONS THAT STABILIZE OR DESTABILIZE THE STRUCTURES OF MULTIPLE HA SUBTYPES.

Lauren Byrd-Leotis, Summer E. Galloway, Evangeline Agbogu, David A. Steinhauer

The work in this chapter was published in 2015 in the Journal of Virology

Article citation: Byrd-Leotis, L., Galloway, S. E., Agbogu, E., & Steinhauer, D. A. (2015). Influenza hemagglutinin (HA) stem region mutations that stabilize or destabilize the structure of multiple HA subtypes. *Journal of Virology*, *89*(8), 4504–4516. http://doi.org/10.1128/JVI.00057-15

Abstract

Influenza A viruses enter host cells through endosomes, where acidification induces irreversible conformational changes of the viral hemagglutinin (HA) that drive the membrane fusion process. The pre-fusion conformation of the HA is metastable, and the pH of fusion can vary significantly amongst HA strains and subtypes. Furthermore, an accumulating body of evidence implicates HA stability properties as partial determinants of influenza host range, transmission phenotype, and pathogenic potential. Though previous studies have identified HA mutations that can affect HA stability, these have been limited to a small selection of HA strains and subtypes. Here we report a mutational analysis of HA stability utilizing a panel of expressed HAs representing a broad range of HA subtypes and strains, including avian representatives across the phylogenetic spectrum and several human strains. We focused on two highly conserved residues in the HA stem region, HA2 position 58 at the membrane distal tip of the short helix of the hairpin loop structure, and HA2 position 112, located in the long helix in proximity to the fusion peptide. We demonstrate that a K58I mutation confers an acid-stable phenotype for nearly all HAs examined, whereas a D112G mutation consistently leads to elevated fusion pH. The results enhance our understanding of HA stability across multiple subtypes and provide an additional tool for risk assessment for circulating strains that may have other hallmarks of human adaptation. Furthermore, the K58I mutants in particular, may be of interest for potential use in the development of vaccines with improved stability profiles.

Importance

The influenza A hemagglutinin glycoprotein (HA) mediates the receptor binding and membrane fusion functions that are essential for virus entry into host cells. While receptor binding has long been recognized for its role in host species specificity and transmission, membrane fusion and associated properties of HA stability have only recently been appreciated as potential determinants. Here we show that mutations can be introduced at highly conserved positions to stabilize or destabilize the HA structure of multiple HA subtypes, expanding our knowledge base for this important phenotype. The practical implications of these findings extend to the field of vaccine design, as the HA mutations characterized here could potentially be utilized across a broad spectrum of influenza subtypes to improve the stability of vaccine strains or components.

Introduction

Nearly every year, seasonal influenza A viruses contribute to hundreds of thousands of human deaths worldwide and place an extraordinary burden on health care systems and the global economy. Of even greater concern is the unpredictable appearance of antigenically novel influenza A strains in humans, with the potential for causing devastating pandemics. A major obstacle for controlling influenza is the diversity of influenza A strains that circulate in the avian species, as this provides a vast genetic pool of viral strains to which the human population is immunologically naïve [244]. Amongst viruses isolated from aquatic birds such as ducks and gulls, 16

antigenically distinct hemagglutinin (HA) subtypes and 9 neuraminidase (NA) subtypes have been identified to date, though over the past century only a small subset of these (H1N1, H2N2, and H3N2) have acquired the capacity to cross species barriers and subsequently establish lineages in the human population. However, there have been numerous examples of limited human infection or outbreaks of H5, H6, H7, H9, and H10 subtype viruses over the past several years [8, 187, 318-321]. Fortunately, such strains were not transmitted efficiently from human to human, but it will be critical to develop a broader understanding of the mechanisms involved in host adaptation, transmission, and pathogenicity of influenza viruses. These multifactorial traits have been genetically linked to a number of the eight gene segments depending on the viral strain, host system, or phenotypic readout utilized in any particular study; however, properties of the hemagglutinin often play a particularly significant role [318, 322-334]. The receptor binding characteristics of HA have long been associated with host specificity [29, 276, 335-338] but more recently, a greater appreciation has developed for the role of HA stability in transmission, adaptation, and pathogenicity phenotypes [49, 196, 279, 339-345].

HA stability phenotypes are intricately related to the pH at which the HA mediates endosomal membrane fusion during the virus entry process, and from a structural perspective, stability relates primarily to the post-cleavage neutral pH conformation of the HA trimer. HA is synthesized as a polyprotein precursor (HA0) that oligomerizes during biogenesis in the endoplasmic reticulum to form homotrimers. Cleavage of HA0 into the disulfide-linked HA1-HA2 subunits is required in order to activate virus infectivity [346-348], as this primes the membrane fusion potential of the

glycoprotein. Upon cleavage-activation, the newly generated hydrophobic N-terminus of the HA2 subunit (i.e. the fusion peptide) is relocated to the interior of the trimer, and this transitions the HA0 structure, which is relatively unresponsive to acidic pH, to a metastable conformation that can subsequently be triggered for membrane fusion activity by acidification of endosomes during virus entry [12, 47]. The conformational changes that accompany membrane fusion result in an energetically stable helical rod structure that relocates the fusion peptide from within the trimer interior, making it available for insertion into the endosomal membrane [48].

For natural isolates, HA subtypes can vary with regard to stability phenotypes as assayed by pH and temperature and cover a range of fusion pH and kinetics of inactivation [349, 350]. In the laboratory, cleaved HAs can be induced to undergo conformational changes at neutral pH by increasing temperature, and these changes are structurally analogous to those that are triggered by acidification [351-353] Furthermore, a direct correlation is demonstrated between fusion pH and temperature at which specific mutants are triggered (i.e. high pH mutants can be triggered at lower temperature) [351]. The differences in fusion pH may reflect the differences in the ecological and host environments in which the distinct subtypes evolve an optimal pH threshold for conformational change that balances the need for stability in the environment with the ability of the virion to uncoat in the endosome. A pH of fusion that is too high can lead to inactivation of the virion prior to receptor mediated endocytosis by the target cell, and one that is too low could lead to viral degradation before the fusion event can occur.

In addition to the potential role for HA stability in the ecology and transmission of influenza viruses, there could also be implications for viral strains to be utilized as

vaccine seed stocks or vaccine components. The issue of stability would be particularly relevant for live attenuated vaccines in regard to both the shelf life of the vaccine and the integrity of the vaccine post-vaccination. Incorporating a more stable HA could support vaccine durability during storage and transport. This increased stability would also enable the vaccine to withstand the natural barriers of the nasal cavity, including a reduced pH environment, prior to mediating infection of the nasal epithelial cells. [354-356].

In order to identify HA mutations that increase or decrease stability across a range of subtypes, we targeted two highly conserved residues in the stem region for further study, K58 and D112 of the HA2 subunit. These residues have been well characterized for H3 HAs, where K58I and D112G mutations are known to increase or decrease HA stability respectively, without compromising the structural integrity of the major antigenic regions [60, 174, 357, 358]. Here we report studies on the stability effects of K58I and D112G mutations introduced into a series of expressed HAs representative of both groups of the phylogenetic spectrum and all five clades. We examined the effects of these mutations by comparing their surface expression, cleavage-activation, and fusion characteristics with wild-type HAs of the same subtype, and we demonstrate that the K58I mutation increases HA stability, and the D112G mutation decreased HA stability, across a broad range of HA subtypes. Amongst the factors involved in risk assessment of circulating influenza A strains for pandemic potential, HA stability is one property that is poorly defined at present [333], and the identification of structural positions involved in HA stability for multiple subtypes should assist in the focus of this task. In addition, the data reported here provide a foundational backbone for vaccine designs and approaches that might benefit from more stable HA glycoproteins.

Materials and Methods

Cells and antibodies. Vero cells (ATCC CCL-81) were used for HA-plasmid transfection to analyze surface expression of wild type and mutant HA proteins. Vero cells were also used as effector cells for transfection of the HA containing plasmids for the quantitative cell-cell fusion assay, described below, and BSR-T7/5 cells (originally obtained from Karl-Klauss Conzelmann) served as the target cells. BHK-21 cells (ATCC CCL-10) were used for transfections of HA-plasmids to analyze fusion via syncytia formation, described below.

The antibodies utilized in this study were described previously [49]. Briefly, the following antibodies were obtained from BEI Resources: goat anti-H1, goat anti-H2, goat anti-$H2^{JAP}$, goat anti-H3, goat anti-H4, goat anti-H5, goat anti-H7, goat anti-H8, goat anti-H10, goat anti-H11, goat anti-$H1^{PR8}$, goat anti-$H5^{VN}$. We used a rabbit anti-X31 serum for detection of the Aichi HA.

*Plasmids***.** The wild-type HA expression plasmids have been described previously [49]. To introduce the 58I and 112G mutations, the wild-type HAs were PCR amplified from the expression plasmids and cloned into pCR-BLUNT, according to the manufacturer's recommendations. The resultant pCR-BLUNT plasmids were utilized as templates to introduce each mutation using the QuikChange methodology. Sequence-verified mutation-positive plasmids were subsequently utilized as a template for PCR using primers designed for ligation independent cloning (LIC), described previously [49]. Briefly, each mutant HA gene was amplified by PCR using a (+) sense primer having the 5' LIC specific flanking sequence of 5'TACTTCCAATCCATTTGCCACCATG, and a (-

) sense primer having the 5' LIC-specific flanking sequence of 5'TTATCCACTTCCATTTCTCA. In addition to the sequences shown, each primer had an additional 12-18 nucleotides of gene-specific sequence following either the start or stop codon. We utilized standard LIC procedures for the generation of each HA plasmid as described previously [49].

Radioactive labeling and Immunoprecipitation. Vero cells were transfected with 1ug of HA plasmid using Lipofectamine and Plus reagent (Invitrogen) according to the manufacturer's instructions. At 16-18 hours post transfection, HA expressing Vero cells were washed twice with PBS and incubated in MEM (- Met-Cys) at 37°C for 30 min. Cell proteins were exposed to a [^{35}S]-methionine pulse by the addition of 25 uCi [^{35}S]-methionine (Perkin Elmer) to the starvation media and incubated for 15 min at 37°C. The cells were then washed with PBS and incubated in complete growth medium supplemented with 20x cold methionine at 37°C for 3 hours. After the chase period, cells were washed once with PBS and treated with either DMEM or DMEM supplemented with 5ug/ml TPCK trypsin (sigma) at 37°C for 30 min. Where noted, surface proteins were biotinylated with 2 mg EZ-link Sulfo-NHS-SS-Biotin (Thermo scientific) in PBS, pH 8.0 at ambient temperature for 30 min. Following biotinylation, the cells were washed with PBS, pH 8.0 supplemented with 50mM glycine to quench the excess biotin. After a final PBS wash, cells were lysed with 0.5 ml RIPA buffer (50mM Tris-HCl, pH 7.4; 150mM NaCl; 1mM EDTA; 0.5% deoxycholate; 1% triton X-100; 0.1% SDS). Cell lysates were centrifuged at 16,000x g for 10 min to pellet cell debris and cleared lysates were harvested.

Protein G dynabeads (Invitrogen) were conjugated to HA-specific antibody in PBS+0.02% Tween-20 at room temperature for 30 min. The beads were then washed with the PBS+0.02% Tween 20 to remove unbound antibody from the solution. The harvested lysates were incubated with 50ul of Protein G dynabeads for 30 min at room temperature to pre-clear any non-specific binding. The pre-cleared lysates were then incubated with Protein-G/antibody complexes for 1 hour at room temperature. Protein-G/antibody/antigen complexes were wash 3x with PBS, resuspended in 35ul 1xSDS buffer, boiled for 5 min, and centrifuged so that the proteins could be separated from the beads and harvested.

For the precipitation of biotinylated proteins, Protein-G/antibody/antigen complexes were washed 3 times with PBS, resuspended in 50ul 50mM Tris-HCl+0.5% SDS, boiled for 5 min and centrifuged so that the bead eluate may be harvested. Of the 50 ul eluate, 25 ul was subsequently precipitated with Streptavdin M-280 Dynabeads (Invitrogen) to isolate cell-surface expressed HA and 25 ul was reserved to determine the total HA of the sample. 100ul of Streptavdin M-280 Dynabeads were washed three times with PBS+0.2%BSA and resuspended in 975ul Streptavidin binding buffer (20mM Tris-HCl, pH8.0; 150mM NaCl; 5mM EDTA; 1% Triton X-100; 0.2% BSA). The 25 ul of eluate was added to the Streptavidin Dynabeads/Streptavidin binding buffer mixture and incubated at room temperature for 1 hour. The unbound HA was then washed from the Streptavidin Dynabead/HA complex with 3 washes of PBS+0.2% BSA. The Streptavidin Dynabead/HA complex was resuspended in 35 ul 1x SDS sample buffer, boiled for 5 min and the bead eluate was harvested. For gel analysis, the 10ul of 3x SDS sample buffer was added to the 25ul total HA sample for a final volume of 35ul.

For gel analysis, 20ul of each sample was resolved on a 12% SDS-PAGE. The gels were fixed with 50% methanol/10% acetic acid solution for 30 min at room temperature and fixed gels were dried under a vacuum for 1 hour at 80°C prior to exposure on a phosphorimaging screen. Phosphor screens were scanned on a Typhoon Trio variable mode imager (GE Healthcare Life Sciences). The intensity of the bands corresponding to HA0, HA1, or HA2 was determined using the ImageQuant software, normalized to methionine content of the appropriate subunit. For analysis of cell surface expressed HA and comparison of wild-type and mutant levels, the total level of HA in each lane was quantified and the amount of surface expressed HA was determined by the following equation, (cell surface HA/ total HA) x100 and then the percent relative to wild-type surface expression was calculated as ((% surface expression mutant HA/% surface expression WT HA) x100). Percent Cleavage was determined using the equation (Ha2/(Ha2+Ha0)) x100% and the percent cleavage relative to wild-type calculated as ((% cleavage mutant HA/% cleavage of WT) x100).

*Fusion Assays***.** HA mediated membrane fusion was examined using a quantitative cell-cell fusion luciferase reporter assay and a qualitative syncytia assay. For the luciferase reporter assay, Vero cells, the effector cells, were transfected with 1 ug of HA plasmid and 1 ug of plasmid containing a firefly luciferase gene under control of a T7 bacteriophage promoter using Lipofectamine and Plus reagent (Invitrogen). 16-18 hours post transfection, the HA expressing cells were washed with PBS and were treated with DMEM+ 5ug/ml TPCK trypsin for 30 minutes and then were washed once more with PBS and treated with DMEM +20ug/ml trypsin inhibitor for 30 min. The Vero cells were then overlaid with the target BSR-T7/5 cells that constitutively express bacteriophage T7

RNA polymerase. The Vero cells plus the BSR-T7/5 overlay were incubated at 37° for 1 hour to allow the BSR-T7/5 cells to adhere to the Vero monolayer. Following this incubation, the plates were washed gently with PBS. The cells were exposed to PBS that had been pH adjusted with 100mM citric acid to the requisite pH and incubated at 37°C for 5 min. At the conclusion of the pH pulse, the pH adjusted PBS was removed and complete growth media was added to neutralize the reaction. The cells were incubated at 37°C for 6 hours to allow for the fusion of the effector and target cells and to mediate the transfer and expression of the T7 luciferase plasmid for the generation of luciferase protein. The cells were washed once with PBS and then lysed with 0.5 ml of Reporter Lysis Buffer (Promega). The cell lysates were frozen for up to 16 hours and then, upon thawing, were centrifuged at 15,000 x g at 4°C to remove debris. 150 ul of the clarified lysate was transferred to a 96-well plate (white, polystyrene, Corning) and the luciferase activity resulting from successful fusion of the target and effector cells was quantified using a BioTek Synergy 2 Luminomter, using 50 ul of luciferase assay substrate (Promega) injected into each well.

For the qualitative syncytia assay, BHK-21 cells were transfected with 1ug plasmid-HA using Lipofectamine and Plus reagent (Invitrogen). 16-18 hours post transfection, HA expressing cells were washed with PBS and treated with 5ug/ul TPCK Trypsin (Sigma) in serum-free DMEM for 15 min at 37°C. The trypsin-treated HA expressing cells were exposed to PBS that had been pH adjusted with 100mM citric acid and incubated at 37°C for 5 min. At the conclusion of the pH pulse, the pH adjusted PBS was removed and the HA expressing cells were neutralized by the addition of complete growth medium and incubated for 2 hours at 37°C to allow syncytia to form. The cells

were then stained with the Hema3Stat Pak according to manufacturer's instruction. Syncytia were visualized and photographed using a Zeiss Axio Observer inverted microscope with attached digital camera.

Results

Viral strains, mutagenesis, cloning, and expression

For our mutagenesis studies, we utilized cloned HA genes derived from WHO reference strains for our complement of avian HA subtypes, a selection of H1, H2, and H3 subtype HA genes from human isolates, a lab-adapted H1N1 vaccine strain, and a well characterized H5N1 isolate (Table 1). These strains were chosen in order to sample a wide distribution of host species, dates and geographic locations of virus isolation, and subtypes that span the range of all phylogenetic clades (Figure 1).

Table 1. Origin of HA subtype proteins

Origin	Subtypes	Strain name	17 mutation	111 mutation
Group 1				
Avian	H1N1	A/duck/Alberta/35/1976	Y17H	H111A
Avian	H5N3	A/tern/South Africa/1961	Y17H	H111A
Avian	H8N4	A/turkey/Ontario/6118/1968	Y17H	H111A
Avian	H11N6	A/duck/England/1/1956	Y17H	H111A
Human	H1N1	A/Puerto Rico/8/1934	Y17H	H111A
Human	H1N1	A/California/04/2009	Y17H	H111A
Human	H2N2	A/Japan/305/1957	Y17H	H111A
Human	H5N1	A/Vietnam/1204/2004	Y17H	H111A
Group 2				
Avian	H3N8	A/duck/Ukraine/1/1963	H17Y	T111H
Avian	H10N7	A/chicken/Germany/N/1949	H17Y	T111H
Human	H3N2	A/Aichi/2/1968	H17Y	T111H

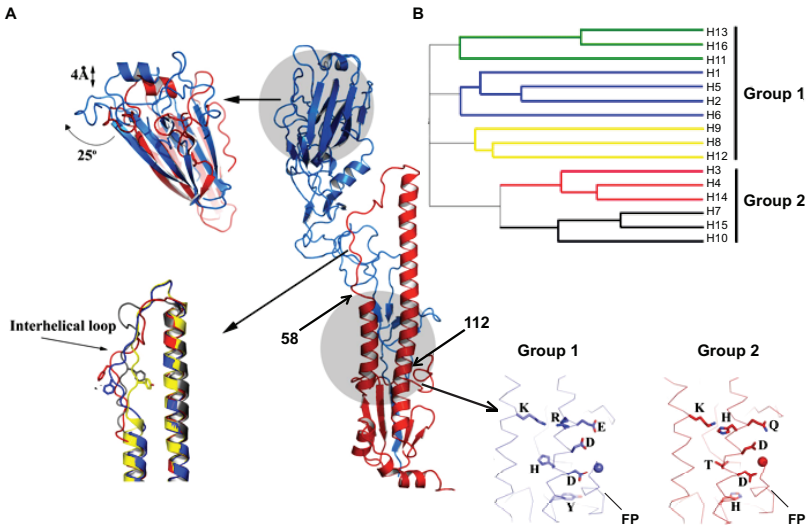

Figure 1. (A) The H3 subtype monomer is shown in the central panel with HA1 depicted in blue and HA2 in red. The structural locations of HA2 K58 and HA2 D112 are indicated. In the upper left region of the figure, the head domains corresponding shaded portion of the monomer are shown, with the H3 head domain (blue) superimposed on the H1 (red). The depiction indicates the higher location relative to HA stems for the H1 subtype, and the "twist" in rotational symmetry. The lower left panel shows the HA2 hairpin structures of representatives of four of the five clades superimposed on one another, and demonstrates that all are very similar in the long helix domain, but vary in structure for the connecting peptide and top of the short helix (color-coded to match panel B). The bottom right panels correspond to the lower shaded region of the monomer structure, and highlight both highly conserved residues and those that segregate in group-specific fashion. HA2 K51, D109, and D112 (top to bottom) are highly conserved, whereas HA2 R/H106, E/Q105, H/T111, and HA1 Y/H17 are conserved within groups. FP indicates the HA2 N-terminal fusion peptide domain, and the spheres denote the HA2 N-terminal glycine residue. (B) This panel shows a phylogenetic tree of the 16 subtypes that circulate in avian species, with the subtypes belonging to Group-1 and Group-2 indicated and the five clades color-coded to designate those subtypes more closely related by sequence and structure.

The codons for HA2 mutations K58I and D112G were introduced individually into the parental WT HA genes by site-directed mutagenesis, and cloned into a pCAGGS vector for mammalian cell expression under the control of the CMV immediate early promoter. Cells were transfected with these HA expression vectors for all experiments described below addressing HA transport to the plasma membrane, cleavage activation of membrane fusion potential, and the pH at which HA-mediated fusion is activated.

Levels of cell surface expression were determined for WT, K58I or D112G HAs by surface biotinylation of expressing cells, followed by immune precipitation with specific antisera. Figure 2 summarizes the results for surface expression of mutant HAs for three or more replicate experiments for each mutant, which we present as the percent surface expression relative to the corresponding wild-type HA. All WT and mutant HAs were found to express on cell surfaces, with an overall range of expression levels comparable to those published previously for mutants HAs [67, 358, 359]. H5 and H7 subtypes are cleaved by endogenous proteases so both the cleaved and the uncleaved forms of HA are detectable in the surface expression assay (Figure 2B).

Cleavage activation of membrane fusion potential

The membrane fusion potential of WT HA for all subtypes examined here can be activated by trypsin cleavage of expressed HA0 into HA1 and HA2 [49]. To address any possible effects that the 58I or 112G mutations might have on cleavage activation, the degree to which exogenous trypsin processed HA0 into HA1 and HA2 was examined. Pulse-chase experiments were carried out with HA-expressing cells using [^{35}S]-methionine, and monolayers were incubated with trypsin (or media), followed by immune precipitation of cell lysates with specific anti-sera and analysis by SDS-PAGE. As shown in Figure 2B and 3, all mutant HAs were cleaved by trypsin or endogenous proteases, with distinct cleavage products corresponding to the HA1 and HA2 subunits. The cleavage efficiency of the mutant HAs was calculated and expressed as the percent cleavage relative to the wild-type HA (Figure 2B, Figure 3). Though a range of cleavage efficiencies were observed amongst the mutant HAs, previous studies on expressed HAs

of multiple subtypes suggest that even HAs in the lower end of these ranges are cleaved sufficiently to mediate membrane fusion activity [49].

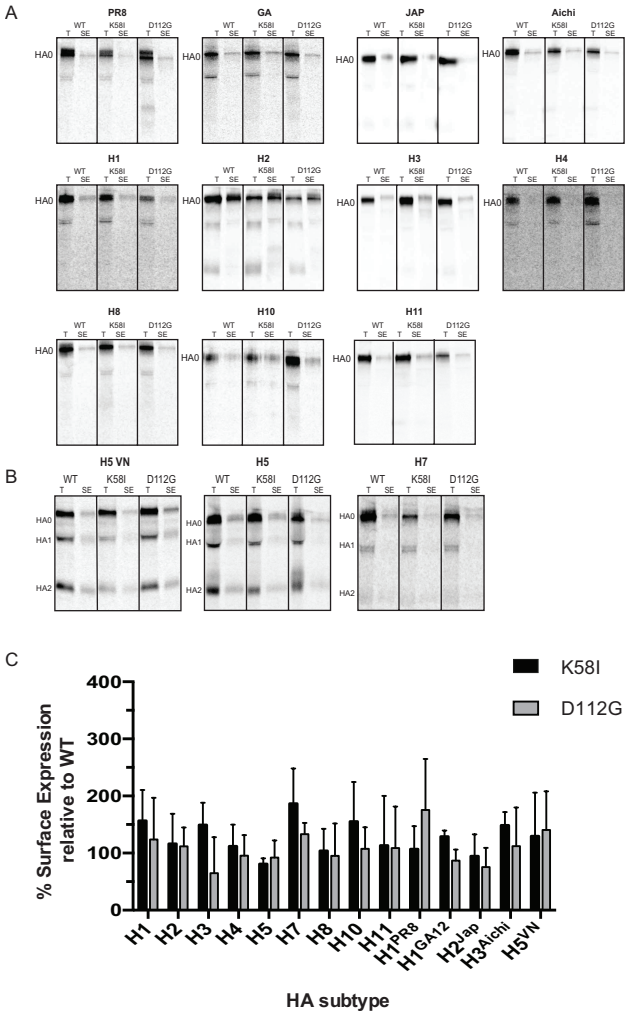

Figure 2. Surface expression of WT and mutant HAs. Radiolabeled, cell surface proteins were biotinylated and precipitated with a HA-specific antibody and then streptavidin where indicated (SE), and resolved by SDS-PAGE. Lanes are denoted T for total HA and SE for surface expressed. (A) Gel images for human and avian subtypes are shown. (B) Gel images for $H5^{VN}$, H5, and H7 are shown. These HAs are expressed in both cleaved and uncleaved forms due to endogenous proteases. (C) Quantitation of the surface expression of mutant HA relative to WT HA. For each WT and mutant HA, the intensity of the bands corresponding to HA0 +streptavidin and HA0 -streptavidin were normalized based on methionine content. Percent surface expression was determined using the following equation (cell surface HA/ total HA)x100 and then the percent relative to wild-type surface expression was calculated as ((% surface expression mutant HA/% surface expression WT HA)x100). Error bars represent the standard deviation of three independent experiments.

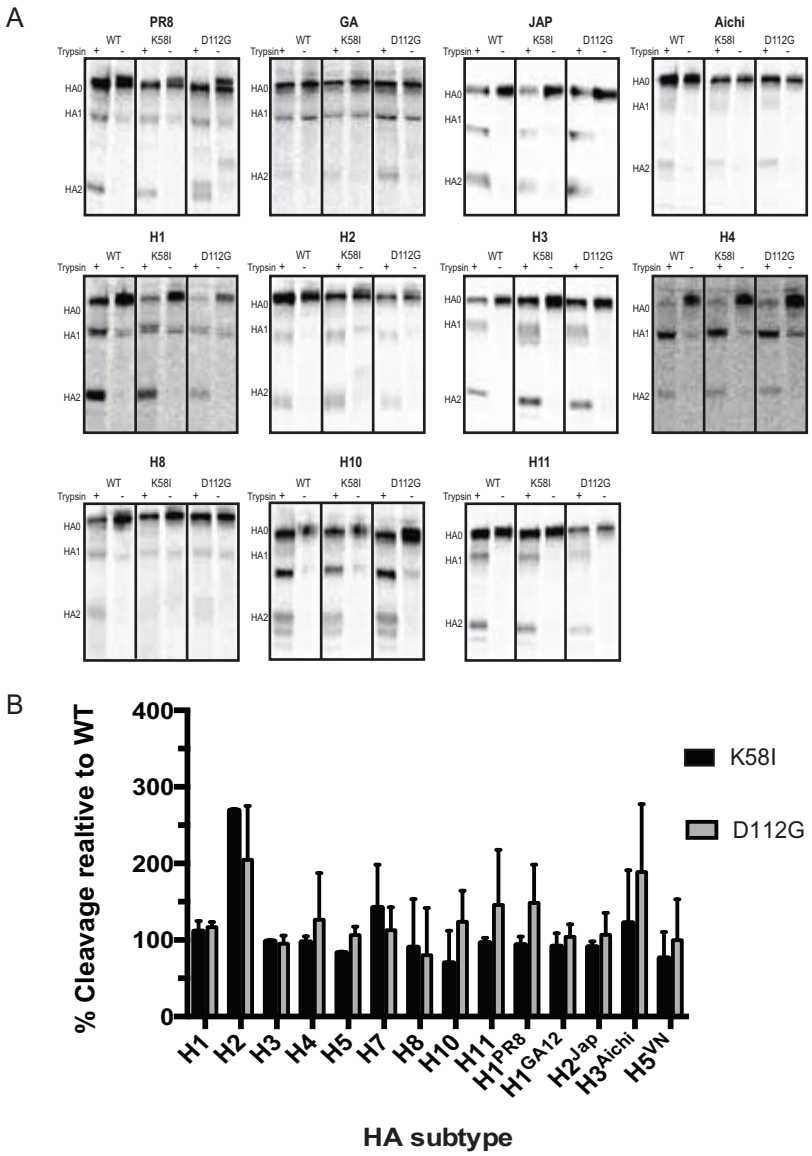

Figure 3. Analysis of proteolytic cleavage of WT and mutant HAs. Radiolabeled, HA-expressing cells were treated with 5ug/ml TPCK trypsin, where indicated. Total cellular HA protein was precipitated from the lysate with a HA-specific antibody and resolved by SDS-PAGE. (A) Gel images for human and avian subtypes are shown. (B) Quantitation of trypsin-mediated cleavage of mutant HA relative to WT HA. For each WT and mutant HA, the intensity of the bands corresponding to HA0 and HA2 were normalized based on methionine content. For the $H5^{VN}$, H5, and H7 subtypes, the cleavage values were determined from the total HA lanes of the surface expression gels shown in Figure 2B. Percent Cleavage was determined using the equation (Ha2/(Ha2+Ha0))x100% and the percent cleavage relative to wild-type calculated as ((% cleavage mutant HA/% cleavage of WT)x100). Error bars represent the standard deviation of three independent experiments.

Membrane fusion pH of mutant HAs by syncytia formation

In order to examine the effects of the 58I and 112G mutations on the fusogenic properties of HA, we employed a qualitative syncytia based fusion assay. BHK cells were transiently transfected with an HA expression plasmid, treated with trypsin (except for H5 and H7 HAs), and subsequently exposed to low pH buffer, and then neutralized. The cells were then incubated for two hours in standard media (during which time syncytia were allowed to form), fixed, stained, and visualized by light microscopy. The pH of fusion was defined as the highest pH value at which extensive syncytia can be detected across multiple fields. Representative photomicrographs are shown in Figure 4.

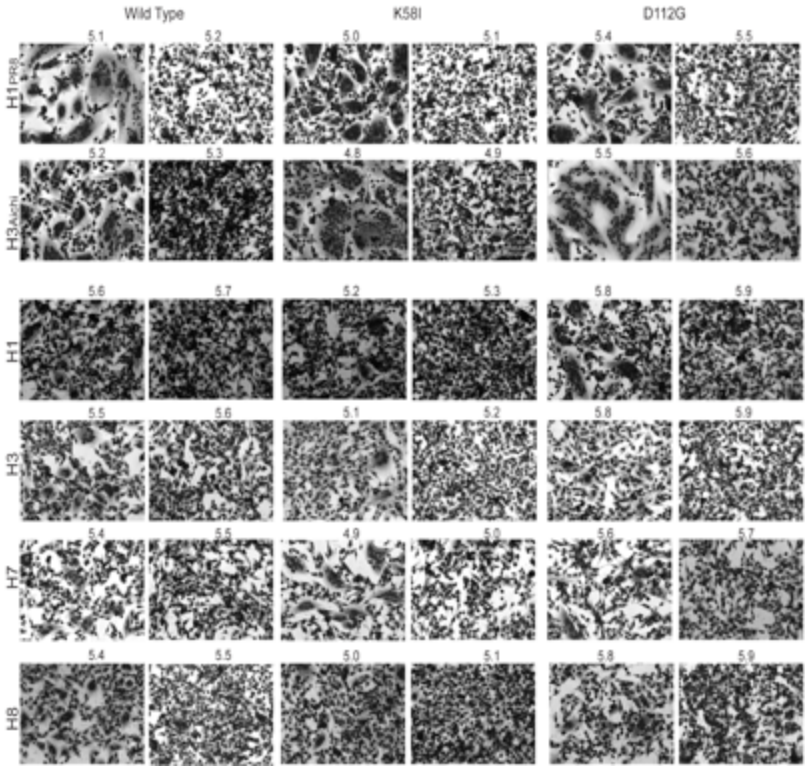

Figure 4. The pH of fusion as detected by syncytia formation. Photomicrographs of syncytia formation assays for Group 1 and Group 2 as well as human and avian representative HAs are shown. HA-expressing BHK cells were treated with TPCK trypsin (5 ug/ml) and exposed to pH adjusted PBS in 0.1 pH unit increments. Photomicrographs corresponding to the highest pH at which syncytia were observed and then 0.1 pH unit higher are shown.

All HAs that were expressed on cell surfaces and cleaved into HA1 and HA2 by trypsin (or endogenous proteases for H5 and H7 HAs) were observed to mediate syncytia formation. In nearly all examples, the K58I mutation led to a lower pH of fusion and the

D112G mutation conferred a high pH phenotype relative to the respective WT HA (Figure 5, Table 2).

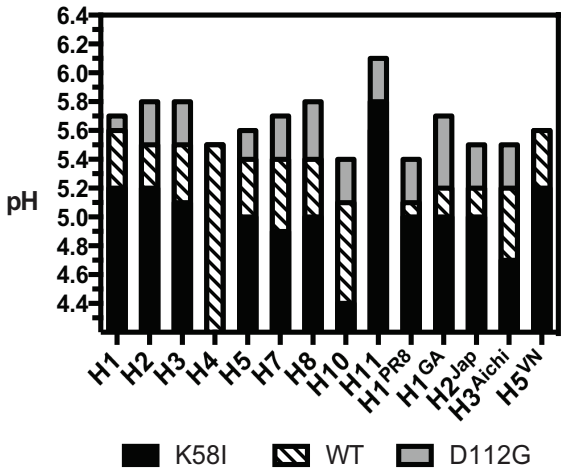

Figure 5. Syncytia formation assay results for all HA subtypes tested. The substitution H4-K58I did not produce syncytia; the H4-D112G did mediate fusion in the syncytia assay though there was no pH difference between WT and D112G (5.5). H11-K58I (pH 5.8) resulted in a higher pH of fusion that the WT H11 (pH 5.6). $H5^{VN}$-D112G did mediate fusion, however the pH of fusion was not higher than WT (5.6).

Membrane fusion pH of mutant HAs by quantitative luciferase assay

We also analyzed fusion activity and compared the fusion pH of WT and mutant HAs using a more quantitative luciferase-based assay. This luciferase reporter gene assay provides a numerical measurement that corresponds to fusion, in which fusion is quantified based on the transfer and subsequent expression of a plasmid encoding firefly luciferase under the control of the T7 bacteriophage promoter from Vero cells to BSR-T7/5 target cells [49, 359]. Assays were carried out using low pH increments of 0.2 pH units, bracketed based on preliminary results and data from the syncytia assays. The luminescence associated with each pH value tested was determined and the pH of fusion was defined as the highest pH value displaying luminescence, after correction by subtracting the value obtained from mock transfected samples or that of the highest pH well (Figure 6).

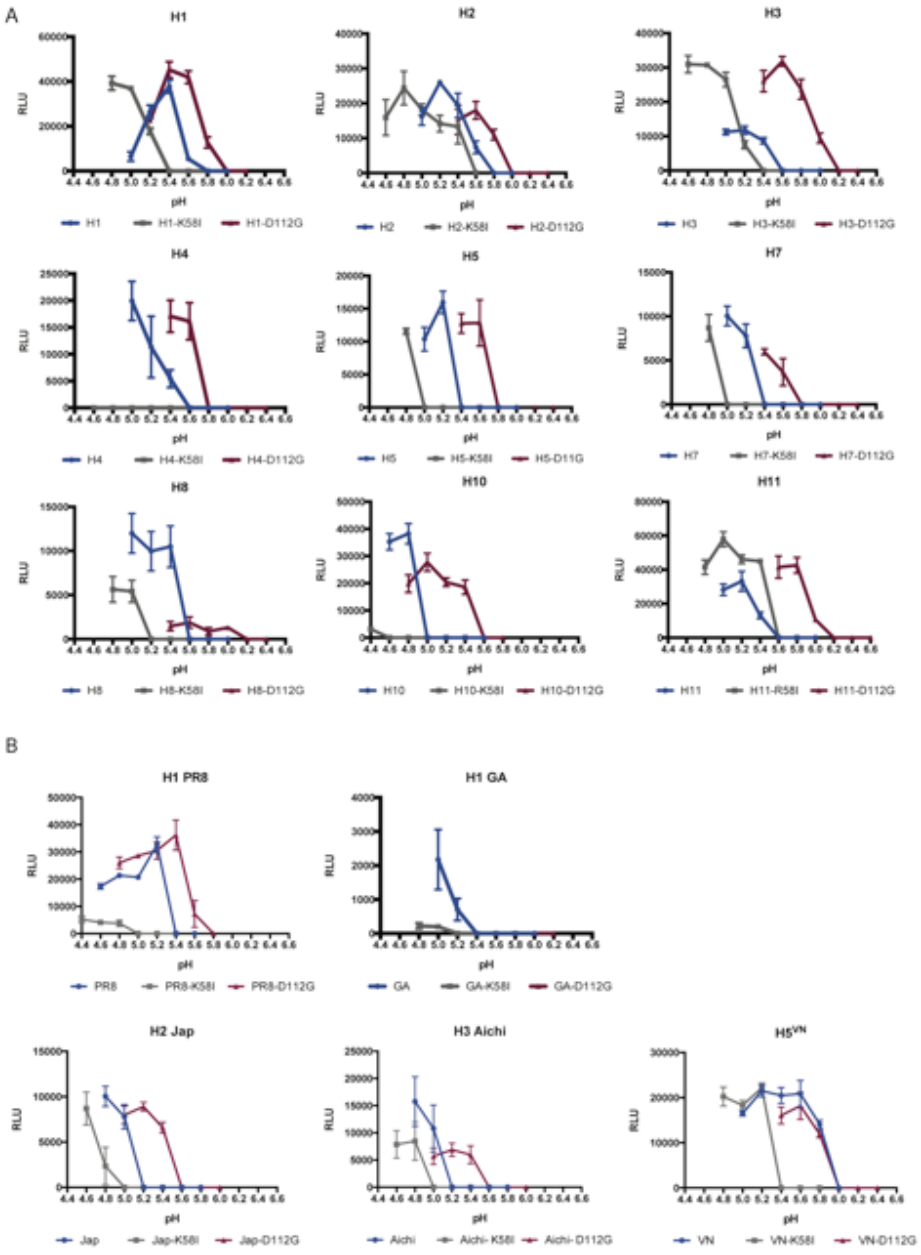

Figure 6. The pH of fusion as detected by the Luciferase reporter gene assay. HA-expressing Vero cells transfected with T7-luciferase plasmid were treated with TPCK-trypsin (5ug/ml) followed by C. soybean trypsin inhibitor (20ug/ml) and then overlaid with BSR-T7/5 target cells that constitutively express T7 RNA polymerase. The mixed cell population was exposed to pH-adjusted PBS in 0.2 pH unit increments and was incubated for 6 hrs at 37°C to allow for cell-to-cell fusion and content mixing leading to expression of firefly luciferase to occur. Luminescence was measured as an indicator of membrane fusion in cell lysates. The graphs show the background-adjusted luminescence. Error bars represent the standard deviation of triplicate experiments. (A) Avian origin HA subtypes. (B) Human origin HA subtypes. No fusion was detected for the $H1^{GA}$ –D112G HA.

The data from the luciferase assay supports the results from the syncytia assay in all examples (Table 2).

Table 2. Fusion pH of wild-type and mutant HAs

Subtype	Wild Type		K58I				D112G			
	Luciferase	Syncytia	Luciferase	ΔpH	Syncytia	ΔpH	Luciferase	ΔpH	Syncytia	ΔpH
H1	5.6	5.6	5.2	**-0.4**	5.2	**-0.4**	5.8	**+0.2**	5.7	**+0.2**
H2	5.6	5.5	5.4	**-0.2**	5.2	**-0.3**	5.8	**+0.2**	5.8	**+0.3**
H3	5.4	5.5	5.2	**-0.2**	5.1	**-0.4**	6.0	**+0.4**	5.8	**+0.3**
H4	5.4	5.5	ND	**ND**	ND	**ND**	5.6	**+0.2**	5.5	**0.0**
H5	5.4	5.4	4.8	**-0.6**	5.0	**-0.4**	5.6	**+0.2**	5.6	**+0.2**
H7	5.2	5.4	4.8	**-0.4**	4.9	**-0.5**	5.6	**+0.4**	5.7	**+0.3**
H8	5.4	5.4	5.0	**-0.4**	5.0	**-0.4**	6.0	**+0.6**	5.8	**+0.4**
H10	4.8	5.1	4.4	**-0.4**	4.4	**-0.7**	5.4	**+0.6**	5.4	**+0.3**
H11	5.6	5.6	5.8	**0.2**	5.8	**0.2**	6.0	**+0.4**	6.1	**+0.5**
$H1^{PR8}$	5.2	5.1	5.0	**-0.2**	5.0	**-0.1**	5.6	**+0.4**	5.4	**+0.3**
$H1^{GA12}$	5.2	5.2	5.0	**-0.2**	5.0	**-0.2**	ND	**ND**	5.7	**+0.5**
$H2^{Jap}$	5.0	5.2	4.8	**-0.2**	5.0	**-0.2**	5.4	**+0.4**	5.5	**+0.3**
$H3^{Aichi}$	5.0	5.2	4.8	**-0.2**	4.7	**-0.5**	5.4	**+0.4**	5.5	**+0.3**
$H5^{VN}$	5.8	5.6	5.2	**-0.6**	5.2	**-0.4**	5.8	**0.0**	5.6	**0.0**

ND- no data available. HA designations from strains in Table 1: PR8 - A/Puerto Rico/8/1934; GA - A/Georgia/F322551/2012; JAP - A/Japan/305/1957; Aichi - A/Aichi/2/1968; VN - A/VietNam/1204/2004

Taken together, the two assays demonstrate that the HAs containing the D112G mutation raise the pH of fusion for nearly all subtypes and strains examined, with most displaying

fusion activity between 0.2 and 0.5 pH units higher than WT HA, depending on the subtype. This result is consistent with previous observations on D112G mutants, and supports a role for the stabilizing effects of hydrogen bonds formed between the highly conserved aspartic acid side chain of D112 and the HA fusion peptide [175, 357]. One exception involved the $H5^{VN}$ isolate HA, for which the D112G mutation appeared to have no effect on the pH of fusion. The $H1^{GA}$ isolate HA containing the D112G mutation demonstrated an increase of the fusion pH of 0.5 pH units in the syncytia assay but did not mediate fusion in the luciferase assay. Also, the H4 subtype HA demonstrated only a moderate increase in fusion pH of 0.2 based on the luciferase assay, and no difference to WT HA was observed by syncytia formation.

Conversely, the K58I mutation lowered the pH of fusion by 0.2-0.5 pH units for all of the HA subtypes examined with the exception of H11. The H11 subtype is unique amongst the HA subtypes, as it is the only one encoding an arginine rather than lysine at the otherwise invariant HA2 position 58. For the H11 subtype, the pH of the wild-type HA was measured to be 5.6 while the pH of the H11-R58I HA was measured to be 5.8. Fusion was undetectable for the H4-K58I mutation in both the syncytia and the luciferase-based assay.

Discussion

The phenotypic characteristics of the influenza A HA glycoprotein play an important role in the process of virus adaptation to varied hosts and ecological niches, and the capacity to modify the stability of HA constitutes one mechanism for adaptation to dynamic environmental pressures. As a general concept, viral envelope components and capsids must evolve a degree of stability sufficient to protect their genomes as they transmit between hosts, yet maintain the capacity to uncoat in response to specific stimuli when appropriate cells at sites of infection are encountered in a new host. For influenza A viruses, the HA-mediated endosomal uncoating process is generally triggered at a pH between 5.0 and 6.0, depending on the viral strain, whereupon the metastable HA structure undergoes irreversible transitions to a highly stable conformation to induce fusion of the viral and endosomal membranes. However, the irreversible HA conformational changes associated with fusion can also be induced by environmental factors such as temperature, resulting in the inactivation of virus infectivity. The broad ecological distribution of influenza A viruses, and the diversity of avian and animal species that act as hosts, require that HA maintain an appropriate balance with respect to stability properties, and be capable of modulating these properties to adapt to different hosts, modes of transmission, or environmental niches.

H5N1 viruses have received particular attention over the past several years, and evidence is accumulating to demonstrate that HA stability can influence replication and pathogenicity characteristics within particular hosts, as well as adaptation and transmission phenotypes. An optimal range of fusion pH can be demonstrated as a

determinant of adaptation and host specificity with avian viruses generally exhibiting a higher activation pH than mammalian strains, presumably corresponding to differences in the sites of infection within these host species. Studies with an avian H5N1 in chickens and ducks reveals an optimal pH range of 5.6-6.0 and an increase in pathogenicity corresponding to an increase in the pH of fusion [339, 340], whereas an avian H5N1 studied in mice exhibits an optimal pH of fusion below 5.6 suggesting adaptation of the avian strain to the mammalian host [360]. HA stability and fusion pH were also implicated as potential determinants for aerosol transmission of H5N1 strains in the ferret model [196, 279, 341].

It would appear likely that observations made with H5 viruses regarding the biological impact of HA stability properties will translate to other subtypes as well. Sequence alignment and structural characterization of the HAs from the 16 influenza A subtypes (excluding the H17 and H18 bat viruses), support the idea that evolutionary pressure operates at the level HA stability and/or membrane fusion properties. The HA subtypes can be segregated into five clades that assemble into two groups (Group-1 and Group-2; Figure 1), and while structural comparison of neutral pH cleaved HAs demonstrates a general degree of similarity, structural distinctions are revealed in regions of the molecule that are rearranged during the fusion process. One difference involves the extended polypeptide chain, that links the long and short helices of HA2, which rearranges during fusion to become part of the post-fusion helical rod structure [48]. Compared to Group-2 HAs, Group-1 HAs contain an extra half turn of the short helix that orients the linking peptide into closer proximity to the long helix, and as the chain traces towards the top of the long helix it forms a “taller” hairpin loop. As a result, the

membrane distal head domains of Group-1 HAs are positioned about 4Å “higher” on the stem domains relative to Group-2 HAs. The head domains, which de-trimerize during fusion, also vary amongst the subtypes by up to 35° with respect to rotational symmetry along the three-fold axes [186, 361]. In addition, group-specific differences are observed in a cluster of residues in close proximity to the fusion peptide in the cleaved, neutral pH structures, a region that is potentially involved in initial triggering of the acid-induced conformational changes, as fusion peptide residues are expelled from the trimer interior prior to being directed toward the target membrane (Figure 1).

The structural locations of HA mutations that influence HA stability have been most extensively studied for the HA of H3 subtype viruses, and can map to positions throughout the HA trimer but concentrate at the interfaces of domains that relocate during fusion [175, 362, 363]. The locations of such mutations are often coincident with the residues and domains defined as variable by the structural comparison of HA subtypes discussed above, but there are few studies that have compared the stability phenotypes of mutant HAs across subtypes. In this report, we focused on two such mutants at positions that are highly conserved amongst influenza A HAs. HA2 residue 58, a lysine in all HA subtypes with the exception of H11 (R58), resides in the region of the membrane distal end of the small α-helix where it meets the extended polypeptide linked to the long helix (Figure 1). As noted above, the small helix of Group-1 HAs is extended by a half turn relative to Group-2 HAs, and in Group-1 structures residue 58 lies within the helix, and the lysine side chain orients towards the trimer interior and interacts with the glutamic acid side chain of conserved residue 97 in the long helix. In Group-1 HAs the short helix contains a serine or glutamine at residue 54, whereas Group-2 HAs contain a group-

specific arginine at position 54, which interacts with the glutamic acid at position 97 of the long helix. As a consequence, the K58 side chain of Group-2 HAs is oriented into solution and the helix is shorter by half a turn. With regard to HA2 residue 112, aspartic acid at this position is completely conserved among all HA subtypes. It is located on the long alpha helix of HA2 and, in the pre-fusion conformation of HA, is buried within the trimer interior. Here it forms several H-bond contacts with residues 3, 4, 5, and 6 of the fusion peptide to stabilize the pre-fusion conformation. When glycine is substituted for aspartic acid, a water molecule occupies the space where the side chain resides in the WT HA, and a weaker network of H-bonds with the fusion peptide are probably responsible for the less stable phenotype [357]. As the HA2 58 region differs in Group-1 and Group-2 HAs, and the region encompassing the HA2 residue 112 contains a number of group-specific ionizable residues that have the potential to influence HA stability (Figure 1), the phenotypes of mutant HAs at these positions were not entirely predictable.

The data presented here show that all mutant HAs were capable of proper folding and transport to cell surfaces. For all surface expressed HAs, trypsin or endogenous proteases were able to activate fusion potential by appropriate cleavage into HA1 and HA2, and all cleaved, surface-expressed HAs demonstrated acid-induced membrane fusion activity. For all of the D112G mutants except the H5 HA of A/Vietnam/1204/04 virus, the mutation caused an elevated pH of fusion relative to the WT HA. This is consistent with results of Russell and colleagues, who observed no change in fusion pH for this mutant HA even though conformational changes could be detected at higher pH than fusion activity [359]. It should be noted that the D112G mutant of H5 HA of A/Tern/South Africa/61 virus (H5N3) showed a higher fusion pH than its parental WT,

similar to all other D112G mutants examined here. For the HAs with the K58I mutation, all that were expressed on cell surfaces displayed an acid-stable phenotype with the exception of the H11 subtype HA, which is the only HA subtype containing arginine rather than lysine at HA2 position 58 in the WT virus (A/Duck/England/56). This H11 HA is also unusual in that it has glutamine rather than glutamic acid at position 97, possibly altering the interactions between the long and short helices of HA2. However, other than the H11 example, the consistent acid-stable phenotype of K58I HAs across the phylogenetic spectrum is interesting, since Group-1 and Group-2 HAs deviate in structure in the region of HA2 58. This is also the region where the group-specific antiviral compound TBHQ binds, and its mode of action has been proposed to involve fusion inhibition due to the stabilization of neutral pH HA during acidification [364, 365]. The direct interpretation of the stabilizing effects of the K58I mutations will require structural characterization of such HAs at high resolution. Generally, the stabilizing K58I HAs were expressed at higher levels on cell surfaces, whereas the D112G HAs more frequently displayed reduced cell surface expression. Overall, the results reported here are consistent with the limited data on the equivalent mutations in other subtypes [174, 359]. The accumulation of data on stability mutants across HA subtypes may provide useful information for identifying viruses with potential for host range adaptation or other biological properties such as transmission and pathogenicity.

The mutant HAs containing K58I, with increased stability properties, could also prove useful as components of influenza vaccines with greater shelf life or as reagents utilized for vaccine assessment. Stability is an issue of universal concern, both for the shelf life of a new vaccine and for the stability of the vaccine particle within the

vaccinated host. For influenza viruses, the problem is even more acute as the viral vaccine strains are frequently changed to reflect the circulating strains and subtypes, and the necessity of a quick turnaround prevents extensive temporal studies on stability and shelf life of the vaccine. Therefore replication characteristics and inherent HA stability, as well as antigenic properties, may be factors to consider for vaccine candidates [356, 366]. Recent experiences with live attenuated vaccine strains of H5N1 viruses, as well as H1N1 pandemic strains, highlight the potential problems associated with vaccine stability and potential solutions that might involve the use of HAs with greater stability to pH and temperature dynamics. For example, inefficient replication properties and immunogenicity of live attenuated candidate H5N1 vaccines [367] were improved by the introduction of the K58I acid-stable HA that we address in the current studies [368]. Similarly, live attenuated vaccine candidates of pandemic H1N1 strains were less immunogenic when 2009 strains from early in the outbreak were utilized, compared to subsequently circulating strains. The critical genetic factor was identified as an HA stalk region HA2 E47K mutation that increased the HA stability of the stains that circulated in the years that followed the initial outbreak [369]. An advantage of stabilizing vaccine candidates using HA stalk mutations is that they would be unlikely to alter the major antigenic sites located on membrane distal HA head domains. Indeed, for the H3 subtype HAs, the K58I mutant and other stalk region mutations have been well characterized for recognition by a wide panel of conformation-specific monoclonal antibodies that target several of the antigenic regions of HA; and in nearly all cases, the mutations have no effect on the antigenic properties of mutant HAs [60, 174, 358]. Acid-stable HAs could also prove useful for improving inactivated vaccines and those based on expressed

recombinant proteins, as these would be less susceptible to HA degradation [370, 371], and the expression and purification of bromelain-released HA ectodomains can prove problematic for HAs with elevated fusion pH phenotypes [60, 372]. Therefore incorporation of stabilizing mutations such as K58I might prove useful to improve yield or shelf life of HAs whether such reagents were to be utilized for vaccine purposes, for generating analytical sera, or assessing immune responses to new vaccine candidates and is broadly applicable to a wide range of subtypes across the phylogenetic spectrum of influenza A viruses.

Acknowledgments

This work was supported by the U.S. Department of Health and Human Services contract HHSN272201400004C (NIAID Centers of Excellence for Influenza Research and Surveillance). We thank members of the Steinhauer lab for their advice and constructive discussions of this work. We also thank Anice Lowen and Robert Berris (Children's Healthcare of Atlanta) for providing the A/Georgia/F32551/2012 (H1N1) clinical isolate; BEI resources for providing several anti-HA antibodies utilized in this study; Konrad Bradley for generating the $H5^{VN}$ subclone; Julia Sobolik for technical assistance.

SHOTGUN GLYCOMICS OF PIG LUNG IDENTIFIES NATURAL ENDOGENOUS RECEPTORS FOR INFLUENZA VIRUSES

Lauren Byrd-Leotis, Renpeng Liu, Konrad Bradley, Yi Lasanajak, Sandra F Cummings, Xuezheng Song, Jamie Heimburg-Molinaro, Summer E. Galloway, Marie Culhane, David F. Smith, David A. Steinhauer, Richard D. Cummings

The work in this chapter was published in 2014 in the Proceedings of the National Academy of Sciences

Article Citation: Byrd-Leotis*, L., Liu*, R., Bradley, K. C., Lasanajak, Y., Cummings, S. F., Song, X., et al. (2014). Shotgun glycomics of pig lung identifies natural endogenous receptors for influenza viruses. *Proceedings of the National Academy of Sciences*, *111*(22), E2241–E2250. http://doi.org/10.1073/pnas.1323162111
*Authors contributed equally to this work.

Abstract

Influenza viruses bind to host cell surface glycans containing terminal sialic acids, but as studies on influenza binding become more sophisticated it is becoming evident that though sialic acid may be necessary, it is not sufficient for productive binding. To better define endogenous glycans that serve as viral receptors, we have explored glycan recognition in the pig lung, as influenza is broadly disseminated in swine and they have been postulated as an intermediary host for the emergence of pandemic strains. For these studies we utilized the novel technology of "shotgun glycomics" to identify natural receptor glycans. The total released N- and O-glycans from pig lung glycoproteins and glycolipid-derived glycans, were fluorescently-tagged, separated by multidimensional HPLC, and individual glycans were covalently printed to generate pig lung shotgun glycan microarrays. All viruses tested interacted with one or more sialylated N-glycans, but not O-glycans or glycolipid-derived glycans, and each virus demonstrated novel and unexpected differences in endogenous N-glycan recognition. The results illustrate the repertoire of specific, endogenous N-glycans of pig lung glycoproteins for virus recognition, and offer a new direction for studying endogenous glycan functions in viral pathogenesis.

Significance statement

Studies using novel “shotgun glycan microarray” technology identify for the first time to our knowledge, the endogenous receptors for influenza viruses from a natural host, the pig. Libraries of total N-glycans from pig lung were probed for binding properties using a panel of influenza viruses isolated from humans, birds, and swine. Natural glycan receptors were identified for all viruses examined, and though some displayed the rather broad α2,3 or α2,6 sialic acid linkage specificity conventionally associated with avian or human viruses, other strains were highly specific, revealing a complexity that has not been demonstrated previously. As pigs are often implicated as intermediate hosts for pandemic viruses, these results and the approaches described, will transform our understanding of influenza host range, transmission, and pathogenicity.

Introduction

Influenza A viruses infect the human population on a yearly basis, causing hundreds of thousands of excess deaths, enormous stress on health care systems worldwide, and extensive economic burden. At unpredictable intervals, viruses with antigenically novel glycoproteins emerge to cause pandemics of even greater concern, and the pig is often implicated as an intermediate host when this occurs [373]. The waterfowl that act as natural reservoirs for influenza A viruses harbor 16 antigenically distinct subtypes of the hemagglutinin (HA) surface antigen, and 9 subtypes of the neuraminidase (NA) envelope protein, but the only subtypes to emerge and circulate broadly in humans over the past century are H1N1 in 1918, H2N2 in 1957, H3N2 in 1968, and H1N1 again in 2009. However, the possible emergence of a novel subtype in humans remains a concern, as highly pathogenic H5 and H7 subtype "bird flu" viruses continue to circulate in avian species, and over the past 15 years have infected humans, with limited ability to transmit between humans. The reasons for such host-species restriction, and mechanisms underlying cross species transmission are thought to be multifactorial, but the receptor binding properties of the HA surface antigen are of paramount significance.

Since the identification of sialic acids (Sia) as critical components of influenza receptors [238, 374], a broadly observable phenomenon has been that avian strains generally prefer binding to glycan receptors with sialic acids containing α2,3 glycosidic linkages to the penultimate galactose in the carbohydrate chain, while human viruses favor binding to substrates with α2,6 linkages [29, 34, 35, 375]. The description of

mutant viruses for which specific changes in the HA receptor binding site result in a switch from one binding preference to the other provides clues on potential mechanisms for altered host range [15, 16, 24, 30, 38, 39, 376], but perhaps leads to the simplified perception that influenza binds rather indiscriminately, as long as the minimal Sia linkage is appropriate. Interestingly, proton-NMR binding data for avian-like or human-like HAs to monosialosides of preferred, or non-preferred linkage, show binding affinity to be generally very weak, with dissociation constants in the millimolar range, and only a 2- to 3-fold difference between cognate pairs and reciprocal pairs [377, 378]. This suggests that productive virus attachment results from the cumulative effects of multiple HA-receptor interactions in which the consequences of very small differences are amplified in a phenotypically distinguishable fashion. However, little more is known with regard to binding affinity for individual glycans of defined structure, or of their presence and distribution in tissues encountered during natural infections.

Initial studies using linkage-specific lectins as an indirect probe for the presence and distribution of potential influenza glycan receptors suggested that the intestinal tract of ducks is rich in α2,3-linked sialic acid and the upper respiratory tract of humans contains an abundance of sialic acid in α2,6 linkage [243]. These observations have been extended considerably, and though the literature on studies applying lectin histochemistry data is complicated, a general consensus suggests that human upper airways contain primarily α2,6-Sia, and the lower respiratory tract contains a mixture with considerable representation of both α2,3-Sia and α2,6-Sia receptor types [40, 254, 379, 380] The respiratory tract of swine also contain both α2,3-Sia and α2,6-Sia, which appear to be distributed similarly to humans [243, 255, 258]. These observations have been used in

support of the hypothesis that the pig may provide an intermediate host for the adaptation of avian strains before emergence in humans, or for the genesis of reassortant pandemic viruses capable of human infection following co-infection with avian and human strains [324].

While lectin histochemistry may provide an indicator for the presence of glycans of particular Sia linkage, it does not identify actual glycan receptors. The continued development and employment of new tools in carbohydrate chemistry and an expanding range of viruses under scrutiny, has made clear that not only Sia linkage, but underlying glycan composition and structure, chain length, and presentation of receptors also play a role in the complex interactions that lead to productive attachment of influenza to host cells. Defined glycan microarrays have been developed and successfully applied to examine the binding specificity of influenza, as well as other viruses and microorganisms [20, 381-387]. However, a limitation of most such arrays, is that they are based on chemically or enzymatically synthesized glycan structures and represent only a subset of the endogenous complex glycomes of natural hosts. The restrictions imposed by the synthetic nature of such arrays is emphasized by the observation that mutant influenza viruses have been identified which replicate both in cell culture or in the mouse respiratory tract, yet exhibit no detectable binding to the glycans on the Consortium of Functional Glycomics (CFG) array [25]. In addition, recent glycan profiles of swine epithelial cells [259], or tissues from human respiratory tissues [380], demonstrate a diversity of glycan structures that are not comprehensively represented on available glycan arrays. Furthermore, the observation that α2,6-linked as well as α2,3-linked sialic acids were identified by mass spectrometry in human lung glycans indicates that alveolar

tropism of influenza virus may not be dictated by its binding only to α2,3 glycans [380]. The available data highlight the need for more focused arrays that represent the distribution of natural endogenous receptors derived from tissues in which influenza replicates in natural hosts. Our group recently developed a novel strategy of Shotgun Glycomics to successfully identify naturally occurring glycoconjugate ligands for Glycan Binding Proteins (GBPs) and serum antibodies [388]. In this strategy summarized in **Fig. 1**, glycans released from naturally-occuring glycoconjugates are labeled with a bifunctional fluorescent tag, fractionated and purified as individual glycans, printed as glycan microarrays, and interrogated with biological targets, such as viruses. The glycans that are strongly bound are considered biologically relevant and are structurally characterized. This novel approach is a shortcut toward defining relevant protein-glycan interactions, as it limits the difficult task of structural characterization of an entire glycome and the laborious chemical synthesis of complex and possibly irrelevant glycans. Utilizing this strategy for the study of influenza virus binding is ideal, as natural glycan microarrays can be prepared from biologically relevant cells and tissues and directly screened with different strains of viruses. In this report we describe the isolation, fractionation, purification, and interrogation of the N-glycome of the pig lung, a potential site of infection for influenza viruses of avian, swine, and human origin, and determine the binding profiles for a panel of influenza viruses that include isolates from each of these host species, and represent several HA subtypes. While some of the expected trends of binding to α2,3- or α2,6-linked sialic acid receptors were observed, the binding profiles did not correlate with those of specific lectins, and receptor recognition was quite selective for particular strains. In several examples, modifications to the glycan backbone

were influential, and for several viruses preferential recognition of branched chain di- and tri-antennary structures suggested a role for multivalent interactions. To our knowledge, this is the first identification of binding characteristics of influenza viruses to specific natural N-glycan derived receptor molecules.

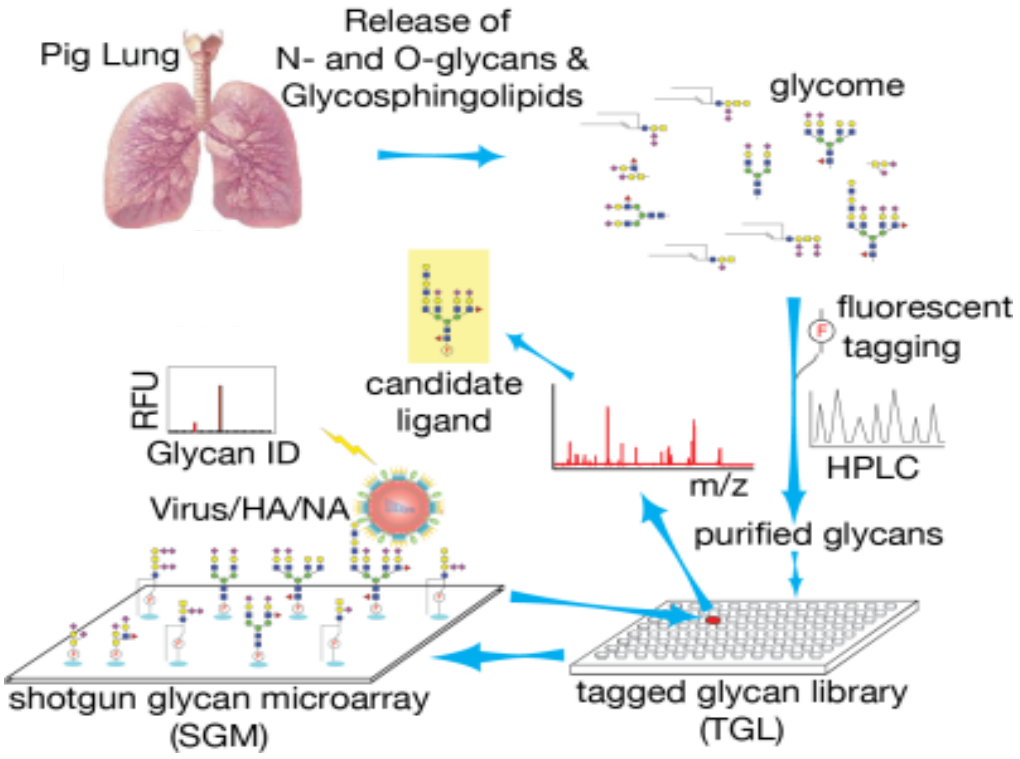

Figure 1. Principle of shotgun glycan microarrays from pig lung. Total glycans are isolated from lung tissue glycoproteins or GSLs, fluorescently tagged and separated by HPLC to generate a tagged glycan library (TGL) of purified fractions collected in 96-well plates. Each glycan fraction is then printed in equal amounts (~1 nmole) on NHS-activated glass slides, and interrogated with fluorescently labeled influenza A virus. The glycans corresponding to bound positions on the slide are retrieved from the TGL and structures determined by mass spectrometry and other methods to identify the candidate ligands for specific viruses.

RESULTS

Pig lung N-glycan library

Pig lung tissue was obtained from a commercial vendor or from a germ-free experimental animal, and in each case, 15 grams of pig lung tissue yielded ~3.1 μmole of total N-glycans. Following separation by HPLC, Lampire lung-derived glycans were determined to be a mixture of neutral (~31%), monosialylated (~23%), disialylated (~40%), and trisialylated (~6%) species (**Fig. S1**). To estimate recovery of the total N-glycans released by N-glycanase from the starting material of tryptic glycopeptides, we followed the distribution of mannose, which is a common constituent of N-glycans. N-glycanase digestion released ~90% of the total mannose while ~5% remained associated with residual N-glycanase resistant glycopeptides. We analyzed total permethylated N-glycans in preparations from the two sources of lung tissue using MALDI-TOF [389, 390]. The results shown in **Fig. S2A** revealed that the N-glycans from the purchased pig lung have compositions that indicate they are dominated by sialylated and fucosylated biantennary complex-type structures (*m/z* 2966.9, 2605.3, etc). A remarkable signal of predicted triantennary complex-type structures (*m/z* 3777.2, etc) is also observed. Signals of high mannose-type N-glycans, ranging from $Man_5GlcNAc_2$ to $Man_9GlcNAc_2$ were also detected in minor abundance (*m/z* 1579.8, 1783.9, 1988.0, 2192.1, and 2396.2). N-Glycolylneuraminic acid (Neu5Gc) (*m/z* 2635.3, 2996.7, etc) and the predicted αGal epitope (Gal-Gal) (*m/z* 2809.5, etc) are also found in the N-glycans. Interestingly, we did not detect significant amounts of glycans with poly N-acetyllactosamine (LacNAc) repeating structures ($-3Gal\beta1\text{-}4GlcNAc\beta1\text{-}_n$). Repeating this analysis on the

permethylated N-glycans from the pathogen-free pig lung gave a similar pattern (**Fig. S2B**), which indicated the reproducibility of our preparative techniques and that the N-glycome was independent of pathogen exposure.

Pig lung N-glycan shotgun glycan microarrays

The released N-glycans were derivatized with 2-amino-N-(2-aminoethyl)-benzamide (AEAB) as described previously [391] and separated in the first dimension using normal phase HPLC. Each peak from the normal phase column was re-chromatographed by HPLC on a porous graphitized carbon (PGC) column to obtain a Pig Lung Tagged Glycan Library (PL-TGL) comprised of ninety-six N-glycan fractions (**Table S1**). This library along with 4 standards, including glycans with α2,3- and α2,6-linked Sia, was printed on NHS-derivatized glass slides to produce v1.0 of the Pig Lung shotgun glycan microarrays (PL-SGM). The N-glycans were quantified based on fluorescence in order to estimate relative abundance (**Table S1**) and prepare them at 100 μM for printing 0.33 nanoliter of each in replicates of 4. Prior to printing, each entry of the PL-TGL was analyzed by MALDI-TOF, to identify the molecular ions in each glycan target. In many cases the unique mass provided monosaccharide composition, and most fractions contained only one or two glycans, thus indicating the relative purity of the isolated glycans.

Lectin binding to pig lung N-glycan microarray

To confirm that the N-glycans were printed on the PL-SGM, we interrogated the array using biotinylated lectins with defined glycan binding specificity and the results are shown in **Table S2**, which provides the average relative fluorescence units (RFU), %CV, and ranking of the glycans in each analysis, as displayed in the histograms in **Fig. 2**.

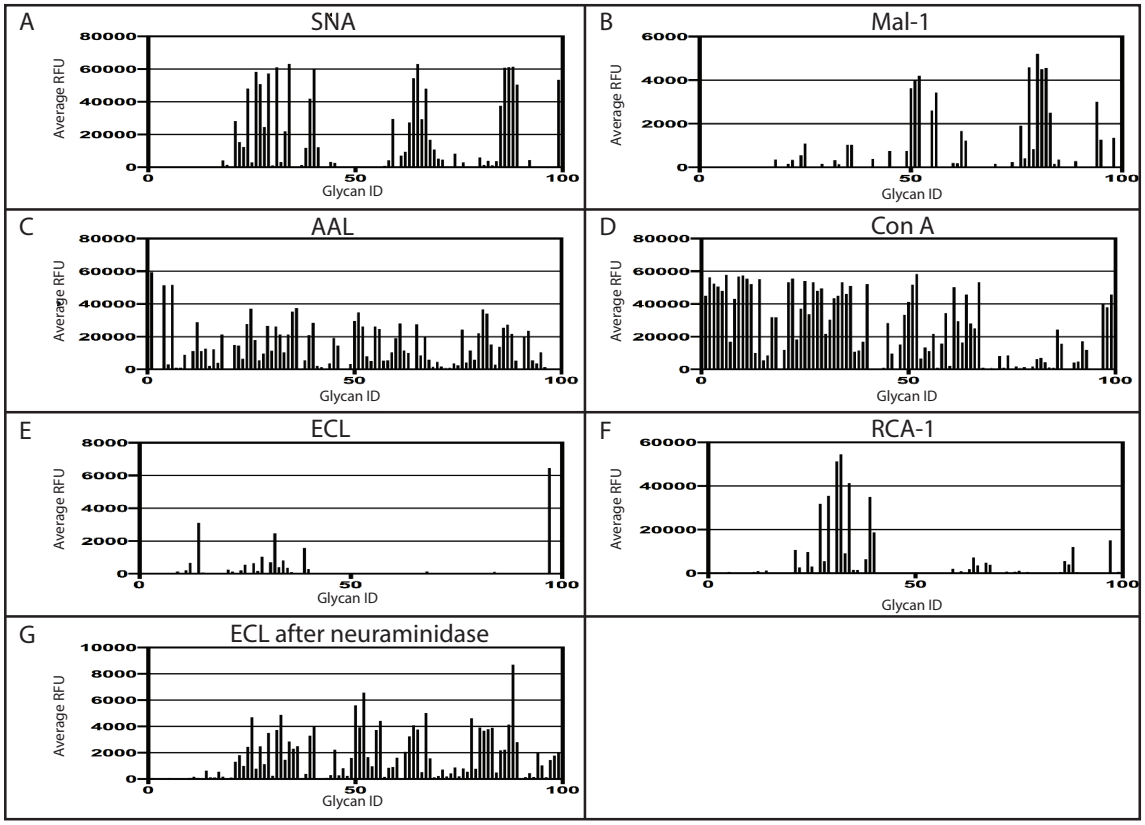

Fig. 2. Lectins binding to pig lung N-glycan micro- array. Glycan microarray TGL fractions were incubated with lectins of different specificity to validate the arrays. The lectins used were: SNA (specific for Sia 2,6Gal-R) (A); MAL-I (specific for Sia 2,3Gal-R) (B); AAL (specific for fucose) (C); ConA (specific for bian- tennary but not triantennary complex N-glycan struc- tures) (D); ECL (specific for terminal galactose) (E); and RCA-I (specific for terminal galactose or 2,6- linked sialic acids but not 2,3-linked sialic acids) (F). The slides were also treated with neuraminidase, fol- lowed by binding of ECL (G) to identify glycans with newly exposed galactose sugars to which sialic acids had been linked. Fractions 1–96 are N-glycans isolated from pig lung: 1–14, neutral; 15–47, monosialyl; 48–77, disialyl; and 78–96, trisialyl. Standards include: 97, NA2 (nonsialylated biantennary N-glycan); 98, NA2-Sia2,3; 99, NA2-Sia2,6; and 100, Man5.

The rank of individual glycans in a binding assay was calculated as a percentile of RFU of the glycan divided by the highest RFU values in that assay. SNA binding to the PL-SGM (**Fig. 2A**) indicates the glycans that possess terminal α2,6-linked sialic acid to galactose [245, 382, 392]. MAL-I binding, which indicates the presence of terminal

sialic acid linked α2,3- to galactose [246] is shown in **Fig. 2B.** Interestingly, most of the glycans appear to be homogeneous with respect to sialic acid linkage since there was very little overlap in the SNA and MAL-I binding profiles. Comparison of the rankings of MAL-I and SNA binding glycans (**Table S2**) indicates significant potential overlap in only 3 glycan fractions, #24, #62 and #63. Binding of these lectins was lost upon treatment of the PL-SGM with neuraminidase, indicating that recognition was Sia-dependent and not due to sulfate; recent studies indicate that SNA and MAL-I can both interact with 6-O- or 3-O-sulfated terminal galactose residues, respectively [393, 394]. The N-glycan PL-SGM was interrogated with other defined biotinylated lectins including AAL, which binds α-linked fucose in a variety of linkages [395] (**Fig. 2C**); ConA, which binds complex-type biantennary, hybrid-type, and high mannose-type N-glycans, but not tri- or tetraantennary complex N-glycan structures [396-398] (**Fig. 2D**); ECL, which binds terminal β1-4-linked galactose [399] (**Fig. 2E**); and RCA-I, which binds terminal β-linked galactose or galactose modified with α2,6-linked sialic acids, but not α2,3-linked sialic acids [400] (**Fig. 2F**). The ECL binding profile after neuraminidase digestion (**Fig. 2G**) indicates that the terminal sialic acids were predominantly linked to galactose in the glycans presented on the PL-SGM. The behavior of lectins binding to the four control glycans is consistent with the known specificity of the lectins and taken together, the data indicate that we were successful in printing N-glycans on the PL-SGM and that these glycans possess both α2,6- and α2,3-linked sialic acid.

Influenza virus binding to N-glycans of the PL-SGM

To explore the range and diversity of potential influenza virus natural glycan receptors present in the pig lung, a panel of viruses isolated from human, swine, and

avian species were examined. The viruses selected represent a broad spectrum of viruses encompassing differing species of origin, time and geographic location of isolation, and various HA subtypes including H1, H2, H3, and H6. (**Table 1**).

Virus	Subtype	Host
Avian isolates		
A/RuddyTurnstone/DE/650625/2002	H6N1	Avian
A/RuddyTurnstone/DE/650645/2002	H1N9	Avian
Contemporary swine isolates		
A/sw/Minnesota/02749/2009	H1N1	Swine
A/sw/Minnesota/02719/2009	H3N2	Swine
A/sw/Illinois/02860/2009	H1N2	Swine
Vaccine strain		
A/Brisbane/59/2007	H1N1	Human
Seasonal		
A/Pennsylvania/08/2008	H1N1	Human
A/New York/55/2004	H3N2	Human
Pandemic H1N1		
A/California/04/2009	H1N1	Human
A/Mexico/InDRE4487/2009	H1N1	Human
A/Texas/15/2009	H1N1	Human

Table 1. The virus strains tested on the microarrays.

Included in the panel were seasonal human isolates of both an H1N1 subtype (A/Pennsylvania/08/2008) and an H3N2 subtype (A/New York/55/2004), as well as 2009 human pandemic (pdm) H1N1 strains A/California/04/2009, A/Mexico/4487/2009, and A/Texas/15/2009, which represent viruses that displaced the previously circulating H1N1 seasonal strains (i.e. A/Pennsylvania/08/2008). These 2009 viruses are direct human isolates (not passaged in eggs) from the H1N1 pandemic, which caused different pathogenic symptoms in humans and have strict α2,6-linked Sia specificities [27]. The contemporary swine viruses of the panel were isolated from pigs at the time of the 2009

human pandemic, and are thought to be representative of viruses with related gene constellations that may have given rise to the human pandemic strains. The three swine strains, A/sw/Minnesota/02719/2009 (H3N2), A/sw/Minnesota/02749/2009 (H1N1), and A/sw/Illinois/02860/2009 (H1N2), have several internal genes in common with one another and with human pandemic strains, but different surface glycoprotein combinations. The Ruddy Turnstone viruses are low-pathogenicity avian H6N1 and H1N9 subtypes. A/Brisbane/59/2007 (H1N1) is a vaccine strain that has been passaged extensively in eggs, and A/New York/55/2004 (H3N2) is a seasonal virus, which was passaged 1-2 times in eggs prior to transfer to MDCK cells. None of the other human or swine viruses analyzed have been passaged in embryonated chicken eggs, a common procedure for growing field or clinical isolates that is known to select for changes in the binding characteristics, including adaptation to α2,3 sialylated receptors [401]. We have shown that A/Brisbane/59/2007 (H1N1) has broad specificity for both α2,3- and α2,6-sialylated receptors [27].

The eleven viruses were labeled with a fluorescent tag and analyzed on the glycan microarray (version 5.1) developed by the Consortium for Functional Glycomics (CFG, www.functionalglycomics.org), which contains 610 immobilized chemo-enzymatically generated glycans, representing a variety of defined glycan epitopes or determinants found on N- and O-glycans and glycosphingolipid-derived mammalian-type glycans. The binding patterns of the viruses on the CFG array demonstrated that all the viruses bound strongest to sialylated N-glycans and common N-glycan epitopes (**Fig. 3**). Each preparation of labeled virus was divided and examined in parallel on the CFG array and on the N-glycans of the PL-SGM. All of the isolates were prepared in this way to

maintain consistency between array experiments. None of the viruses bound to neutral glycans, but many mono-, di-, and tri-sialylated N-glycans were bound by the different virus strains (**Fig. 3**), and each of the viruses displayed a distinct binding pattern to the PL-SGM.

Waterfowl isolates –The binding patterns of A/Ruddy Turnstone/650625/2002 (H6N1) and A/Ruddy Turnstone/DE/650645/2002 (H1N9) were compared on the CFG glycan array with the help of the Cross Analysis tool in the GlycoPattern website (https://glycopattern.emory.edu). This comparison indicated a clear relationship between these two strains. Both avian strains demonstrated a definite specificity for NeuAcα2,3Gal terminating glycans. Of the two strains, A/Ruddy Turnstone/DE/650645/2002 (H1N9) demonstrated a much more restricted specificity, binding primarily to linear fucose-containing glycans. Interestingly, all of the glycans bound by strain A/Ruddy Turnstone/DE/650645/2002 (H1N9) were also bound by strain A/Ruddy Turnstone/650625/2002 (H6N1); however, A/Ruddy Turnstone/650625/2002 (H6N1) bound many more glycans with lower ranking (14 to 40 percentile), many of which were branched glycans. When a similar comparison was made between these two strains on the PL-SGM (**Fig. 3 and Table S4**), no such overlap was observed. The A/Ruddy Turnstone/650625/2002 (H6N1) strain bound 34 glycan fractions ranked between 100 and 20 percentile, while the 4 glycans bound strongest (ranked 73-100) by strain A/Ruddy Turnstone/DE/650645/2002 (H1N9) were among the weaker binding glycans for strain A/Ruddy Turnstone/650625/2002 (H6N1).

Swine isolates – The three swine isolates A/swMinnesota/02749/2009 (H1N1), A/sw/Minnesota/02719/2009 (H3N2), and A/sw/Illinois/02860/2009 (H1N2) were

analyzed on the defined glycan microarray from the CFG and the PL-SGM (**Fig. 3 and Table S4**) in parallel. These three isolates were all generally specific for α2,6-linked sialic acids and bound strongest to sialylated linear and branched lactosamine- or polylactosamine-containing glycans on the CFG array. When analyzed on the PL-SGM, binding of the 3 swine isolates correlated well with SNA binding, which was consistent with the swine isolates being generally specific for α2,6-Sia. The three strains analyzed bound a number of common glycan fractions including glycans identified with Chart ID #64-67 and #85-89 (**Fig. 3 and Table S4**)

Human Isolates – We analyzed a vaccine strain, A/Brisbane/59/2007 (H1N1), seasonal strains A/Pennsylvania/08/08 (H1N1) and A/New York/55/2004 (H3N2), and 3 pandemic strains of H1N1 A/California/04/2009, A/Mexico/INDRE4487/2009, and A/Texas/15/2009 side-by-side on defined glycan microarrays of the CFG and the PL-SGM (**Fig. 3 and Table S4**). The vaccine strain A/Brisbane/59/2007 (H1N1), which had undergone multiple passages in eggs, had an extremely broad specificity, binding approximately 100 of the 158 sialylated glycans on the CFG array, including 50 of the 88 glycans that have α2,3-linked sialic acid. Among the seasonal and pandemic strains analyzed, the seasonal strain A/Pennsylvania/08/08 (H1N1) had the broadest specificity, binding 55 glycans in the top 80 percentile ranking, which included only 11 glycans containing only α2-3-linked sialic acid. The other seasonal strain A/New York/55/2004 (H3N2) displayed the most restricted specificity on the CFG defined array with binding to only 10 glycans considered as significant; all of which contained α2-6Sia, and in most cases these terminated linear lactosamine and polylactosamine structures. Among the pandemic strains from 2009, A/Texas/15/2009 (H1N1) showed the broadest specificity,

binding 38 sialylated glycans, all containing α2,6-linked sialic acid. Glycans bound by the other pandemic strains, A/California/04/2009 (H1N1) and A/Mexico/INDRE4487/2009 (H1N1), were also bound by A/Texas/15/2009. When the human isolates were analyzed on the PL-SGM, the vaccine strain A/Brisbane/59/2007 (H1N1) appeared to have the broadest specificity for the pig lung N-glycans, binding 28 of the 96 glycans printed on the PL-SGM (**Fig. 3 and Table S4**), which is consistent with the broad specificity of this strain on the defined CFG array. Similar to its behavior on the CFG array, the seasonal strain A/New York/55/2004 (H3N2) showed the most restricted specificity on the PL-SGM (**Fig. 3 and Table S4**), with only 4 glycans bound to significant levels. Thus, the general behavior of the human isolates on the PL-SGM was very similar to their behavior on the defined glycan array.

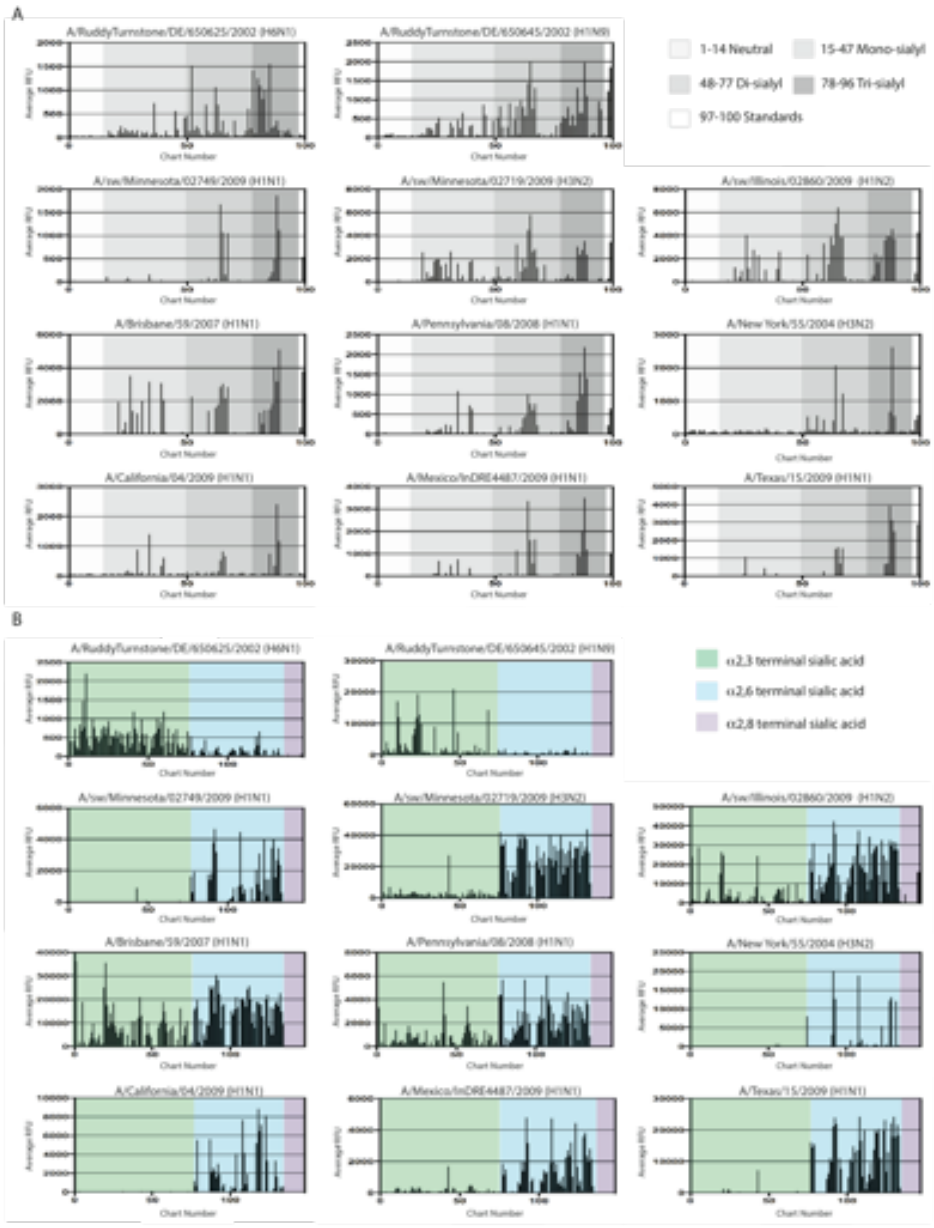

Figure 3. **Influenza virus binding to glycan microarrays.** Eleven viruses have been tested including isolates from vaccine (A/Brisbane/59/2007), human (A/New York/55/2004, A/Pennsylvania/08/2008, A/California/04/2009, A/Mexico/INDRE4487/2009, and A/Texas/15/2009), avian (the Ruddy Turnstone viruses) and swine (A/sw/Minnesota/02719/2009, A/sw/Minnesota/02749/2009, and A/sw/Illinois/02860/2009). (A) PL-SGM array. Fractions 1-96 are N-glycans isolated from pig lung: 1-14, Neutral; 15-47, Mono-sialyl; 48-77, Di-sialyl; 78-96, Tri-sialyl. Standards include 97: NA2; 98: NA2-2-3 Sia; 99: NA2-2-6 Sia; 100: Man5. (B) CFG array. This microarray contains 610 immobilized glycans, representing a variety of defined glycan epitopes or determinants. Only the epitopes containing terminal sialic acid are represented here. The glycans are grouped by terminal linkage with the α2,3 linkage type highlighted in green, the α2,6 linkage highlighted in blue and the α2,8 linkage highlighted in purple.

Some general observations from the CFG and the PL-SGM data can be made when comparing the isolates, especially as they are grouped by specificity. The avian isolates, which demonstrated a preference for terminal α2,3Sia, preferentially bound to glycans displaying core fucosylation of N-glycans, especially A/Ruddy Turnstone/DE/650645/2002 (H1N9). For both avian viruses, residues of the same structure tend to bind with greater apparent affinity if a core fucose is present. However, the subset of viruses that bind terminal α2,6Sia do not show a preference for core fucosylated glycans. For example, the A/sw/Minnesota/02749/2009 (H1N1) virus binds two structures in the highest percentiles (100 and 96) that differ only in the addition of core fucose residues. For the mammalian viruses the sialic acid linkage and composition of the terminal sugars seem to be more critical determinants of binding, as all glycans with these terminal characteristics are bound with similar affinity, regardless of chain length or whether they are branched or unbranched. This finding suggests that for the recognition of terminal α2,6-Sia, it is the extreme reducing end of the glycan structure that is important, and this may be due to the way the terminal sialic acid in the α2,6 conformation fits into the binding pocket on the HA. The avian viruses seem to rely more on core structure and modification for binding preference in comparison with the mammalian strains, which could be a consequence of the HA-receptor interactions beyond the sialic acid binding pocket of HA.

Characterization of glycans that may function as Influenza virus receptors

The N-glycans on the PL-SGM that were consistently bound at high levels by labeled viruses were considered candidates as natural receptors for influenza and chosen for further structural analysis. Glycans #34, 64, 67, and 88 showed relatively strong

binding by human, swine and avian influenza virus strains while glycans #56, 81, and 83 were recognized by the avian virus strains and the human and swine strains, A/Brisbane/59/2007 (H1N1) and A/sw/Illinois/02860/2009 (H1N2), that showed a broader specificity of binding (**Fig. 3 and Table S4**). Therefore, the structures of these glycans were analyzed by MALDI-TOF, tandem mass (MS/MS) spectrometry, and the pattern of binding by lectins with defined specificities (**Tables S2** and **S5**), to allow a prediction of glycan structure using the general approach of Metadata-Assisted Glycan Sequencing (MAGS) [402].

The glycans were analyzed in both positive and negative mode MALDI-TOF to check for sulfate groups in the glycans. A difference of m/z 78 (or 56 due to sodium adduct) indicated a sulfo group. The glycan structures were also analyzed by MS/MS to determine the backbone structures. In addition, the glycans were further treated with neuraminidase to demonstrate the sialic acid moiety and linkage, which is also easier for MS/MS characterization of glycan backbones. For example, when glycan #67 was treated with neuraminidase, its HPLC profile was shifted, indicating Sia removal (**Fig. 4A**). MS revealed glycan #67 has a molecular mass of 2553.2 $[M+Na]^+$, very close to calculated molecular mass of 2554.9 $[M+Na]^+$, indicating a composition of five hexoses (Hex), four acetyl hexosamines (HexNAc), two sialic acids (Neu5Ac), and one fucose (Fuc) ($Fuc_1NeuAc_2Hex_5HexNAc_4$) (**Fig. 4B**). Together with the molecular weight change determined by MS (**Fig. 4C**), we propose two sialic acids in the glycan moiety. The MS/MS further confirmed the backbone structures (**Fig. 4C**).

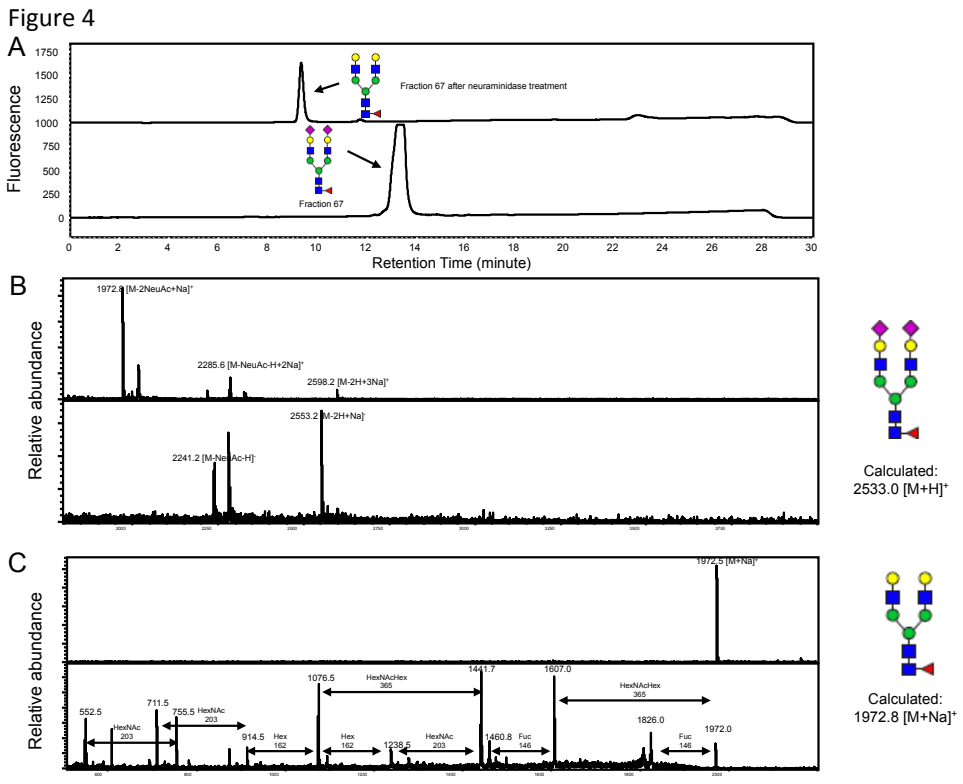

Figure 4. **Determination of the structure of Fraction 67.** (A) HPLC profile of fraction 67 before and after treatment of neuraminidase. (B) The MS spectra of fraction 67, in both positive (top panel) and negative (bottom panel) mode. (C) The MS (top panel) analysis of fraction 67 after treatment of neuraminidase and MS/MS (bottom panel) analysis of parent ion 1972.

Consistent with the MS data, The glycan was bound by SNA and RCA-I, which is consistent with Siaα2-6Galβ1-4GlcNAc, while ConA binding is consistent with a biantennary N-glycan (not a triantennary complex N-glycan structure) and AAL binding with the presence of fucose. Taken together these results indicate that glycan #67 is a biantennary complex-type N-glycan terminated with Siaα2-6Galβ1-4GlcNAc and containing a core fucose linked to the reducing end GlcNAc, as shown in **Fig. 5**. This structure is consistent with no binding by ECL (free terminal galactose) or MAL-I (α2,3-linked sialic acids). The MS analysis of glycan #64 predicts a biantennary complex-type

N-glycan with no core fucose (**Fig. 5**), and a lectin binding pattern identical to glycan #67 with the exception of AAL, which is consistent with the absence of fucose in this glycan. In addition, Glycan #64 demonstrated an identical lectin binding profile as the standard glycan #99; glycans #64, 67, and 99 all showed similar virus binding profiles.

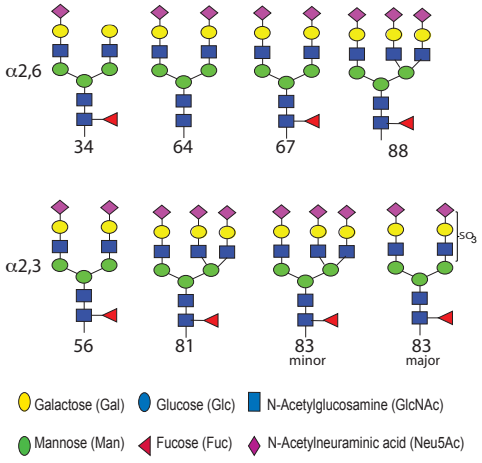

Figure 5. **The structures of selected N-glycans.** The bound glycans were identified as bi-and tri-antennary complex-type N-glycans as well as a sulfated biantennary structure with α2,6-linked sialic acids or α2,3-linked sialic

Based on a similar approach, the other glycans were identified as bi-and triantennary complex-type N-glycans (**Fig. 5**), as well as a sulfated biantennary structure (#83). The Sia linkages were identified from the lectin binding profiles (SNA and MAL-I). All of the candidate virus-binding receptors terminated in α2,6-Sia except glycans #56, #81, and #83, which terminated in α2,3-Sia based on lectin binding. Based on these predicted structures, comparisons to the structures present on the CFG array can be made. Glycan #64 and #67 have cognate structures on the CFG array; #55, #318, #325, and #366 correspond to #64 on the PL-SGM, and #482 and #483 correspond to #67 on the PL-SGM. The remaining structures from the PL-SGM that we have characterized are not represented on the CFG array. This finding confirms the novelty and significance of the

shotgun array technique. These data demonstrate, for the first time, the direct association of naturally occurring N-glycans from pig lung with binding of influenza viruses, supporting their function as potential receptors for these influenza viruses *in vivo*.

Studies on virus binding to O-glycan and glycolipids

While the above results define the ability of influenza viruses to recognize endogenous N-glycans, we also explored the potential of viruses to bind other classes of glycans, including O-glycans and glycolipids. Using the shotgun glycomics approach described previously [388], we prepared total O-glycans and glycolipids. These were derivatized with AEAB, separated by multidimensional HPLC, and printed on glycan microarrays. Although a wide variety of glycans were detected by specific lectin binding (**Fig. S3 and S5**), as might be expected from previous studies of lung tissue glycomics of other species, no significant binding of influenza viruses was observed on shotgun microarrays of the O-glycans or glycolipid-derived glycans (**Fig. S4 and S6**). Therefore, based on our available data, pig lung-derived N-glycans are recognized by all of the influenza viruses studied, but we observed no significant binding to pig lung-derived O-glycans or glycolipids.

Discussion

The data presented here provide novel and fundamental contributions to the understanding of several separate but interrelated areas involving host-pathogen interactions. From a broad perspective, it represents the first interrogation of the pig lung glycome, and opens up the field for investigating numerous economically important respiratory diseases of swine. Furthermore, the extension of the technology, reported here, to human tissue should pave the way for the understanding of various human respiratory diseases and promote the development of novel therapeutic intervention strategies. Our results also reveal novel insights into the recognition of natural glycan receptors in the pig lung by a diverse array of influenza viruses and show that binding does not necessarily follow basic assumptions that have been made regarding α2,3-Sia and α2,6-Sia linkage specificity for avian and human viruses, respectively.

Since swine are susceptible to both avian and human Influenza viruses and are considered a possible intermediate host for the generation of pandemic human viruses, there has been significant interest in characterizing the glycome using glycomic profiling of cells and tissues by mass spectrometry [259, 265]. These studies reveal the presence of a diverse range of glycans terminating in Galα1-3Gal or sialic acid in both α2,3- and α2,6- linkages, where NeuAc was more prevalent than NeuGc. Glycan microarray analyses of the same viruses that were used to infect primary swine respiratory epithelial cells demonstrated the viruses preferred α2,6-linked sialic acid on the array, and infectivity studies showed a clear dependence of surface α2-6-linked sialic acid for

influenza infection [259]. These studies indicated that NeuAcα2,6 containing N-glycans are important for virus infection, but structural definition of the natural glycan receptors was predicted only by comparison of the similarity of the predicted glycan structures determined by MS analysis with the defined glycans on the CFG glycan microarray and therefore these studies are correlative. In addition, glycans expressed by cultured cells isolated from organs may be misleading, and not necessarily reflective of glycans in the native organ, since cell cuture conditions have been known to select for changes in glycan structures [403, 404]. Our approaches involve direct analysis of glycan structures in the relevant tissue. We analyzed two independent samples of pig lung tissue, observing glycans in the range of 1,500 to 5,000 daltons, and the data are similar to the profiles reported previously for trachea, lung and primary swine respiratory epithelial cells. While the MS profile of primary swine respiratory epithelial cells observed glycans over an extended mass range of 1,500 to 8,000 [259], the large, multiantennary polylactosamines-containing glycans that constitute the high end of the mass range were present in vanishingly low amounts. We were unable to detect these glycans on the lung sample we analyzed, and they were not reported as present in trachea or lung by Sriwilaijaroen et al. [265], however no testing of influenza binding to these glycans was performed in this study. The defined glycan microarray currently available from the CFG contains a variety of multiantennary glycans possessing long stretches of polylactosamine terminated in sialic acid, and numerous analyses of influenza virus binding to this array of defined glycans demonstrate strong virus binding to such structures. Based on these data, it has been suggested that such long sialylated polylactosamine structures may be important in productive virus infection [405, 406]. Such conclusions, however, may be

open to question, since the amounts of such structures actually identifiable in the tissues appears to be extremely low or undetectable. As we have demonstrated, if sufficient material is available to undergo detailed structural analysis, the shotgun glycan microarray approach makes it possible to identify potential receptors based on their presence in natural tissue and their ability to participate in functional binding.

A significant body of work has accumulated from many investigators on analyses of influenza A virus binding to defined sialylated glycans on glycan microarrays and in spite of this novel approach, we still have not defined the exact structure of a glycan receptor that functions in productive infection. These data were recently documented in a multidisciplinary study of influenza A virus-glycan interactions using a glycomics approach [380]. In this extensive study the N-glycan and O-glycan composition of human lung and bronchus were analyzed by mass spectrometry. A wide spectrum of Siaα2,3- and Siaα2,6-terminated glycans were found in both the lung and the bronchus. These results indicate that alveolar tropism by influenza viruses appears to involve both Siaα2,3- and Siaα2,6-terminated glycans and emphasizes the complexity of this system where the cell surface glycans as well as glycoconjugates of the respiratory tract fluid probably play important but undefined roles. The mass spec data allowed for structural predictions that were used in combination with influenza A virus binding data from four published glycan arrays comprised of defined glycans to determine if they could predict replication of human, avian, and swine viruses in human *ex vivo* respiratory tract tissues. The CFG defined glycan microarray was the most comprehensive of the four evaluated. Although the CFG array possessed the greatest diversity of sialylated glycans, the influenza A binding data from this array was not predictive of productive virus

replication in human respiratory tract tissue. The study concluded that more comprehensive and focused arrays need to be developed to evaluate emerging influenza A viruses. It is tempting to conclude that the solution to this dilemma is simply to synthesize the glycans corresponding to the sialylated glycans predicted by glycomics analyses. However, the glycan structures based on profiling are predicted structures, and details of all the structures are not available. Furthermore, synthesis of large N-glycans is an extremely difficult task, and synthesis of all possible glycans predicted by MS analysis of the human respiratory tract tissues is currently not possible. Thus, the shotgun glycomics approach, which will obtain and identify the glycans from the natural source of tissue or glycoconjugate, has a high probability of presenting cellular glycans that function as viral receptors.

With regard to the specific binding properties of influenza viruses, our data is generally consistent with the well documented observations that some strains bind preferentially to either α2,3-Sia or α2,6-Sia, and that these specificities can provide useful indicators for potential involvement in host species specificity. However, our results also indicate that influenza virus receptor recognition is much more complicated than might be ascertained by such basic assumptions. One important observation is that virus binding profiles do not directly correlate with the recognition profiles determined for the lectins SNA-I and MAL-I, which are often utilized to assay for the abundance of specific "receptors" of α2,6-Sia or α2,3-Sia linkages, respectively [40, 243, 255, 379, 407]. While some viruses, such as the vaccine strain A/Brisbane/59/2007 (H1N1), and low-pathogenicity avian isolates, A/Ruddy Turnstone/650625/2002 (H6N1) and A/Ruddy Turnstone/650645/2002 (H1N9), bound to glycans that broadly reflected the profile

observed with the specific lectins, other viruses, such as pdmH1N1 strains, A/California/04/2009, A/Mexico/INDRE4487/2009, and A/Texas/15/2009 and seasonal strains A/Pennsylvania/08/2008 (H1N1) and A/New York/55/2004 (H3N2), bound to highly specific subsets of glycans. Interestingly, for a number of virus strains, significant binding was observed to glycans recognized by neither SNA or MAL-I. In other examples, viruses bound efficiently to both α2,3-Sia and α2,6-Sia linked glycans. A/swine/Minnesota/02719/2009 (H3N2) and A/swine/Illinois/02860/2009 (H1N2) each bind the same 3 glycans that are recognized as α2,3-Sia and α2,6-Sia. Similarly, three glycans of both specificities are bound by A/Brisbane/59/2007 (H1N1), A/California/04/2009 (H1N1), and A/New York/55/2004 (H3N2). This dual specificity may have been expected for the vaccine strain A/Brisbane/59/2007 (H1N1), as it represents a human strain that had been subsequently passaged in embryonated chicken eggs, where recognition of α2,3-Sia linkages may have been selected, but was unexpected for other viruses that bound the same glycans or for the two avian strains A/Ruddy Turnstone/DE/650645/2002 (H1N9) and A/Ruddy Turnstone/650625/2002 (H6N1). While these avian strains showed the expected binding to α2,3-Sia glycans that were not recognized efficiently by human or swine strains, they also bound to several of the α2,6-Sia containing glycans. The swine viruses A/sw/Minnesota/02749/2009 (H1N1), A/sw/Minnesota/02719/2009 (H3N2), and A/sw/Illinois/02860/2009 (H1N2) were all isolated in 2009, but displayed broad differences with respect to the number of glycans recognized, with the A/sw/Minnesota/02749/2009 (H1N1) virus showing a much more restricted binding profile. Though these swine viruses were isolated in the US Midwest in the same year, they are different HA and NA subtypes. Another illuminating

observation relates to the valency of receptors recognized, as some of the more highly specific strains were more selective for di- and triantennary glycans. Interestingly, the 2009 human pandemic strains known generally to have low binding activity [27, 28], were more selective for the multivalent receptors.

The glycans that bound virus and generated a ranking of greater than 40% for at least one of the viruses interrogated are shown in **Table S3**. The glycans selected for further analysis were glycans #34, 56, 64, 67, 81, 83, and 88, and their structures are shown in **Fig. 5**. The characterized glycans do have some similarities which suggest that these features might be relevant determinants of binding. Each structure is branched, either biantennary or triantennary, and of the 8 structures characterized, 7 contain a core fucose modification. The motif of terminal Sia-Gal-GlcNac is represented in all of the structures that have been characterized which is in accordance with general observations of influenza binding. These structures were chosen because of their abundance, purity, and relative ease of characterization. Each is a principal binder for at least one and often many of the viruses tested, but they are not necessarily the highest binding structure. Further structural characterization of the components of the PL-SGM will reveal the true relevance of these complex N-glycan structures with respect to influenza binding.

The observation that swine and human isolates recognize a number of the same glycans is consistent with our knowledge of the swine as a suitable host for a range of influenza viruses, and this is supported by the observation that avian isolates examined here also recognized a range of both α2,3-Sia or α2,6-Sia linked receptors. The extension of the pig lung glycan array technology reported here to human respiratory tract tissues,

and to the tissues of the intestinal tract of avian species, will be required to identify whether specific receptors exist that are critical determinants of host range.

Our current understanding of influenza binding specificity has been based largely on studies of binding to artificial receptor analogs of defined α2,3-Sia or α2,6-Sia linkage, or to heterogeneous collections of glycans present on cell surfaces characterized only by reactivity with specific lectins. Such studies have proven useful for broad generalizations of species specificity, by relating them to the amino acid composition, and structural aspects of the HA binding site using viruses isolated from different hosts. However, a striking feature of these results presented here relates to distinct differences in the binding profiles detected, even amongst strains that would be broadly classified in the same category based on overall α2,3-Sia or α2,6-Sia preference. These distinctions relate to glycan backbone, modifications, and valency of the receptor species, and highlight a level of complexity that is not easily explained based on our current knowledge of HA structures. When considering productive virus attachment in the context of a natural host, the situation becomes even more complicated, as factors relating to NA activity and specificity, relative ratios and distribution of HA and NA glycoproteins on viral surfaces, and virion morphology may all play a role. The mechanisms by which individual virus strains modulate their detailed selectivity for receptors, and the implications for host range and pathogenicity, are not currently appreciated. However, our current studies on swine tissue suggest that it will require a much broader understanding of the identity, density, and distribution of natural endogenous receptors at sites of infection in many of the natural hosts for influenza viruses.

Experimental Methods

Materials. Pig lung was purchased from Lampire Biological Products (Piperville, PA) or obtained from germ free animals from the College of Veterinary Medicine, University of Minnesota, St. Paul, MN and stored at −80°C until use. All chemicals were purchased from Sigma-Aldrich and used without further purification. HPLC solvents were purchased from Fisher Scientific. An Ultraflex-II TOF/TOF system (Bruker Daltonics) was used for MALDI-TOF mass spectrometry analysis. Both reflective positive and reflective negative modes were used as indicated in the figures. The 2,5-dihydroxybenzoic acid (5 mg ml^{-1} in 50% acetonitrile, 0.1% TFA) was freshly prepared as the matrix and 0.5 μl matrix solution was spotted on an Anchorchip target plate (200 μm or 400 μm) and air-dried. Then 0.5 μl sample solution was applied and air-dried. An ozone generator (model OZV-8, Ozone Solutions) was used to generate ozone from high purity oxygen.

Isolation of N-linked Glycans. Frozen pig lung (free of trachea) was homogenized at 4°C and adjusted to a chloroform/methanol/water ratio of 4:8:3 (v/v/v). The soluble fraction was reserved as a source of glycolipids and the insoluble material, collected by centrifugation, was resuspended in in 8M GuHCl in 0.2 M Tris (pH 8.2) and subsequently reduced by dithiothreitol (DTT) and alkylated by iodoacetamide. Denatured material was dialyzed against water overnight and lyophilized. The lyophilized proteins were digested with trypsin in 50 mM phosphate buffer (pH 8.2) to generate glycopeptides that are susceptible to digestion with Peptide *N*-Glycosidase F (PNGase F, New England Biolabs). After PNGase F digestion, the released N-glycans

were obtained in the run-through of C-18 cartridges (Waters) and collected by subsequent application to and elution from a Carbograph cartridge (AllTech), and subsequently the free glycans were derivatized with AEAB as previously described (38). The bifunctional fluorescent AEAB tag permits quantification of total glycans and provides a primary amino group for coupling to NHS activated glass surfaces when printed as microarrays.

Isolation of O-glycans and Glycolipids. O-glycans were isolated following the non-reductive elimination procedure using ammonium hydroxide/ammonium carbonate developed by Huang et. al. [408]. The free reducing glycans were conjugated with AEAB as described for N-glycans. Free glycans from glycosphingolipids were isolated following the ozone-mediated non-reductive de-lipidization [409]. The free reducing glycans were conjugated with AEAB as described for N-glycans. One-dimensional HPLC using a normal phase column was carried out for both O-glycans and glycans from glycolipids. Fractions were collected, lyophilized, quantified based on fluorescence and printed without second dimensional HPLC separation. No apparent binding was observed for these microarrays.

*Permethylation of Glycans***.** For structural profiling by MALDI-TOF analysis the N-glycans were permethylated using sodium hydroxide and iodomethane in DMSO [390] prior to derivatization with AEAB. The permethylation reaction was quenched with water after 1 hour, and the samples were extracted with chloroform. The organic phase was washed three times by ddH_2O and gently dried with nitrogen gas under a hood and re-dissolved in 1:1 methanol:water. The samples were loaded onto C-18 cartridge and eluted stepwise with water, 15%, 35%, 50%, and 75% aqueous acetonitrile.

Permethylated glycans were usually present in the 35%, 50%, and 75% ACN fractions. The glycans were annotated with the help of the GlycoWorkbench tool.

HPLC separation of AEAB. An HPLC CBM-20A system (Shimadzu), coupled with a UV-light detector (SPD-20A) and a fluorescence detector (RF-10AXL), was used for HPLC analysis and separation of AEAB conjugated glycans. 2D-HPLC separation, utilizing normal phase and reverse phase columns as previously described [391] provided multiple fractions that were largely homogeneous. The quantified fractions obtained after 2 dimensional HPLC were then lyophilized and adjusted to 200 μM with deionized water and stored frozen as the PL-TGL.

Viruses and cells. Virus stocks representing swine, human, and avian isolates were selected based on their availability and the relevance of the strain with respect to circulation in a population. The virus stocks were grown in Madin-Darby canine kidney cells (MDCK) cells that were maintained using DMEM supplemented with 5% fetal bovine serum (FBS) and penicillin-streptomycin. Briefly, 85 to 90% confluent MDCK cells grown in T175 flasks were washed twice with phosphate-buffered saline (PBS), overlaid with 10 ml of serum-free Dulbecco's modified Eagle's medium (DMEM) supplemented with 1 μg/ml tosylsulfonyl phenylalanyl chloromethyl ketone (TPCK) trypsin, and infected with a 1:1,000 or 1:10,000 dilution of the original virus stock. Cells were incubated with rocking for 1 hour at ambient temperature, the inoculum was removed, and 30 ml of serum-free DMEM supplemented with 1 μg/ml TPCK trypsin was added. The flasks were incubated at 37°C for 2 to 3 days until monolayers were 80 to 90% destroyed. Virus was then harvested in the infected cell supernatant and frozen at −80°C for subsequent purification. The stocks of all viruses utilized in these studies were re-

sequenced after the limited amplification in MDCK cells prior to labeling for glycan array analysis. We detected no sequence changes and no evidence for observable heterogeneity.

Purification of virus strains. Preparations of each virus were done so that each would yield enough volume for multiple experiments so that essentially the same preparation could be used on each array at the same time. For virus preparations, infected cell supernatants were clarified by low speed centrifugation, then pelleted through a 25% sucrose cushion in NTE buffer (100 mM NaCl, 10 mM Tris, 1 mM EDTA). Purified viruses were pelleted by centrifugation in a SW32 rotor at 28,000 rpm for 2 h, resuspended in 2 ml of PBS buffer, aliquoted, and frozen at −80°C. Frozen, purified virus strains were later thawed, and the hemagglutination units (HAU) and plaque forming units (PFU/ml) titers were determined using standard techniques.

Agglutination of erythrocytes. Chicken erythrocytes were acquired from Lampire Biologicals as whole-blood preparations. Whole-blood preparations were washed two times with 1× PBS and diluted to 0.5% for hemagglutination experiments, which were performed using standard techniques. Briefly, 0.5% erythrocyte preparations were added to 2-fold serial dilutions of 50 µl of virus stock for 1 h to determine the HA titer. This procedure was done before and after labeling the virus with Alexa Fluor 488 to monitor the HA titer during the labeling process. Infectious titers of virus stocks were also determined by plaque assay on MDCK cell monolayers.

Fluorescently labeled viruses. Binding of fluorescently labeled influenza virus was performed as previously described [27, 410, 411]. Briefly, 200 µl of virus was incubated with 25 µg of Alexa Fluor 488 (Invitrogen) in 1 M $NaHCO_3$ (pH 9.0) for 1 h at room

temperature. Labeled viruses were dialyzed against PBS using a 7,000-molecular-weight-cutoff (MWCO) Slide-A-Lyzer mini-dialysis unit (Thermo Scientific) overnight at 4°C. In all cases, labeled viruses were used in experiments the following day.

Microarray Preparation and Analysis. NHS-activated slides (Nexterion H) were purchased from SCHOTT North America, Inc. (Louisville, KY). Corning Epoxy slides were purchased from Corning Incorporated Life Sciences (Tewksbury, MA). Noncontact printing was performed using a Piezoarray printer (Perkin Elmer) as previously described [412]. All samples were printed within 10% variation of 0.33 nL at a concentration of 100 μM in phosphate buffer (300 mM sodium phosphate, pH 8.5). Before assay, the slides were rehydrated for 5 min in TSM buffer (20 mM Tris-HCl, 150 mM sodium chloride (NaCl), 0.2 mM calcium chloride ($CaCl_2$) and 0.2 mM magnesium chloride ($MgCl_2$)) and the analyses were carried out for lectins and viruses as previously described for one hour at 4°C to prevent neuraminidase activity [410, 412]. Biotinylated lectins (Vector Labs) were used as controls in the binding assay and the bound lectins were detected by a secondary incubation with cyanine 5–streptavidin (5 μg ml^{-1}, Invitrogen). For multi-panel experiments on a single slide, the array was constructed according to the dimension of a standard 16-chamber adaptor. The adaptor was applied to the slide to separate a single slide into 16 chambers sealed from each other during the assay. The slides were scanned with a ProScanArray microarray scanner (Perkin Elmer) equipped with 4 lasers covering an excitation range from 488 nm to 637 nm and the scanned images were processed to Excel spreadsheets as previously described [410, 412]. For cyanine 5 fluorescence, 649 nm (ex) and 670 nm (em) were used. For Alexa Fluor 488 fluorescence, 495 nm (ex) and 519 nm (em) were used.

Acknowledgments

This work was supported by the U.S. Department of Health and Human Services contracts HHSN266200700006C and HHSN272201400006C (National Institute of Allergy and Infectious Diseases Centers of Excellence for Influenza Research and Surveillance), and NIH grants GM098791 (RDC) and GM085448 (DFS).

SUPPLEMENTARY MATERIAL: SHOTGUN GLYCOMICS OF PIG LUNG IDENTIFIES NATURAL ENDOGENOUS RECEPTORS FOR INFLUENZA VIRUSES

Lauren Byrd-Leotis, Renpeng Liu, Konrad Bradley, Yi Lasanajak, Sandra F Cummings, Xuezheng Song, Jamie Heimburg-Molinaro, Summer E. Galloway, Marie Culhane, David F. Smith, David A. Steinhauer, Richard D. Cummings

The work in this chapter was published as supporting information in 2014 in the Proceedings of the National Academy of Sciences

Article Citation: Byrd-Leotis*, L., Liu*, R., Bradley, K. C., Lasanajak, Y., Cummings, S. F., Song, X., et al. (2014). Shotgun glycomics of pig lung identifies natural endogenous receptors for influenza viruses. *Proceedings of the National Academy of Sciences*, *111*(22), E2241–E2250. http://doi.org/10.1073/pnas.1323162111
*Authors contributed equally to this work.

Supplementary Figure 1

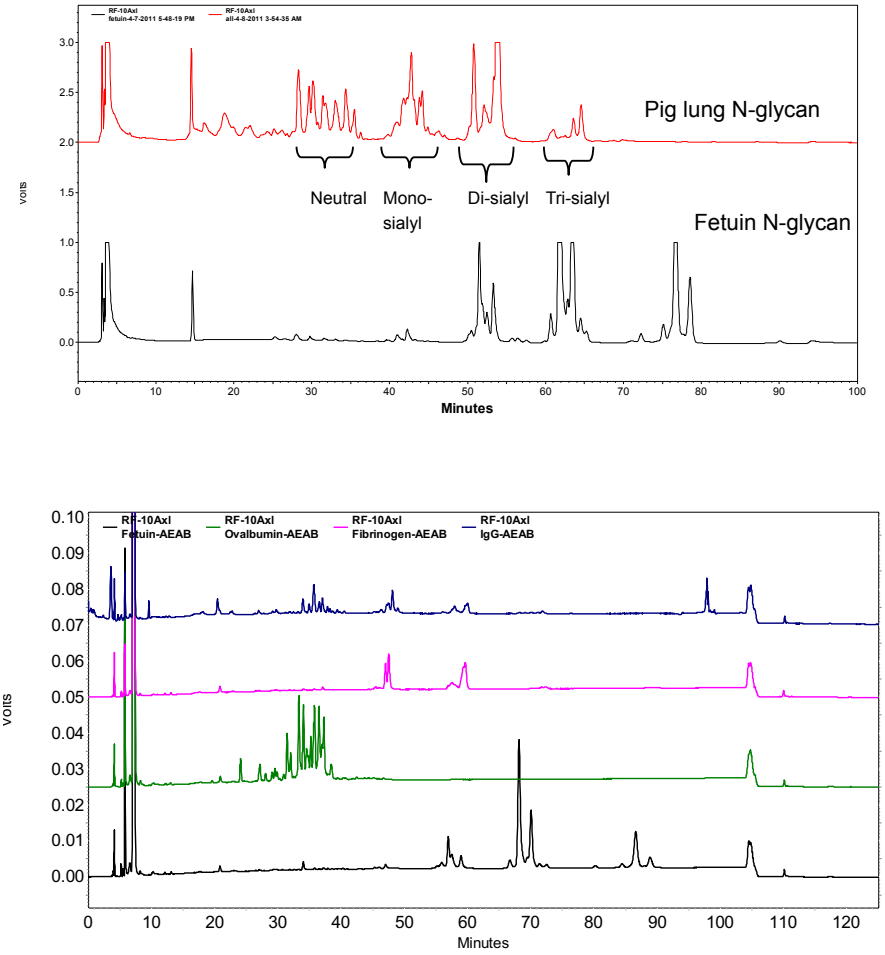

Supplementary Figure 1. **HPLC profile of pig lung N-glycans.** (A) Fetuin was treated in the same procedure as pig lung to release N-glycans and the N-glycans were linked with AEAB and used as a standard to indicate the position of neutral, mono, di and tri-sialyl N-glycans by charge separation. (B) Profiles of additional glycoproteins, ovalbumin, fibrinogen, and IgG, to highlight the regions of neutral, mono, di, tri, and larger glycans in the profile.

Supplementary Figure 2

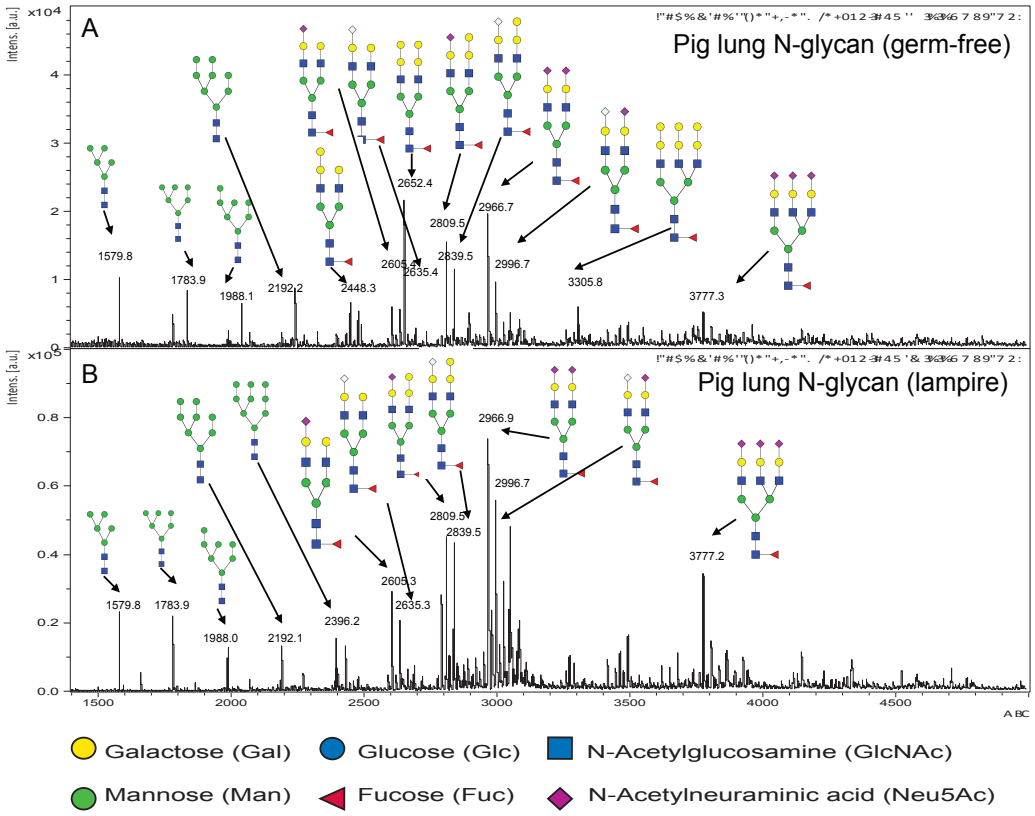

Supplementary Figure 2. **Pig lung N-glycan profiles.** (A) N-glycans from germ-free pig lung. (B) N-glycans from pig lung purchased from Lampire. The glycans were derivatized by permethylation and analyzed by MALDI-TOF.

Supplementary Figure 3

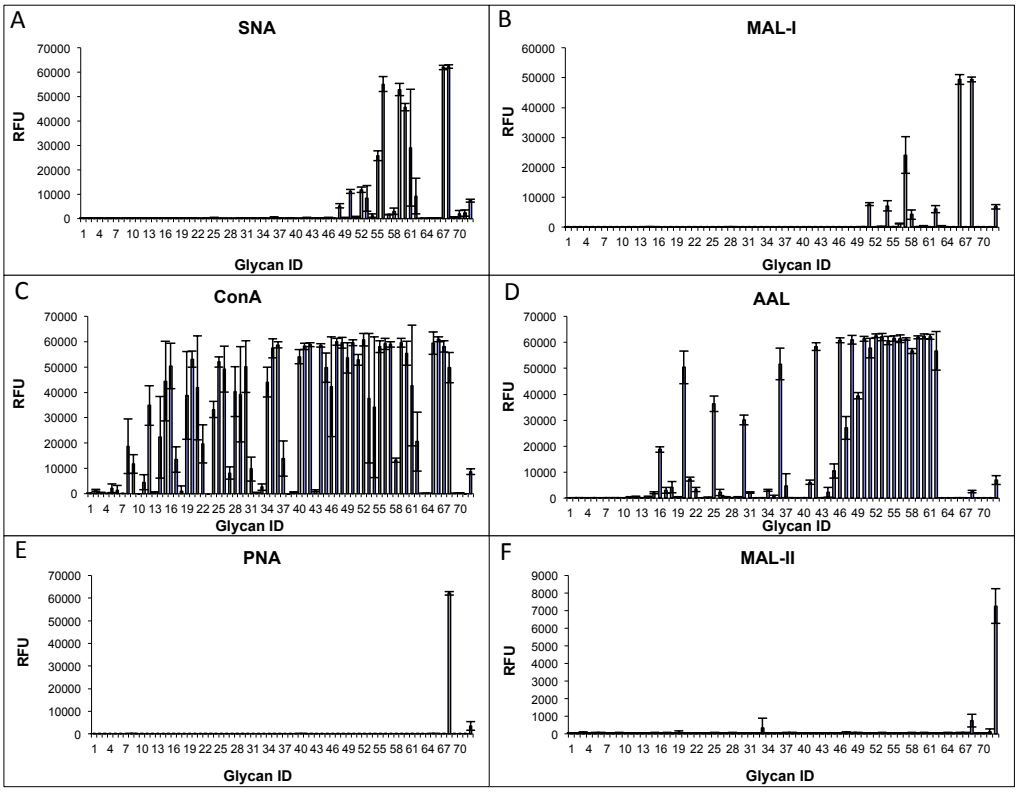

Supplementary Figure 3. **Standard lectin binding to the pig lung O-glycan microarray.** (A) The binding of SNA (binds to Sia α2-6Gal-R). (B) The binding of MAL-I (binds to Sia α2-3Gal-R). (C) The binding of ConA (binds biantennary, but not triantennary complex N-glycan structures). (D) The binding of AAL (binds fucose). (E) The binding of PNA (binds de-sialylated core 1 structure), and (F) the binding of MAL-II (binds to α2,3-linked sialic acids). Fraction 1-62 are O-glycans isolated from pig lung; standards include 63: LNnT; 64: LNT; 65: NA2; 66: NA2-2-3 Sia; 67: NA2-2-6 Sia; 68: Fetuin; 69-71: PBS; and 72: Biotin.

Supplementary Figure 4

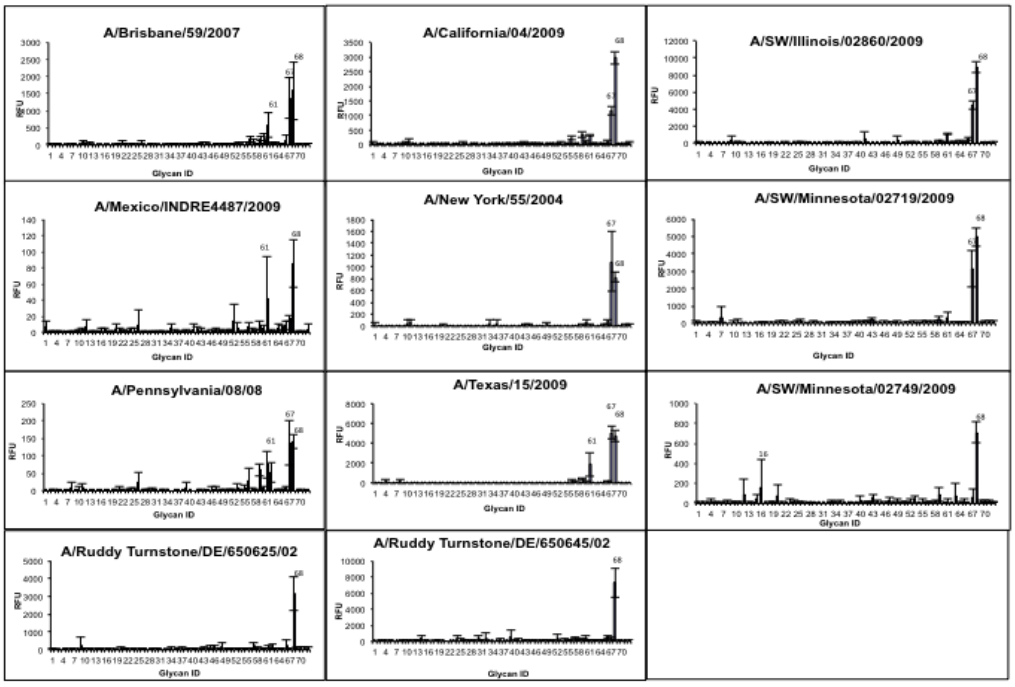

Supplementary Figure 4. **Influenza virus binding to O-glycan microarray.** Fraction 1-62 are O-glycans isolated from pig lung; standards include 63: LNnT; 64: LNT; 65: NA2; 66: NA2-2-3 Sia; 67: NA2-2-6 Sia; 68: Fetuin; 69-71: PBS; and 72: Biotin

Supplementary Figure 5

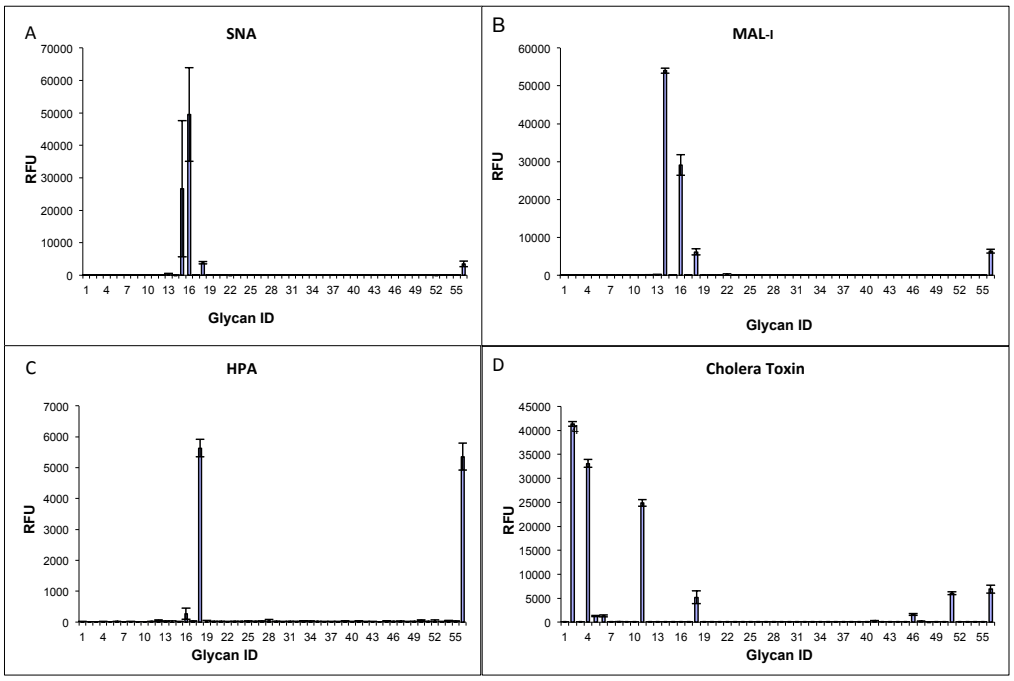

Supplementary Figure 5. **Lectin binding to pig lung GSL microarray.** (A) The binding of SNA (binds to Sia α2-6Gal-R). (B) The binding of MAL-I (binds to Sia α2-3Gal-R). (C) HPA (binds to terminal GalNAc) and (D) cholera toxin (binds to GM1). Fraction 19-54 are free glycans from GSLs; standards include 1-10 are lipid control, 11: GM1; 12: LNT; 13: NA2; 14:NA2-2-3 Sia; 15: NA2-2-6 Sia; 16: Fetuin; 17 and 55: PBS; 18 and 56: Biotin.

Supplementary Figure 6

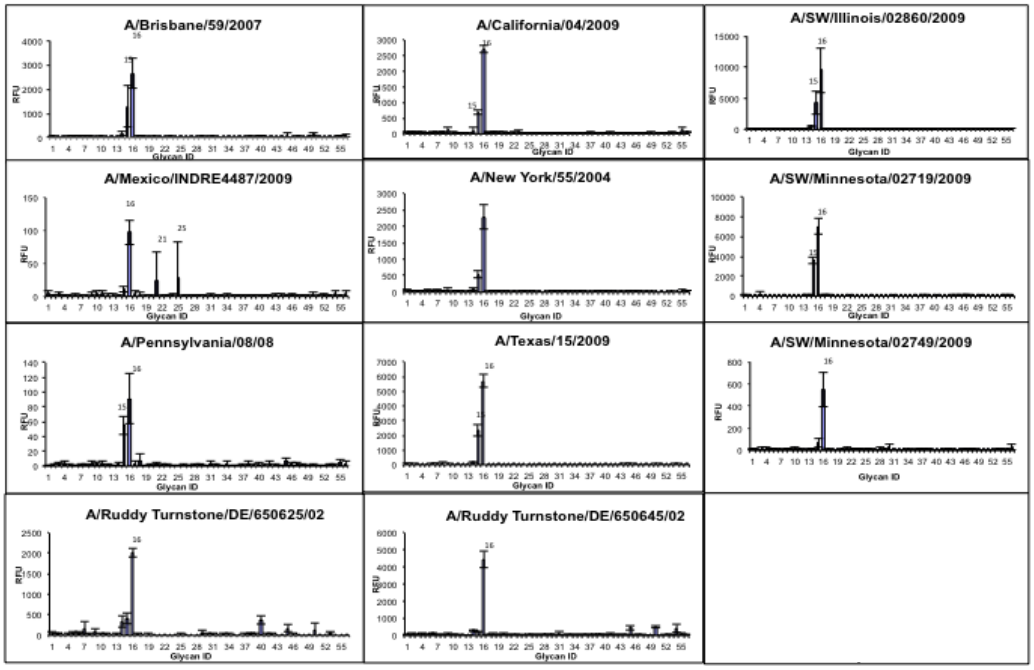

Supplementary Figure 6. **Influenza virus binds to pig lung GSL microarray.** Fraction 19-54 are free glycans from GSLs; standards include 1-10 are lipid control, 11: GM1; 12: LNT; 13: NA2; 14: NA2-2-3 Sia; 15: NA2-2-6 Sia; 16: Fetuin; 17 and 55: PBS; 18 and 56: Biotin.

SUPPLEMENTARY TABLES

Supplementary Table 1. Summary of 96 fractions of N-glycan array.

Fraction Number	**Amount (n mol)**	**Relative abundance (%)**
1	4.6	0.48%
2	4.6	0.48%
3	28.7	3.00%
4	1.9	0.20%
5	8.1	0.85%
6	10.5	1.10%
7	37.2	3.89%
8	37.6	3.94%
9	35.8	3.75%
10	28.1	2.94%
11	7.0	0.73%
12	7.1	0.74%
13	1	0.10%
14	1.4	0.15%
15	0.7	0.07%
16	2	0.21%
17	1.8	0.19%
18	4.8	0.50%
19	0.9	0.09%
20	1.1	0.12%
21	2	0.21%
22	1.6	0.17%
23	4	0.42%
24	1	0.10%
25	5.1	0.53%
26	6.0	0.63%
27	11.4	1.19%
28	10.7	1.12%
29	5.7	0.60%
30	1.2	0.13%
31	6	0.63%
32	1.1	0.12%
33	3.7	0.39%
34	50	5.23%
35	25.5	2.67%
36	16.7	1.75%
37	6.5	0.68%
38	6.7	0.70%

39	3.3	0.35%
40	25	2.62%
41	12.1	1.27%
42	4.7	0.49%
43	1.2	0.13%
44	5.4	0.57%
45	10.4	1.09%
46	5.6	0.59%
47	0.8	0.08%
48	3.8	0.40%
49	13.1	1.37%
50	6	0.63%
51	15.5	1.62%
52	20.4	2.14%
53	3	0.31%
54	2	0.21%
55	34.8	3.64%
56	11.5	1.20%
57	7	0.73%
58	4	0.42%
59	3.7	0.39%
60	8.2	0.86%
61	17.7	1.85%
62	8.7	0.91%
63	5.7	0.60%
64	9.6	1.01%
65	29.3	3.07%
66	15.5	1.62%
67	164	17.17%
68	8	0.84%
69	3.7	0.39%
70	3.2	0.34%
71	1.8	0.19%
72	0.8	0.08%
73	0.8	0.08%
74	3.8	0.40%
75	1.3	0.14%
76	0.8	0.08%
77	0.9	0.09%
78	2.7	0.28%
79	1	0.10%
80	11	1.15%
81	2.1	0.22%
82	4.7	0.49%
83	7.2	0.75%

84	11	1.15%
85	6.1	0.64%
86	4.6	0.48%
87	7.8	0.82%
88	11.1	1.16%
89	7.9	0.83%
90	0.7	0.07%
91	1.3	0.14%
92	0.9	0.09%
93	1.1	0.12%
94	2.6	0.27%
95	3	0.31%
96	1.5	0.16%

Supplementary Table 2. Lectin binding to the Pig Lung Shotgun glycan microarray.

See online material- Proceedings of the National Academy of Sciences, 2014 vol. 111 (22) pp. E2241-E2250

Supplementary Table 3. Virus binding to Pig Lung Shotgun glycan microarray

See online material- Proceedings of the National Academy of Sciences, 2014 vol. 111 (22) pp. E2241-E2250

Supplementary Table 4. Viruses binding to the Pig Lung Shotgun glycan microarray and rationale for characterization

See online material- Proceedings of the National Academy of Sciences, 2014 vol. 111 (22) pp. E2241-E2250

Supplementary Table 5. Structural analysis of selected fractions with HPLC profiles and MALDI spectrum

Fraction Number	**MS (positive) Da (treated with neuraminidase)**	**MS (negative) Da (treated with neuraminidase)**	**HPLC (normal phase)**	**Proposed structure (Hex, HexNAc, Fuc, NeuAc)**
34	1973		mono	5411 (α 2-6)
64	1827		Di	5402 (α 2-6)
56	1973		Di	5412 (α 2-3)
81	2338		Tri	6513 (α 2-3)
83	2338 (minor)	2028 (major)	Tri	5412 + sulfate (major), 6513 (α 2-3)
88	2337		Tri	6513 (α 2-6)

Fraction 34 HPLC

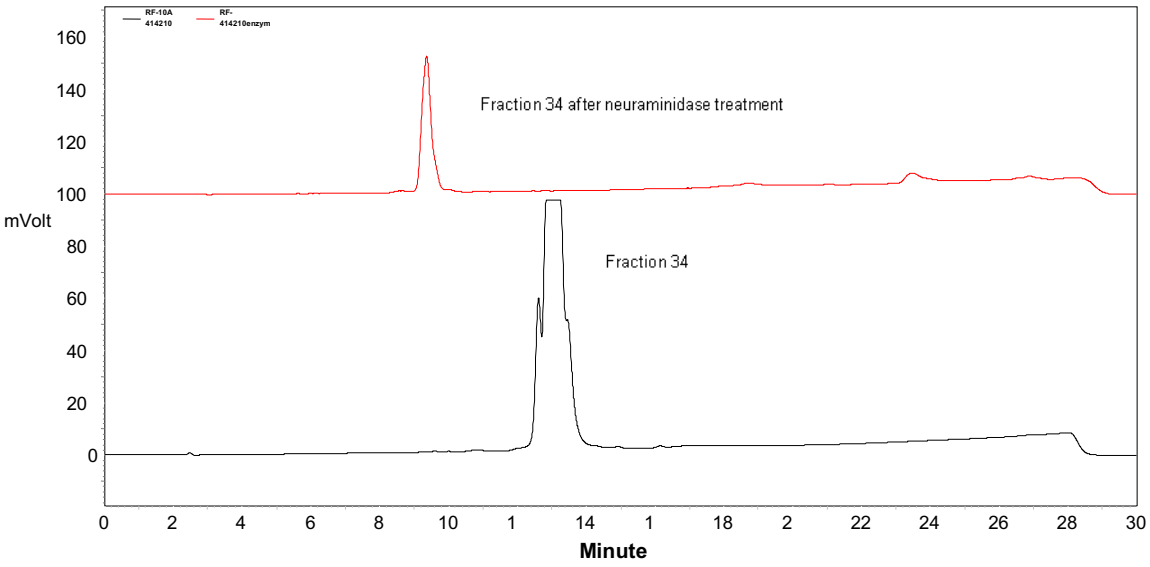

Fraction 34 after neuraminidase treatment (positive)

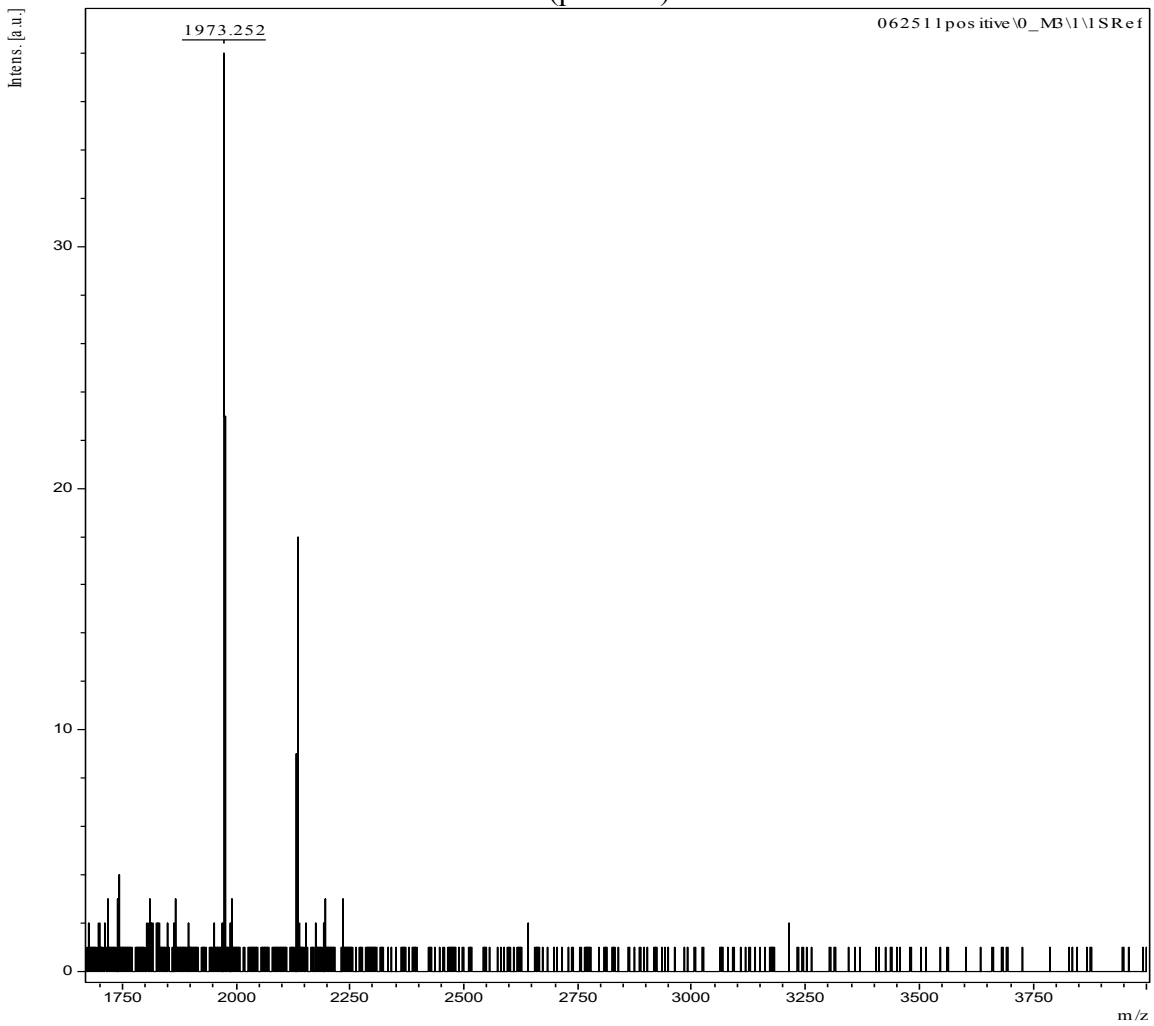

Fraction 56 HPLC

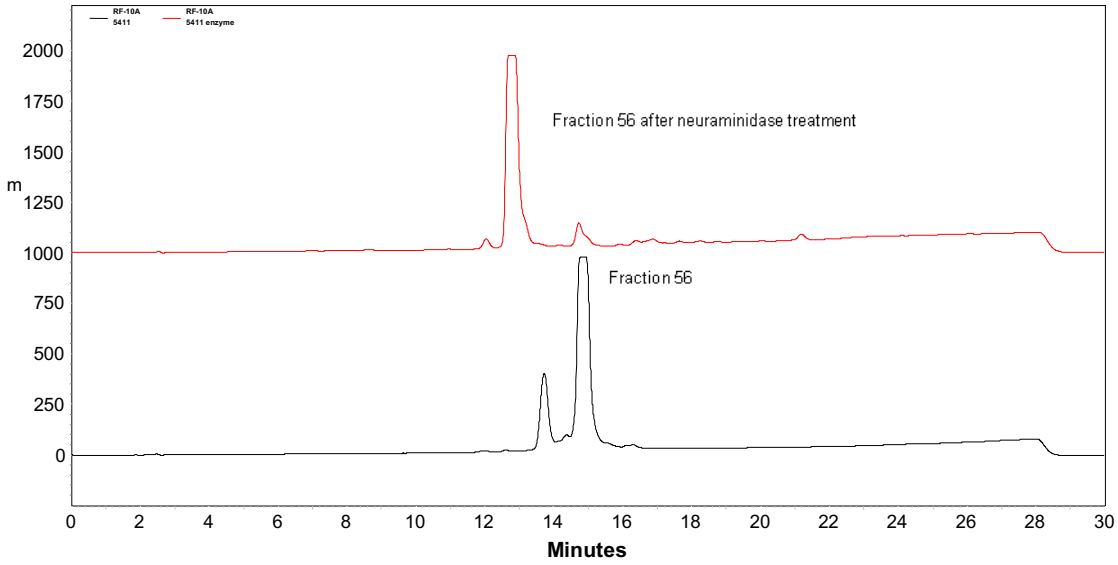

Fraction 56 after neuraminidase treatment (positive)

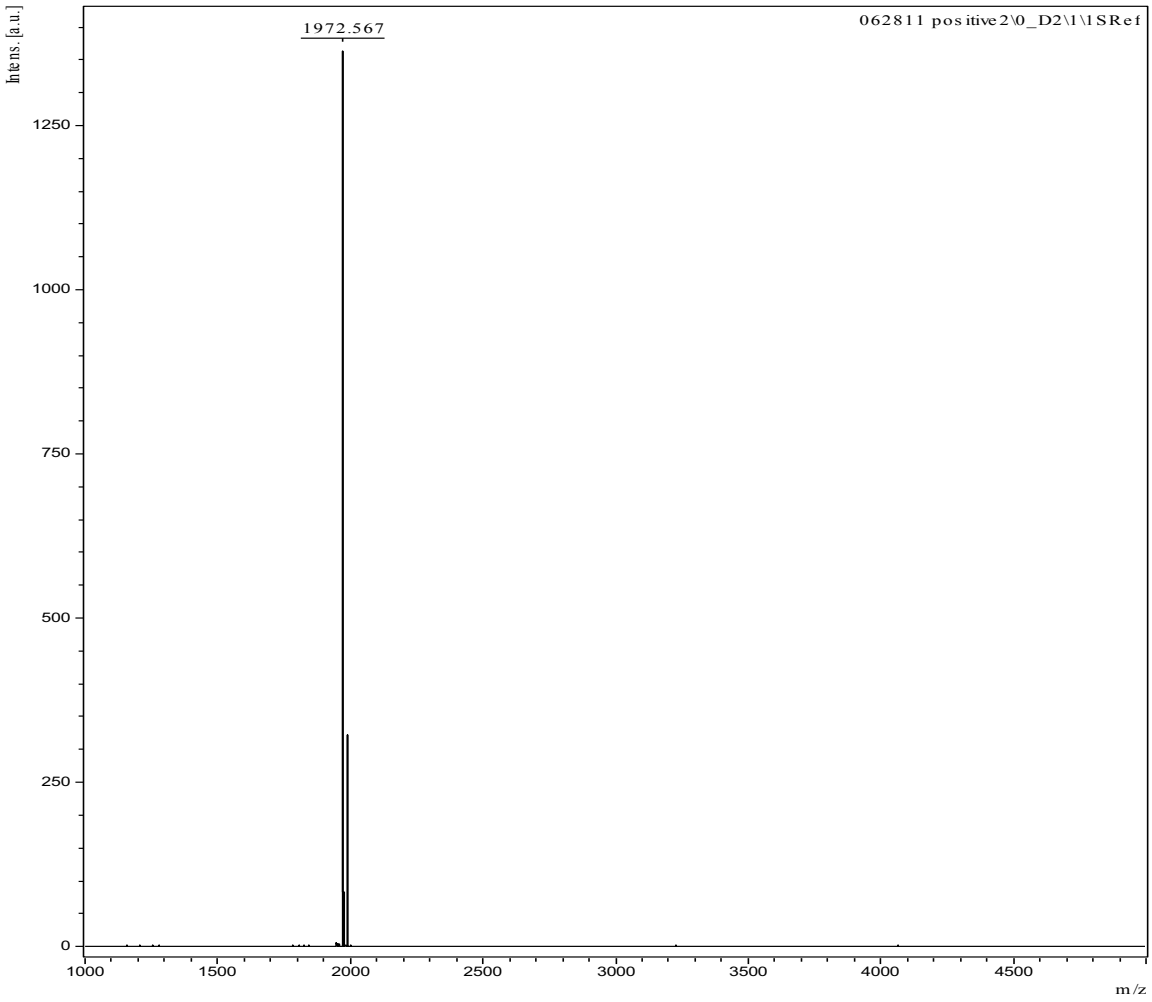

Fraction 64 HPLC

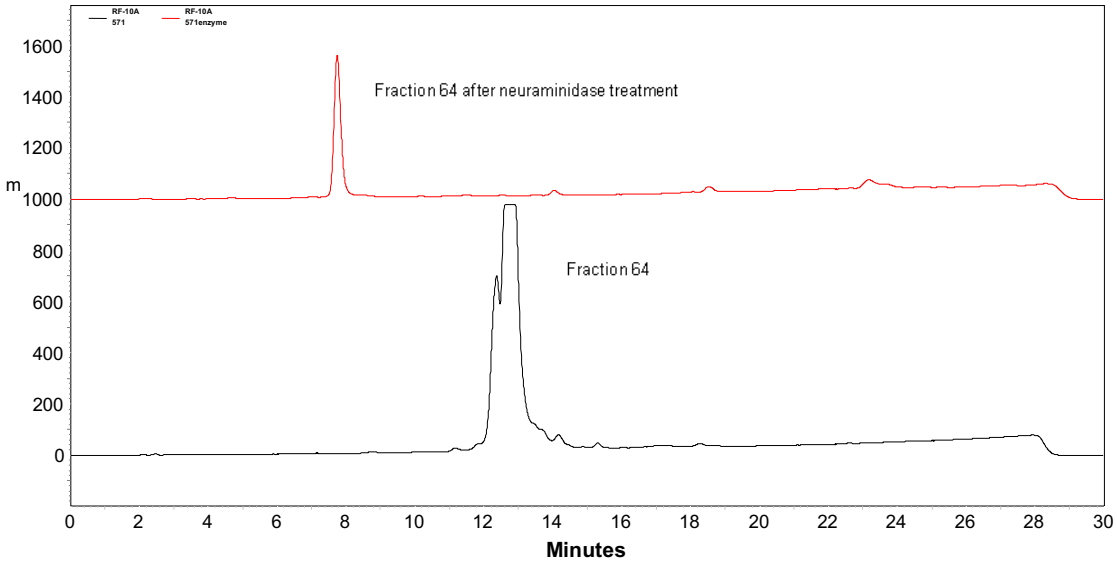

Fraction 64 MS after neuraminidase treatment (positive)

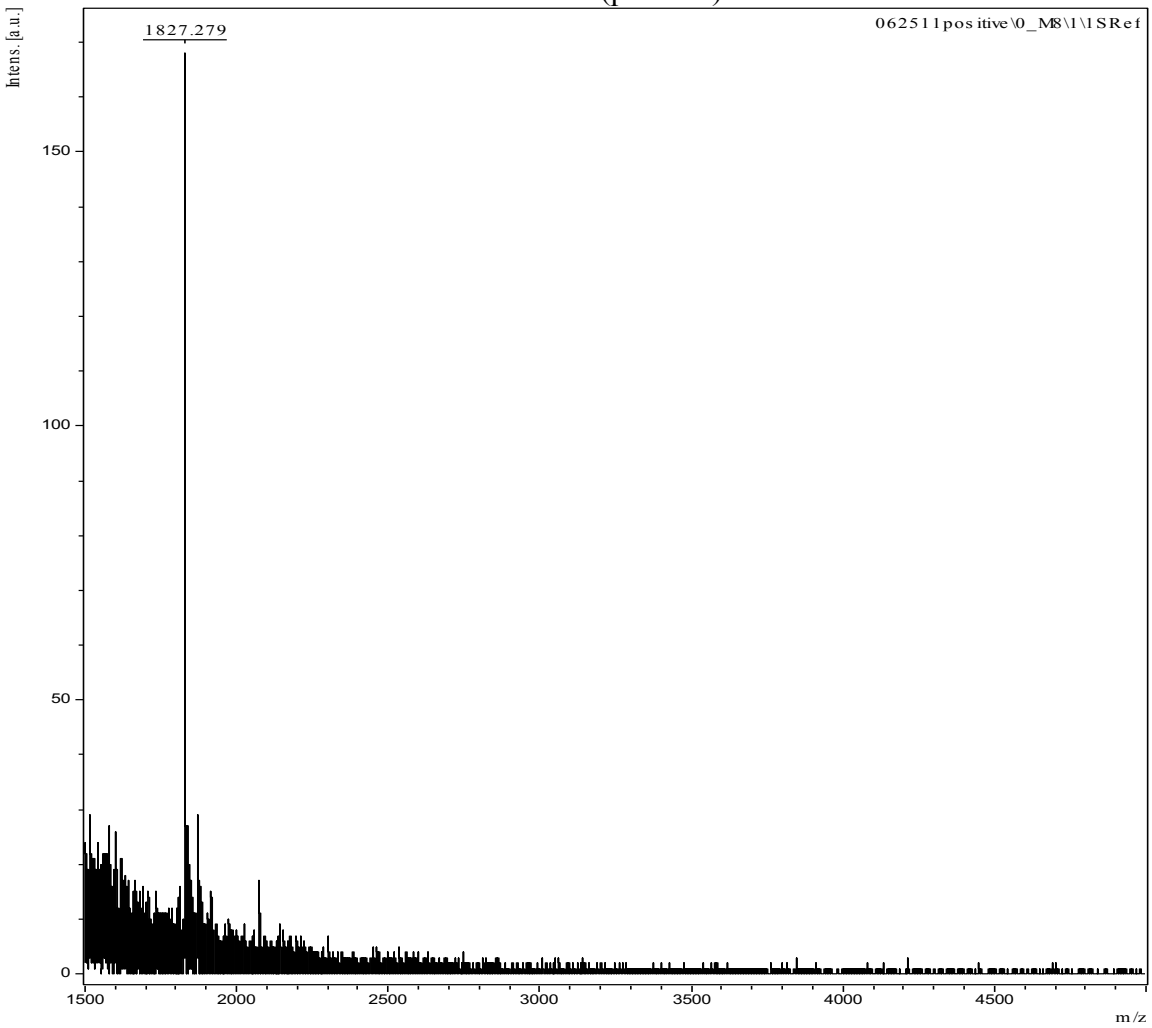

Fraction 81 HPLC

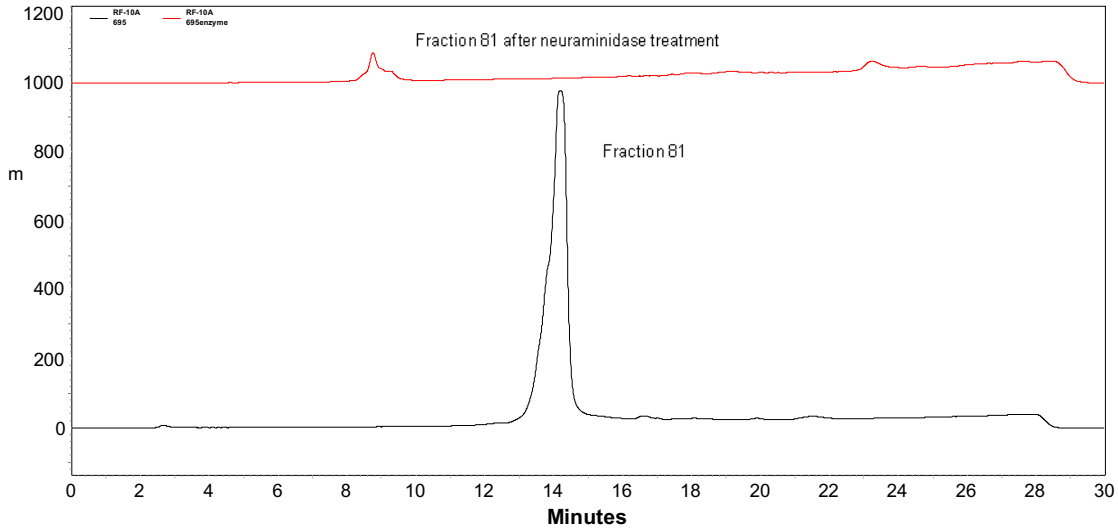

Fraction 81 MS after neuraminidase treatment (positive)

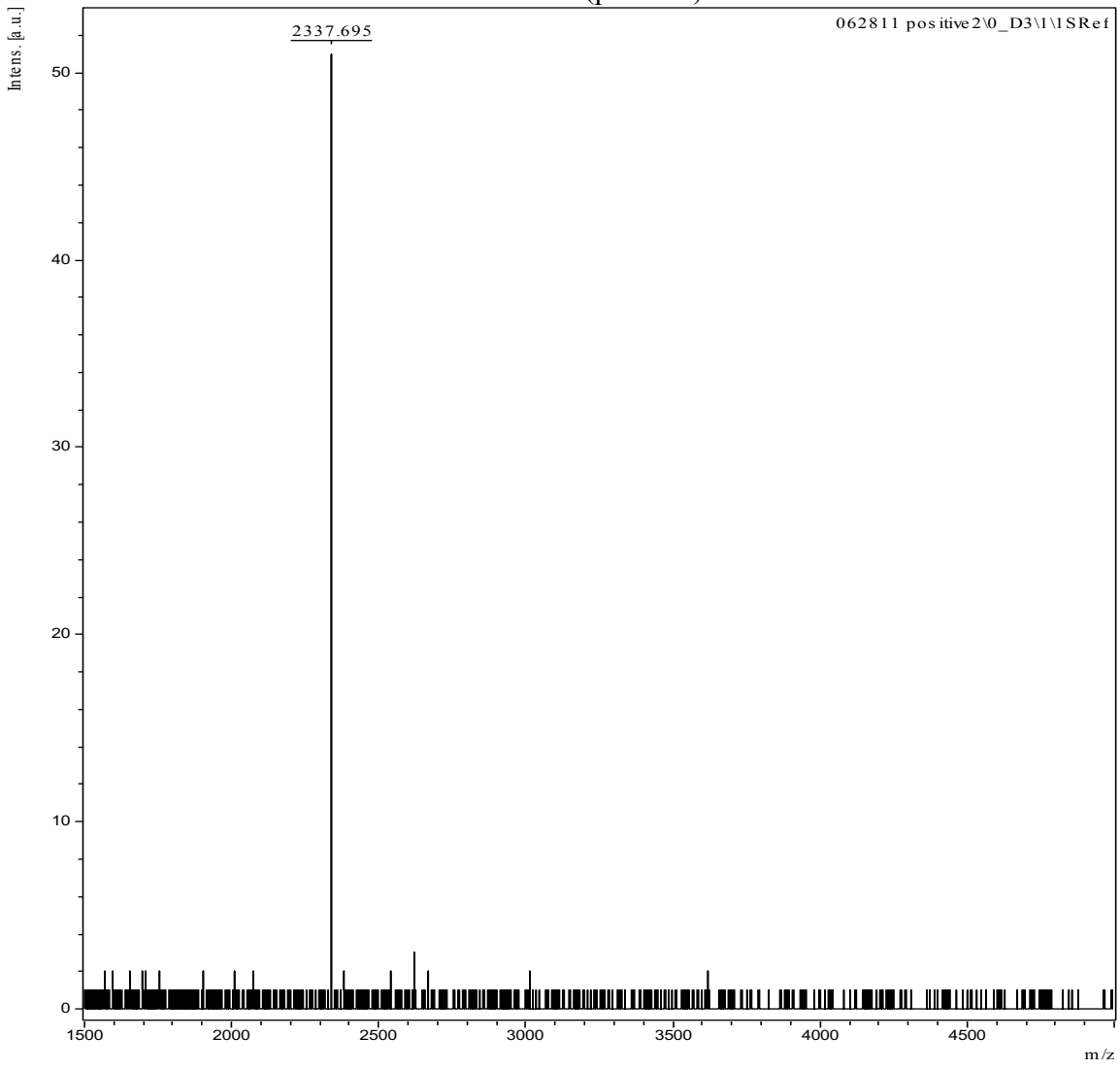

Fraction 83 HPLC

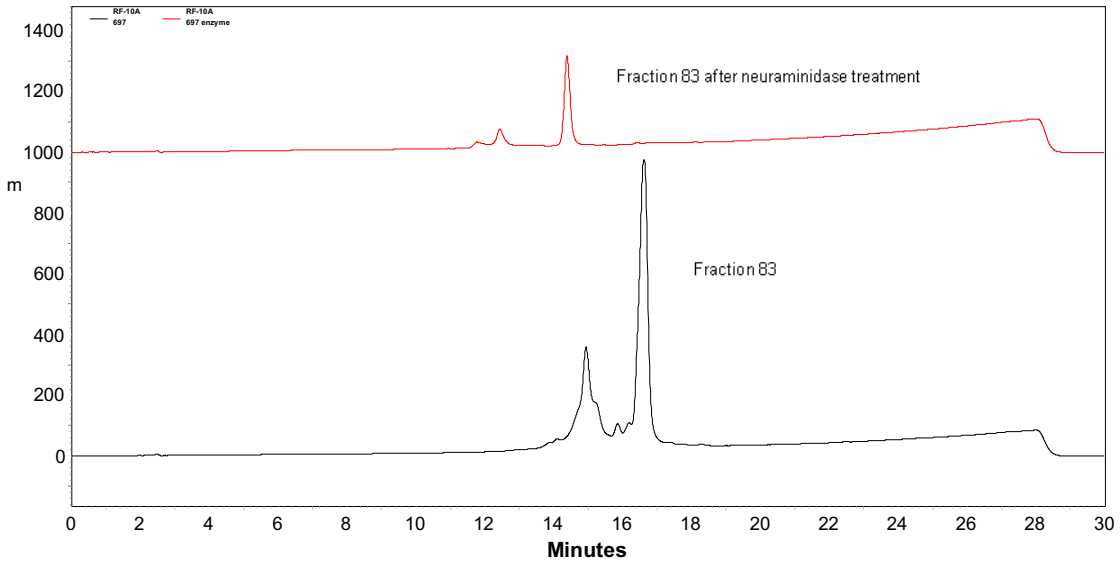

Fraction 83 MS after neuraminidase treatment (negative), major fraction

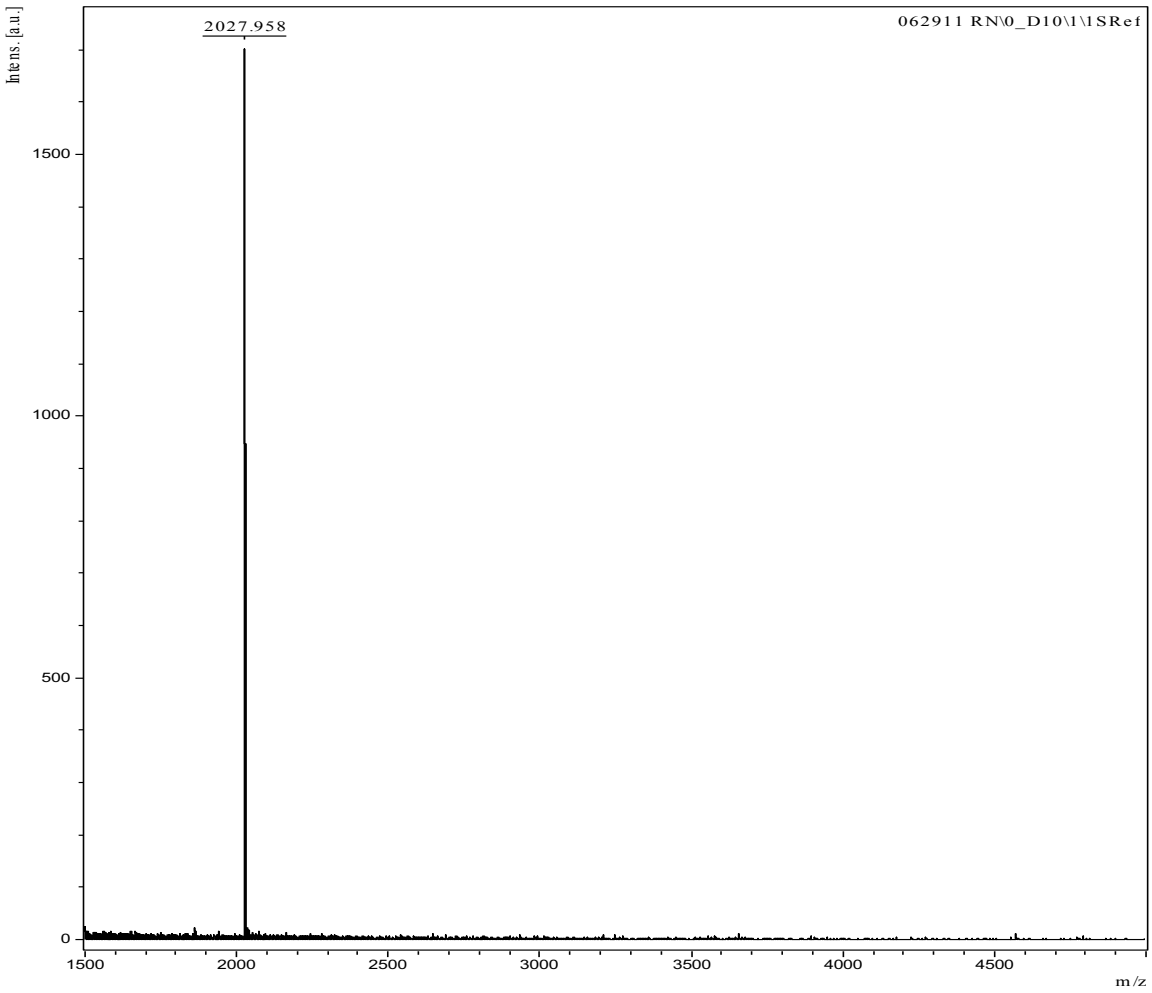

Fraction 83 MS after neuraminidase treatment (positive), minor fraction

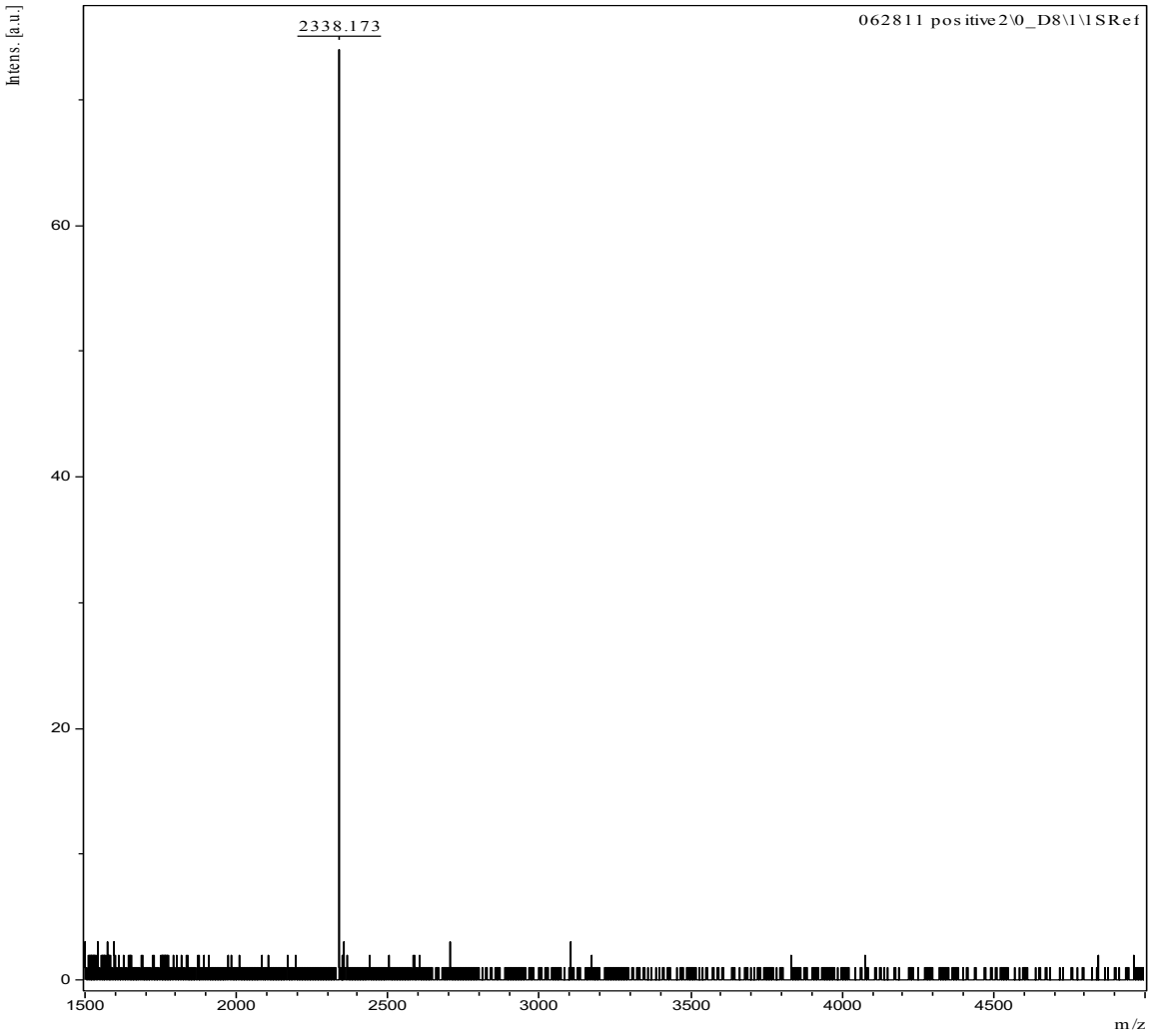

Fraction 88 HPLC

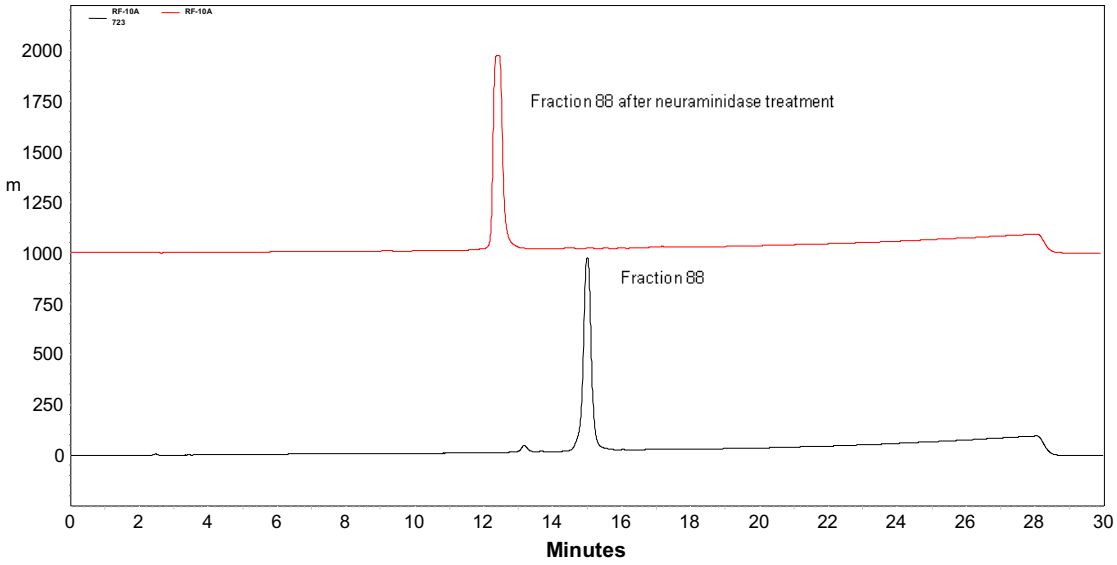

Fraction 88 MS after neuraminidase treatment (positive)

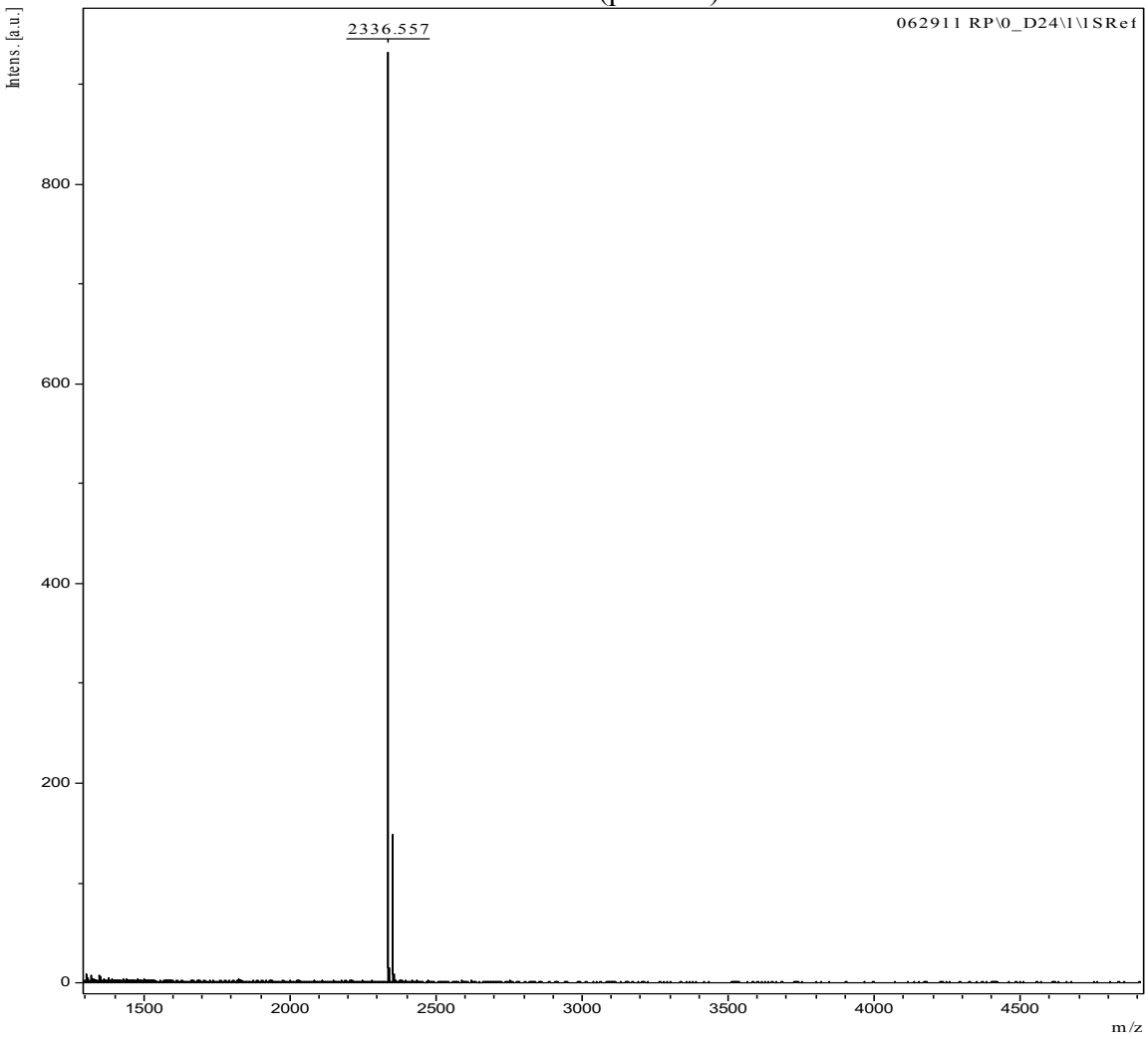

CONCLUSIONS AND FUTURE STUDIES

The processes of interspecies transmission and host adaptation are multi-factorial and just beginning to be understood. In order to gain a deeper insight and, potentially, a more effective level of preparedness, the study of these process must be widened to a systems approach instead of a narrow emphasis on one protein or aspect of influenza biology. This work has focused on the process of initiation of influenza A virus infection mediated by the hemagglutinin protein with future work planned to examine the role of the neuraminidase. In addition to addressing these questions, we sought to increase the biological relevance of our assays and as such, created revolutionary technology that allowed for the isolation of natural endogenous receptor structures for influenza. Our approach, combining the strengths of molecular virology and glycomics allows for the development of innovative assays to study of the process of influenza infection within the context of host biology.

The work presented here examines the process of entry in reverse chronological order starting with HA mediated fusion, then HA receptor binding and the glycans present in natural lung tissue. As discussed, fusion occurs once the virion has been internalized by the target cell and the low pH environment of the endosome induces the structural rearrangement of the HA protein. Through structural studies and experiments with fusion mutants, the conformational change of HA has been described with specific emphasis placed on the function of potential ‘trigger’ residues. Conserved residues 58 and 112 had previously been identified as important for HA stability in an H3 subtype

[60, 174, 357, 358]. Here we have expanded those studies to include characterization of additional subtypes representative of both group 1 and group 2 HAs and found that for most of the strains we examined, a K58I mutation lowers the pH of fusion, increasing the acid stability of the HA. The orientation of the sidechain of the original amino acid, lysine, at position 58 is shifted between the two groups, tilting towards the interior of the trimer in group 1 HAs and out in solution for group 2 HAs. It is interesting then, that the original residue is conserved between groups and that this particular mutation can have the same effect for all HA subtypes. A D112G mutation has the opposite effect, raising the pH of fusion and highlighting a necessary interaction mediated by the longer side chain of aspartic acid that is abrogated by the exchange for glycine. Though these mutations were induced in an experimental setting and not necessarily characterized in isolated strains, such mutations that do increase acid stability have been identified upon a transmission event [369, 413, 414]. For the H1, H2, and H3 subtypes, the K58I mutation lowers the pH of fusion of the avian strain to the threshold pH for the wildtype human strains of the same subtypes. This particular residue may not be frequently mutated in interspecies transmission events, but it does illustrate the changes needed for lowering the pH of fusion that may be required for adaptation to a mammalian host. In continuation of this work, we have begun to examine the roles of residues 17 and 111 in the acid stability of the HA (Appendix I). These residues are conserved within HA group classifications, with group 1 HAs including a tyrosine at 17 and a histidine at 111 and group 2 HAs including a histidine at 17 and a threonine at 111. The histidine is found in both groups, though in different positions and indicates that the sum of the hydrogen bond interactions may be greater than the interactions mediated by individual residues. The same principle

may apply to residue 58, conserved though positioned differently with consistent mutation phenotypes across the groups. The compound interactions determined by the structural order of residues is different between the group classifications making it possible that group specific mutations may be identified that lead to a propensity for interspecies transmission or increased virulence.

Prior to HA-mediated fusion, the cell must endocytose the virion based on recognition of and interaction with the receptor, also facilitated by HA. We studied this functionality in the context of natural receptors and the differences in receptor preference between mammalian and avian strains. Though the accepted dogma reduces receptor binding specificity to the terminal sialic acid linkage, we've found that proximal glycan determinants narrow the preferred range of receptors. The new dogma might be that influenza A viruses bind to a specific set of glycan structures terminating in sialic acid and while avian and mammalian viruses typically bind within their accepted linkage group (2,3 vs 2,6) not all available glycans are utilized as receptors. Our work has identified 8 natural endogenous receptors in the swine lung that are recognized by a quorum of the panel of viruses studied. Features of the common receptors include branched structures and core fucose moieties. In the isolation of the glycans, we learned valuable information about the glycomic composition of the swine lung. We were able to isolate N-glycans, O-glycans, and glycolipids, though only N-glycans were bound by our panel of viruses. We did not find large polylactosamine structures that have been implicated in receptor binding previously and did find structures not represented on the CFG arrays, highlighting the significance of these natural studies which lend more biological relevance to the virus-receptor interaction.

Future directions involve exploring the glycomics of both the swine lung and the human lung. A new method, oxidative release of natural glycans or ORNG, has been developed and will be used to release the glycans from lung tissue [415]. Previous methods, including those described in our shotgun glycomics work, have relied on enzymes such as PNGaseF, with protocols targeted to processing small amounts of tissue, to release the N-glycans. The ORNG method is appropriate for large scale preparation of glycans and is based on a chemical reaction with sodium hypochlorite, a much cheaper alternative to the enzymatic reactions used previously. The N-glycans from the pig lung will be extracted and compared to the number and range of glycans isolated using the traditional method. This comparative experiment will validate the use of the ORNG method, and the re-extraction of the pig lung glycans will allow us to selectively compartmentalize the tissue prior to homogenization so that localization of glycan species within the lung can be determined. The glycans will be used to generate a new set of PL-SGM slides, with presumably more structures available since the sodium hypochlorite will release those glycans that might have been unable to be acted on by PNGaseF. These slides will continue to be useful for influenza binding studies, especially in the characterization of strains primed for interspecies transmission. Ultimately having the natural tissue array will be very useful in regular surveillance of commercial porcine and avian populations, tracking the receptor recognition properties of circulating strains with an eye for transmission potential and disease implications.

In addition to using the ORNG method for treatment of swine lung, we have begun work on glycan extraction of human lung tissues using donor organs deemed unfit for transplant. This study will not only be the first characterization of the glycome of a

human organ, but will also provide an unparalleled look into influenza receptor binding on a large scale. We will follow the model of our work with the swine lung, and print a shotgun array, without characterizing the glycan species prior to binding studies. We will interrogate the arrays with the same representative panel of viruses for initial characterization and will identify the glycans to be structurally analyzed based on binding. MAGS-based approaches, described in our shotgun glycomics work, will be used to sequence the glycans. We expect the initial characterization to reveal endogenous natural receptors of influenza virus in the human lung and that the array will become an invaluable tool for the continued study and surveillance of influenza. In addition to the significance for the field of influenza research, this work will provide the first comprehensive description of the glycome of a human organ. Of the 4 major biological components: nucleic acids, proteins, lipids, and carbohydrates, carbohydrates are by far the most diverse group and also the least well characterized. The implications for basic biology and disease are profound, as evidenced by genetic disorders related to carbohydrate synthesis and metabolism. Having a depiction of the glycan representation of an organ will advance the field of glycomics significantly and will be the first step in identifying and characterizing the human glycome. These arrays and the glycan extraction procedure will become tools, useful for comparing the representative glycome of human to swine species with interest in viral transmission, for examining a range of pathogen interactions including other respiratory viruses and bacterial pathogens such as *Pseudomonas aeruginosa*, for exploring host glycosylation deficiencies, and for characterizing the effects of age, environment, smoking etc. on the glycan presentation in the human lung.

In addition to using the natural lung arrays to identify biologically relevant structures recognized by HA for binding, we will examine the role of NA, characterizing the preferred substrates and then examining the functional balance with HA in the context of receptor interaction prior to entry. As previously discussed, the necessity of a functional balance of the activities of HA and NA has been well-established both in collected clinical isolates and in experimental settings. The general idea of influenza replication relegates the functions of neuraminidase to cleaving sialic acid off would-be inhibitory mucins and facilitating the release of nascent virions by removing sialic acid that would encourage HA-mediated aggregation. However, we postulate that neuraminidase may play an important role at the cell surface, impacting the receptor binding by acting on receptors that could be bound by HA. We expect the field of endogenous HA receptors identified on the natural arrays in the absence of NA activity to be narrowed by the introduction of a functional NA. In addition to the balance of HA affinity with NA activity, we expect that a balance of substrate specificity also exists and may have untold implications for receptor specificity and cellular tropism. Currently, studies to assay the specificity and activity of neuraminidase rely on artificial substrates, sialyllactose derivatives and 2'-(4-Methylumbelliferyl)-a-D-N-acetylneuraminic acid, MUNANA. Though these substrates give a general idea of linkage based specificity, they don't reflect the structures in natural infection or even generic N-glycans. For this reason, we are designing and constructing a set of glycans that more closely represent the structures isolated from natural tissue (Figure 1).

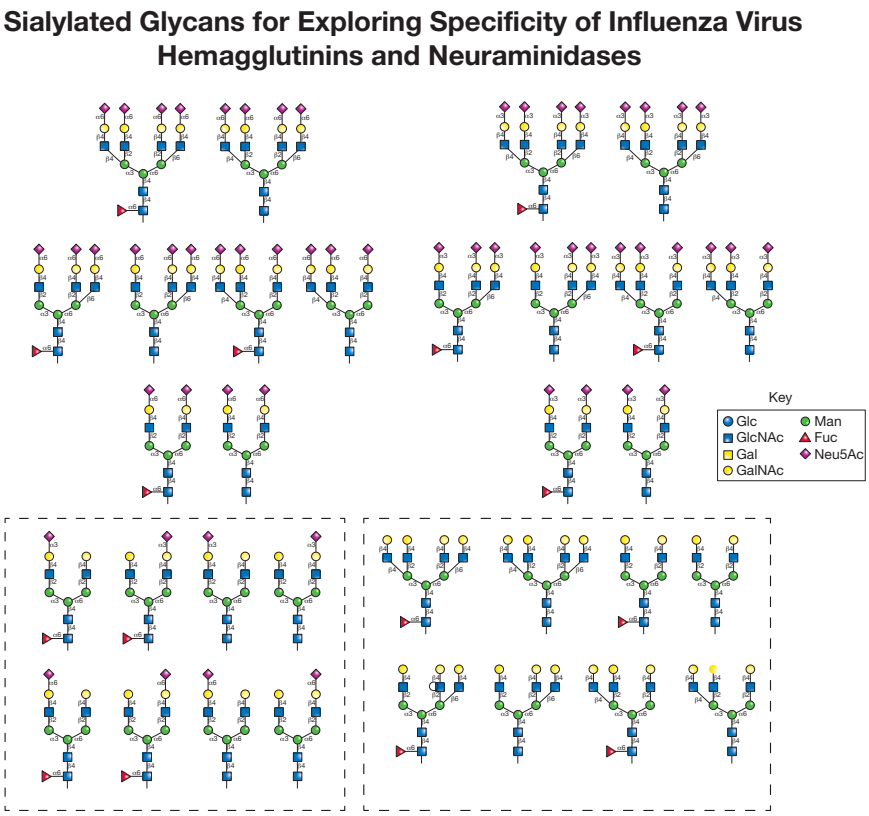

Figure 1. Core set of glycans developed for neuraminidase assays. The same basic structure is represented with terminating sia of both linkage types and no sialylation.

This core set of glycans will range from bi-antennary to tetra-antennary and will include both 2,3- and 2,6- terminal sialic acids for each backbone. The entire set will also be replicated with a core fuscose and without sialylation. The core set of glycans will all start from a precursor siayloglycopeptide isolated from egg yolks [416]. This structure will be fluorescently tagged and then modified by a series of enzymes to introduce the structural features necessary to create the different glycan species.

This core set of glycans will be utilized in three separate assays used to determine the specificity of the neuraminidase. The first of these assays will take advantage of the charged natured of the sialic acid. We will utilize ion exchange chromatography, with QAE-sephadex columns in a high pH Tris buffer. The QAE is highly positively charged

and will be bound by negatively charged sialylated glycans. We will treat each linkage pair of our core set of glycans with whole virus at 37°C to allow for sialidase activity. We will then be able to run the entire preparation over the column and measure, via fluorescence activity, the concentration of desialylated glycans in the run through. Comparison of the desialylation of the 2,3 linked structure versus its cognate 2,6 linked structure will enable us to characterize the substrate specificity of different NAs and should allow for the study of the enzymatic rate kinetics. The second assay will utilize the glycan reductive isotope labeling, GRIL, technique [417] to label one linkage representative of each pair, such that the structures can be identified separately via MALDI mass spectrometry. For this procedure, one glycan structure will be labeled with a heavy isotope, aniline C-13, that will result in a 6 dalton shift of the MALDI spectrum of the labeled glycan in comparison to the original unlabeled glycan. A population of glycans will be treated with virus under conditions that allow for neuraminidase activity. At the conclusion of the reaction, that population plus the cognate, unlabeled, untreated population will be mixed together and analyzed via MALDI-mass spectrometry. The untreated glycans will serve as internal controls, while the treated glycans should be reduced in amount corresponding to the cleavage activity of the neuraminidase. This assay will allow for a quantitative measurement of structural and linkage preference by different influenza NAs. Finally, the complete set of core glycans will be printed in a microarray format in order to assess the potential impact on HA binding. The arrays will be treated with virus at 37°C to allow for NA activity. Lectin profiles before and after neuraminidase treatment will be compared. Sialidase activity will be revealed by a decrease in SNA or MAL binding on the treated slide compared to an untreated slide. To

examine the effect on HA receptor availability, the treated slide will be treated again with labeled virus to obtain an HA binding profile. Just as with the lectin profile, this will be compared with the HA binding to an untreated slide. We expect to see a reduction in the number of structures bound by the HA, indicating the NA-mediated cleavage of potential receptors.

Our work on HA has scrutinized and continued characterization of both functions related to entry: fusion and receptor binding. We have examined the importance of conserved residues within the fusion peptide pocket identifying their impact on fusion conditions, with implications for vaccine stability and for understanding transmission determinants. We have also characterized the broad receptor preference trends of avian, swine, and human strains of IAV. We determined the structural composition of glycans that can be utilized by the HA for receptor binding and then isolated and identified the endogenous glycans bound in swine lung tissue. By narrowing the field of potential glycan receptors, we have a greater understanding of receptor determinants and virus-receptor interaction within the host. The analysis of human lung tissue will allow for the identification of the receptors available to and bound by influenza A viruses in the course of human infection. The implications of these results are far reaching, impacting our understanding of not only virus-receptor interactions, but also receptor localization within the general site of infection and even host adaptation processes. The characterization of NA specificity, in the context of further defining HA:NA balance, will expand our knowledge of the functionality of both surface proteins with implications for the greater issues of influenza biology such as host adaptation and interspecies transmission as the virus mediates natural infection.

APPENDIX: ANALYSIS OF FUSION PEPTIDE POCKET RESIDUES OF INFLUENZA A VIRUS HEMAGGLUTININ AND THEIR EFFECT ON THE PH STABILITY OF THE PROTEIN.

Lauren Byrd-Leotis, Wei Wang, and David Steinhauer

The work in this appendix is being prepared for publication.

Abstract

Much is known about the process of structural rearrangement and about the importance of regions within the fusion peptide pocket of IAV HA, however the impact of individual residues HA1 position 17 and HA2 position 111 on HA stability and pH of fusion have not been characterized outside a select few subtypes. Both residues have been postulated to be involved in the triggering process, as HA1 17 is buried within the trimer upon cleavage activation, making contacts within the fusion peptide pocket, and HA2 111 is found in the portion of the long helix that restructures allowing for the direct 180° bend of the molecule as it transitions to the post-fusion conformation. The residues are highly conserved within the confines of the HA group classifications. Our results indicate that for the group 2 HAs which incorporate a tyrosine at position 17, the stability of the HA was increased and the pH of fusion was lowered by the incorporation of the histidine at that position. For the group 1 HA subtypes, fusion is dependent on the contacts made by the histidine at position 111. Removing the polar functional groups by incorporating an alanine at that position completely prevents fusion despite the protein's unchanged susceptibility to proteases and expression at the surface. A mutation to histidine at this residue for the group 2 HAs, a reversion to the group 1 sequence, increases the pH of fusion. These results present an extensive characterization of the significance of both positions in the fusion process and provide additional insight into HA stability phenotypes in the context of group classifications.

Introduction

The hemagglutinin (HA) protein of influenza A virus mediates the fusion of the virion membrane with that of the endosome to allow for the genetic complexes, the vRNPS, to enter the cell and begin replication. HA is a type 1 transmembrane protein that associates as a homotrimer on the surface of the virion and adopts three conformations throughout the course of entry. The first, HA0, is the pre-cleaved, pH neutral form of the trimer. Upon cleavage by host proteases, the HA assumes a fusion primed state with the N-terminus of the fusion peptide internalized within the fusion peptide pocket [346-348]. Acidification of the environment induces the conformational changes that result in the extrusion of the fusion peptide and insertion into the target membrane [12, 47]. The stability of the HA molecule relates to the pH of fusion at which acid-induced conformational changes occur. It has been postulated that the environmental pH at the sites of infection in different host species could be a barrier to cross species transmission. Several factors have been implicated in the successful transmission of an avian virus to mammalian host such as HA receptor binding and recently, HA stability [29, 196, 276, 279, 335, 337-343, 345]. Currently only three of the sixteen hemagglutinin (HA) subtypes circulating within the avian reservoir have successfully crossed the species barrier to become established in human hosts [244]. For all HA subtypes, proteolytic activation and fusion have been extensively characterized [49] and residues important for stability phenotypes such as 17, 58, 106, 111, and 112, etc. have been identified and studied in some subtypes [68, 174, 357-359].

Of particular interest are the residues of HA1 position 17 and HA2 position 111 (Figure 1). These residues are highly conserved among the structural classifications of group 1 and group 2 HA subtypes [186, 361].

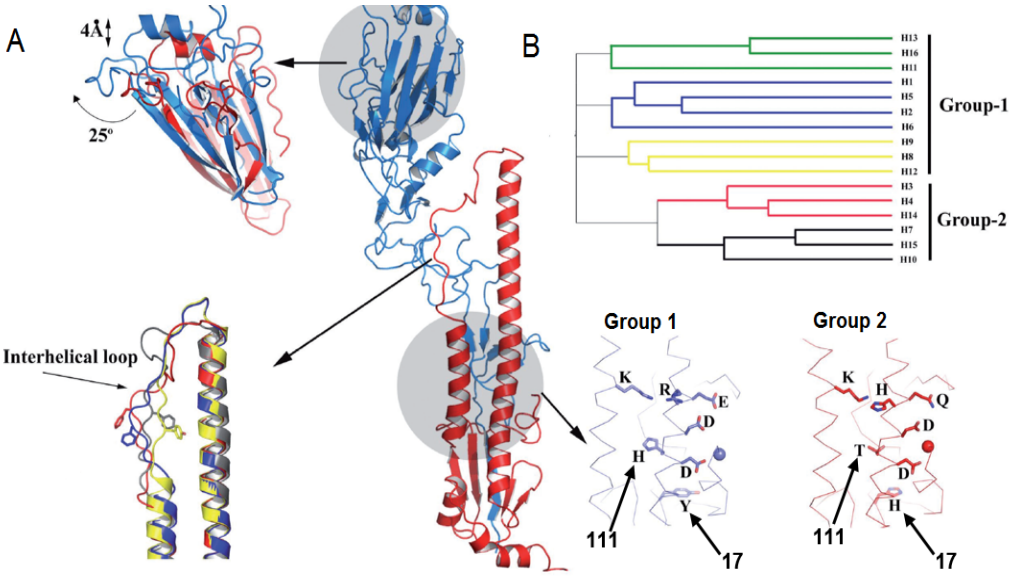

Figure 1. Structural and phylogenetic comparison of group 1 and group 2 HAs **A**. The structure of two superimposed HA monomers, group 1 and group 2, with the fusion peptide pocket expanded for both. The residues at positions 17 and 111 are highlight. **B**. The division of IAV subtypes into groups and clades.

The HA1 17 residue is internalized within the fusion peptide pocket after cleavage of the HA0. There it makes contacts with other residues in the pocket that are lost upon acidification. For Group 1 HAs, this residue is a tyrosine and group 2 HAs, it is a histidine. The ability of this residue to form hydrogen bond contacts with the fusion peptide relates to the stability of the activated pre-fusion structure and directly affects the pH of fusion. The HA2 111 residue is located in the long central helix, in an area that undergoes the helix-to-loop transition as the HA moves from the pH neutral to the acidified form. This loop structure allows for the formation of the rod-like structure of the transmembrane domain and fusion peptide which will ultimately insert into the target

membrane. In group 1 HA subtypes, the amino acid at residue 111 is histidine and in group 2 HA subtypes, it is threonine [12, 30, 186, 358, 361, 418-422] . While others have shown the importance of these residues in the triggering of fusion for some subtypes [358, 359], an extensive characterization has not yet been completed. The goal of this work is to examine the effect of mutating these conserved residues in a range of subtypes representative of both groups and also avian and human strains.

Materials and Methods

Cells and antibodies. Vero cells (CCL-81) were obtained from ATCC and were used for transfections for the following assays: luciferase based reporter assay to assay fusion, western blot, radioactive labeling and immunoprecipitation, and flow cytometry to assay cleavage and surface expression. BSR-T7/5 cells (originally obtained from Karl-Klauss Conzelmann) served as the target cells in the luciferase-reporter based assay. For the syncytia formation assay, BHK-21 cells (ATCC CCL-10) were transfected with HA-plasmids to analyze fusion, described below.

The HA specific antibodies utilized in this study were described previously [49, 68]. BEI Resources provided the following: goat anti-H1, goat anti-H2, goat anti-$H2^{JAP}$, goat anti-H3, goat anti-H4, goat anti-H5, goat anti-H8, goat anti-H10, goat anti-H11, goat anti-$H1^{PR8}$, goat anti-$H5^{VN}$. Aichi HA was detected using rabbit anti-X31 serum.

Plasmids. The wild-type HA expression plasmids have been described previously [49, 68]. To introduce the Y17H, H17Y, H111A and T111H mutations, the wild-type HAs were PCR amplified from the expression plasmids and cloned into pCR-BLUNT,

according to the manufacturer's instructions. The pCR-BLUNT plasmids containing the HA gene of interest were modified using QuikChange site-directed mutagenesis to incorporate each mutation. Ligation independent cloning (LIC) procedures were used for the generation of the final plasmids. For LIC, the mutant HA genes in the sequence-verified pCR-BLUNT clones were amplified using LIC specific primers: a + sense with the 5' flanking sequence 5'TACTTCCAATCCATTTGCCACCATG, and a (-) sense primer with the 5' flanking sequence of 5'TTATCCACTTCCATTTCTCA. Standard LIC procedures described previously [49, 68] were used for the generation of each of the WT and mutant plasmids.

Radioactive labeling and Immunoprecipitation. 1 ug of plasmid containing the WT or mutant HA was complexed with Plus reagent and transfected using Lipofectamine (Invitrogen) into Vero cells. After an incubation of 16-18 hours, the cells, now expressing HA, were washed 2x with PBS and incubated at 37°C in starvation media, MEM (-Met –Cys), for 30 min. A 15 min pulse with 25 uCi of [^{35}S]-methionine (Perkin Elmer) followed, after which the cells were washed with PBS and incubated at 37°C in complete media with excess (20x) cold methionine for a 3 hour chase period. To assay for cleavage, the cells were washed once with PBS and incubated in DMEM or DMEM plus 5ug/ml TPCK trypsin (Sigma) at 37°C for 30 minutes. For the examination of surface expression, surface proteins were biotinylated using 2 mg EZ-link Sulfo-NHS-SS-Biotin (Thermo Scientific) in PBS pH 8.0 for an incubation time of 30 minutes at ambient temperature. After incubation, biotinylated samples were washed with 50mM glycine in PBS, pH 8.0 to quench the excess biotin. Cells were washed a final time with PBS and were lysed by the addition of 0.5ml RIPA buffer (50mM Tris-HCl, pH 7.4; 150mM

NaCl; 1mM EDTA; 0.5% deoxycholate; 1% triton X-100; 0.1% SDS). A 10-minute centrifugation at 16,000x g pelleted the cell debris to leave cleared lysates remaining.

For the antibody pull-down, HA specific antibodies were conjugated to Protein G dynabeads (Invitrogen) in PBS + 0.02% Tween-20 for an hour at room temperature. Unbound antibody was removed following a wash step with PBS+ 0.02% Tween-20. The lysates were also pre-cleared using the Protein G dynabeads for an hour at room temperature. The Protein G/ antibody complexed beads were incubated with the pre-cleared lysates for an hour at room temperature. Following incubation, the beads complexed now with the specific HAs were washed three times with PBS and resuspended in 30 ul 1x SDS buffer. A 5 min boil and brief centrifugation step removes the proteins from the beads.

For the precipitation of biotinylated proteins, the beads complexed with Protein-G/antibody/antigen were washed 3 times with PBS and resuspended in 50ul 50mM Tris-HCl+0.5% SDS. The beads were boiled for 5 minutes and centrifuged to dissociate the proteins, so that they may be collected. 25 ul of the eluate is used for a subsequent pull down of the biotinylated proteins using Streptavidin M-280 Dynabeads (Invitrogen) to isolate and precipitate cell-surface expressed HA. 100 ul of beads per sample were washed three times with PBS + 0.2% BSA and then resuspended in 975ul streptavidin binding buffer (20mM Tris-HCl, pH8.0; 150mM NaCl; 5mM EDTA; 1% Triton X-100; 0.2% BSA). The eluate (25 ul) was added to the beads in the streptavidin binding buffer and incubated for 1 hour at room temperature. The beads were then washed with PBS+ 0.2% BSA to remove unbound substrates and resuspended in 35ul 1x SDS sample buffer. The beads were boiled for 5 min and centrifuged to collect the dissociated proteins. The

remaining 25 ul of the immunoprecipitation elution was used to determine the total amount of HA protein in the sample. 10ul of 3x SDS sample buffer was added to the total HA sample for a final volume of 35ul.

For gel analysis, 18 ul of samples were loaded and run on 12% pre-cast SDS-PAGE gels. The gels were fixed with 50% methanol/10% acetic acid solution at room temperature for 30 minutes and dried under a vacuum for 1 hour at 80°C. Once dried, the gels were stored in a cassette for exposure to a phosphorimaging screen. The Phosphor screens were scanned on a Typhoon Trio variable mode imager (GE Healthcare Life Sciences). ImageQuant software was used to determine the intensity of the HA0, HA1 and HA2 bands. The values were normalized to methionine content of the appropriate subunit. Percent Cleavage was determined using the equation (Ha2/(Ha2+Ha0)) x100% and the percent cleavage relative to wild-type calculated as ((% cleavage mutant HA/% cleavage of WT) x100). To examine surface expressed HA and for the comparison of wild-type and mutant levels, the total level of HA in each lane was quantified and the amount of surface expressed HA was determined by the following equation, (cell surface HA/ total HA) x100 and then the percent relative to wild-type surface expression was calculated as ((% surface expression mutant HA/% surface expression WT HA) x100).

Fusion Assays. Membrane fusion mediated by the HA proteins was measured in 2 assays: a qualitative syncytia assay and a quantitative luciferase reported based assay. For the syncytia assay, BHK-21 cells were transfected with 1ug of HA containing plasmids complexed with Plus reagent and Lipofectamine (Invitrogen) per manufacturer's instructions. 16-18 hours post-transfection, the cells were washed with PBS and were treated with serum-free DMEM plus 5ug/ul TPCK-trypsin (Sigma) for 15 min at 37°C.

The trypsin containing media was removed and the cells were washed with PBS and then exposed to low pH PBS, adjusted with 100mM citric acid, for 5 min. The low pH was neutralized by the removal of the PBS and the immediate addition of complete growth media (CGM). The cells were incubated in CGM for 2 hours at 37°C and then were fixed and stained using a Hema3Stat Pak () for visualization. Syncytia formation was imaged and recorded using a Zeiss Axio Observer inverted microscope with attached digital camera.

For the quantitative luciferase-based reporter assay, 1ug HA-plasmid and 1 ug of plasmid containing the gene for firefly luciferase under a T7 bacteriophage promoter were complexed with Plus reagent and transfected into Vero cells using Lipofectamine (Invitrogen). 16-18 hours after transfection, the cells were washed with PBS and treated with 5ug/ul TPCK trypsin in serum-free DMEM for 30 minutes. The trypsin treatment was followed by a wash and a 30-minute incubation in serum-free DMEM plus 20ug/ul trypsin inhibitor to neutralize any remaining trypsin activity. BSR-T7/5 cells, which constitutively express bacteriophage T7 RNA polymerase, were overlaid on to the Vero cells expressing HA at the cell surface. The combined cell populations were incubated for 1 hour at 37°C to allow for the BSR-T7/5 cells to adhere to the existing monolayer of Vero cells. Non-associated cells were removed via a gentle PBS wash. The combined monolayer was exposed to low pH PBS, adjusted with 100mM citric acid, and incubated for 5 minutes at 37°C. The acidified PBS was removed and the low pH environment was neutralized by a wash and then the addition of complete growth media. The combined cell populations were incubated at 37°C in the CGM for 6 hours to allow for fusion and the transfer of the T7 polymerase and expression of the T7-luciferase plasmid. The cells

were then washed with PBS and lysed with 0.5ml of Reporter Lysis Buffer (Promega). The lysates were frozen for 16-18 hours and then collected. Cell debris were removed following centrifugation at 15,000 x g at 4°C and 150ul of the clarified lysate was transferred to a white, flat bottom, polystyrene 96-well plate (Corning). 50ul of luciferase assay substrate (Promega) was injected into each well and luciferase activity, indicating a successful fusion event between the two cell populations, was quantified using a BioTek Synergy 2 Luminometer.

Results and Discussion

The HA subtypes used for this study (Table 1) are representative of both group 1 and group 2 HA structures, as well as human and avian strain HAs. For the study of the residue at HA1 position 17, we mutated the amino acid to reflect the residue conserved in the other structural group so that the group 1 HAs incorporated a Y17H mutation and the group 2 HAs incorporated a H17Y mutation. The HA2 111 residue is highly volatile in the group 1 HAs and the only certain mutations were tolerated at that position. Previous work by our group and others failed to express any substitution other than alanine and even the H111A substitution significantly destabilized the HA [359]. For the group 2 HAs, we were able to incorporate a histidine at residue HA2 111 (T111H). Site directed mutagenesis was used to generate the mutant HAs and each was sequence verified.

Table 1. Origin of HA subtype proteins

Origin	Subtypes	Strain name	17 mutation	111 mutation
Group 1				
Avian	H1N1	A/duck/Alberta/35/1976	Y17H	H111A
Avian	H5N3	A/tern/South Africa/1961	Y17H	H111A
Avian	H8N4	A/turkey/Ontario/6118/1968	Y17H	H111A
Avian	H11N6	A/duck/England/1/1956	Y17H	H111A
Human	H1N1	A/Puerto Rico/8/1934	Y17H	H111A
Human	H1N1	A/California/04/2009	Y17H	H111A
Human	H2N2	A/Japan/305/1957	Y17H	H111A
Human	H5N1	A/Vietnam/1204/2004	Y17H	H111A
Group 2				
Avian	H3N8	A/duck/Ukraine/1/1963	H17Y	T111H
Avian	H10N7	A/chicken/Germany/N/1949	H17Y	T111H
Human	H3N2	A/Aichi/2/1968	H17Y	T111H

To confirm that the effect of the mutations was not related to a disruption in protein presentation, the surface expression of each HA mutant subtype was compared to its wild-type counterpart. By biotinylating and precipitating the surface expressed HA with a streptavidin pull down assay, it was determined that the HA1 17 mutants were expressed at levels ranging from 82% to 157% of wild-type indicating that the incorporation of histidine or tyrosine, respectively, did not significantly alter the expression profile of the HA. For the HA2 111 mutants, surface expression relative to WT ranged from 44% to 192%, indicating that the HA2 111 mutations also did not affect the surface expression of the protein (Figure 2).

In order to be primed for the conformational change enabling fusion, the HA0 form must be able to be cleaved by host proteases. To confirm that the incorporation of the mutant amino acids at residue HA1 17 and HA2 111 did not alter the cleavage phenotype or susceptibility to trypsin, HA proteins were expressed, labeled with [^{35}S]-

methionine and treated with exogenous trypsin. After immunoprecipitation with HA subtype specific antibodies, levels of uncleaved HA0 were compared to the cleaved forms, HA1 and HA2 for mutant HAs relative to wild type. For the HA1 17 mutations, percent cleavage compared to wild-type ranged from 70% to 143% indicating that mutations at this residue did not significantly impact the susceptibility to trypsin. For the HA2 111 mutations, overall levels of percent cleavage compared to wild type were lower, ranging from 43% to 144% with both H5 subtypes (avian H5 and human $H5^{VN}$) exhibiting levels as low as 2-5 percent. (Figure 3) The results recapitulate the findings of Reed et al who also described a non-cleavage phenotype for the H5 H111A mutant [359].

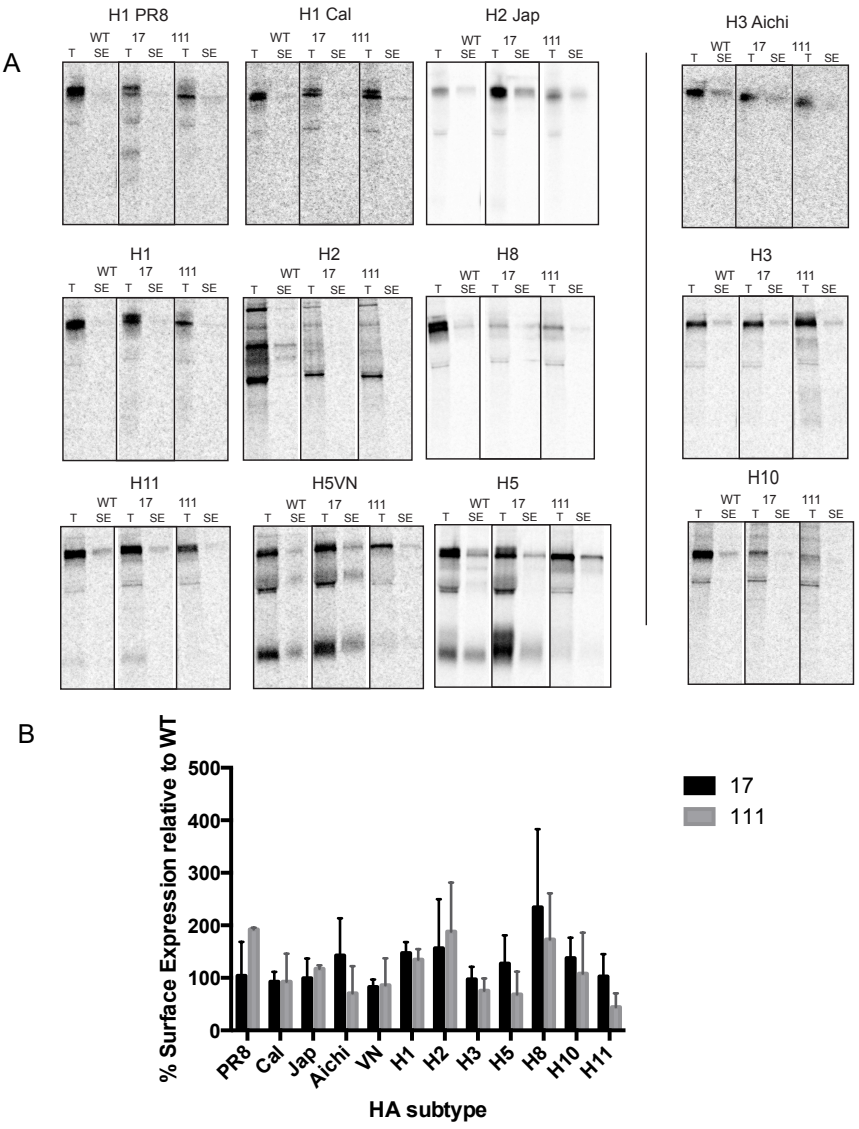

Figure 2. Surface expression of WT and mutant HAs. Radiolabeled, cell surface proteins were biotinylated and precipitated with a HA-specific antibody and then streptavidin where indicated (SE), and resolved by SDS-PAGE. Lanes are denoted T for total HA and SE for surface expressed. (A) Gel images for human and avian subtypes are shown, with group 1 and group 2 separated by a black line. (B) Quantitation of the surface expression of mutant HA relative to WT HA. For each WT and mutant HA, the intensity of the bands corresponding to HA0 +streptavidin and HA0 -streptavidin were normalized based on methionine content. Percent surface expression was determined using the following equation (cell surface HA/ total HA)x100 and then the percent relative to wild-type surface expression was calculated as ((% surface expression mutant HA/% surface expression WT HA)x100). Error bars represent the standard deviation of three independent experiments.

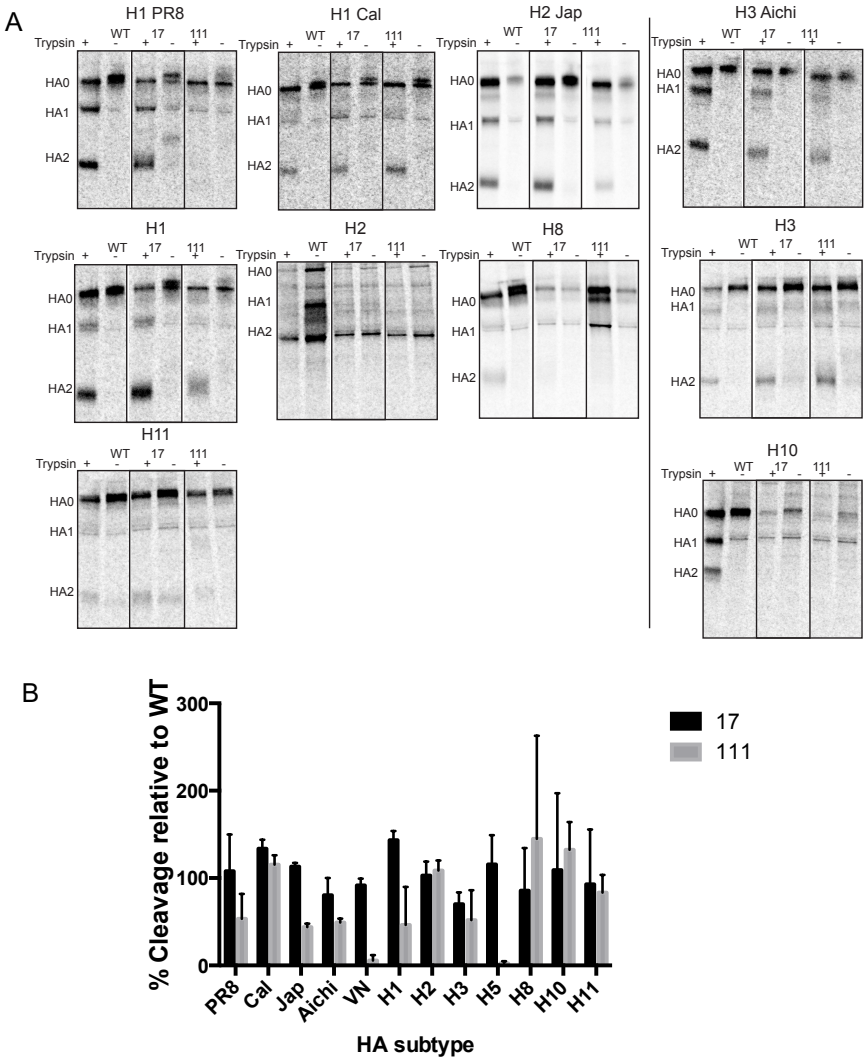

Figure 3. Analysis of proteolytic cleavage of WT and mutant HAs. Radiolabeled, HA-expressing cells were treated with 5ug/ml TPCK trypsin, where indicated. Total cellular HA protein was precipitated from the lysate with a HA-specific antibody and resolved by SDS-PAGE. (A) Gel images for human and avian subtypes are shown, with group 1 and group 2 subtypes separated by the black line. (B) Quantitation of trypsin-mediated cleavage of mutant HA relative to WT HA. For each WT and mutant HA, the intensity of the bands corresponding to HA0 and HA2 were normalized based on methionine content. For the $H5^{VN}$ and H5 subtypes, the cleavage values were determined from the total HA lanes of the surface expression gels shown in Figure 2B. Percent Cleavage was determined using the equation (Ha2/(Ha2+Ha0))x100% and the percent cleavage relative to wild-type calculated as ((% cleavage mutant HA/% cleavage of WT)x100). Error bars represent the standard deviation of three independent experiments.

The importance of the conserved residue at each the 17 and 111 position for the stability of HA was determined using assays that establish the pH of fusion. Two assays were utilized, the first a qualitative syncytia assay, which allows for the visualization of fusion events resulting in the formation of syncytia at incremental pH units. The second assay is the quantitative luciferase based reporter assay which involves the transfection of the HA containing plasmid along with a plasmid containing the gene for luciferase under the control of a T7 promoter. The transfected cells are overlaid with BSR-T7 cells containing the T7 polymerase and exposed to a low pH environment. The HA expressed on the transfected cells should mediate fusion between those and the BSR-T7 cells allowing for the transfer of the T7 polymerase and the expression of the luciferase. Luciferase expression is measured by a luminometer and plotted over a range of pH values.

The results of both the syncytia assay and the luciferase reported based assay reveal that the HA1 17 mutation does facilitate fusion for a majority of the HA subtypes (exceptions: H2, H5, and H8) and that the effect is group specific. As mentioned previously, this residue lies in the fusion peptide pocket in the post cleavage form of HA and makes hydrogen bond contacts with the histidine at position 18, water, and the carbonyl oxygen of residues HA1 6 and 10, stabilizing the protein structure [175]. For the group 1 HAs, the change from tyrosine to histidine destabilized the HA fusion peptide pocket and resulted in an increase in the pH fusion of +0.2 to +0.6 pH units compared to the wild-type subtype. These results are consistent with previous work documenting an increase in the pH of fusion of H3 subtypes when the amino acid substitution resulted in the introduction of a glutamine, arginine, or alanine, all of which reduce the hydrogen bond interactions [60, 358, 423-425]. For the group 2 HAs, the H17Y mutation resulted

in a stabilization of the fusion peptide pocket, decreasing the pH of fusion by 0.4 pH units for each subtype. (Table 2, Supplemental figures 1 and 2) These results are consistent with other group 2 HA studies using only H3 subtypes and substituting histidine for tyrosine [358]. The differences in amino acid interactions have been modeled and suggest that the longer functional group of the tyrosine may form a more extensive network of hydrogen bonds interacting directly with residues 10 and 12 of HA1 [358].

Table 2. Fusion pH of wild-type and mutant HAs

	pH and △pH values for wild-type and mutant HAs									
		Wild type		**17 mutation**				**111 mutation**			
		Luciferase	**Syncytia**	**Luciferase**		**Syncytia**		**Luciferase**		**Syncytia**	
	Subtype			pH	△pH	pH	△pH	pH	△pH	pH	△pH
Group 1	**H1**	5.4	5.4	5.8	0.4	6	0.6	<4.4	ND	<4.4	ND
	H5	5.2	5.2	<4.4	ND	<4.4	ND	<4.4	ND	<4.4	ND
	H8	5.4	5.4	<4.4	ND	<4.4	ND	<4.4	ND	<4.4	ND
	H11	5.6	5.6	6.0	0.4	6.0	0.4	<4.4	ND	<4.4	ND
	$H1_{PR8}$	5	5	5.6	0.6	5.6	0.6	<4.4	ND	<4.4	ND
	$H1_{CA}$	5.2	5.4	5.4	0.2	5.8	0.4	<4.4	ND	<4.4	ND
	$H2_{JAP}$	5	5.2	5.4	0.4	5.4	0.2	<4.4	ND	<4.4	ND
	$H5_{VN}$	5.6	5.6	6.0	0.4	6.0	0.4	<4.4	ND	<4.4	ND
Group 2	**H3**	5.4	5.2	5	-0.4	4.8	-0.4	5.6	0.2	5.4	0.2
	H10	5	5	4.6	-0.4	4.4	-0.6	5.4	0.4	5.4	0.4
	$H3_{Aichi}$	5	5	4.6	-0.4	4.6	-0.4	5.6	0.6	5.6	0.6
	ND- No fusion detected at pH at 4.4										

The fusion data for the HA2 111 mutant subtypes is also conserved by group as all of the group 1 HAs incorporating the H111A mutation were unable to facilitate fusion in either the syncytia or the luciferase reporter-based assay. We have demonstrated that the HA proteins are being expressed at the surface and that some percentage of the surface expressed HAs are, in fact, cleaved, so the inability to detect fusion likely illustrates the need for the histidine mediated interactions with the fusion peptide pocket within the structural group 1 HA subtypes. These results reiterate those demonstrated by Reed et al for the H5 subtype [359]. For the group 2 HAs, the T111H mutation led to an increase in the pH of fusion indicating a destabilization of the HA compared to wild type. (Table 2, Supplemental figures 1 and 2) The amino acid at residue 111, either threonine or histidine, forms contacts with a series of surrounding group-specific amino acids, residues HA1 18, HA1 38 and HA2 21 [186, 358], so it follows that a substitution with alternate structural interactions and bond chemistry could lead to a reduction in stability of the region.

Our results indicate that both residues HA1 17 and HA1 111 have significant roles in maintaining the stability of the fusion-primed conformation and may function for all HA subtypes as triggering residues that, upon acidification, induce the final conformational change that allows for the insertion of the fusion peptide into the target membrane. As HA stability emerges as a factor that is potentially involved in cross species transmission, understanding the implications of the structural group differences and specific residues involved reveals predictors for stability phenotypes that might increase the probability of a transmission event.

Acknowledgments

This study was supported by the U.S. Department of Health and Human Services contract HHSN272201400004C (NIAID Centers of Excellence for Influenza Research and Surveillance. L.B.L. is supported by Ruth L. Kirschstein NRSA F31 Fellowship 1F31AI115968-01. W.W. was supported by China Scholarship Council. We also thank BEI for providing anti-HA antibodies; Evangeline Agbogu for generating the HA plasmids; and Jess Trost for help with the IP experiments.

Supplemental figure legends

Figure 1. The pH of fusion as detected by syncytia formation. Photomicrographs of syncytia formation assays for Group 1 and Group 2 as well as human and avian representative HAs are shown. HA-expressing BHK cells were treated with TPCK trypsin (5 ug/ml) and exposed to pH adjusted PBS in 0.1 pH unit increments. Photomicrographs corresponding to the highest pH at which syncytia were observed and then 0.1 pH unit higher are shown for wild-type. For subtypes with no fusion phenotypes, the photomicrograph taken at the lowest testes pH unit, 4.4, is shown.

Figure 2. The pH of fusion as detected by the Luciferase reporter gene assay. HA-expressing Vero cells transfected with T7-luciferase plasmid were treated with TPCK-trypsin (5ug/ml) followed by C. soybean trypsin inhibitor (20ug/ml) and then overlaid with BSR-T7/5 target cells that constitutively express T7 RNA polymerase. The mixed cell population was exposed to pH-adjusted PBS in 0.2 pH unit increments and was incubated for 6 hrs at 37°C to allow for cell-to-cell fusion and content mixing leading to expression of firefly luciferase to occur. Luminescence was measured as an indicator of membrane fusion in cell lysates. The graphs show the background-adjusted luminescence. Error bars represent the standard deviation of duplicate experiments. (A) Avian origin HA subtypes. For H2, H5 and H8, no fusion was detected with Y17H mutation. For the group 1 HA subtypes, no fusion was detected in the H111A mutant strain. (B) Human origin HA subtypes. Similar to the avian subtypes, no fusion was detected for the group 1 HA subtypes with the H111A mutation.

Supplemental Figures

Supplemental Figure 1. Fusion pH as detected by syncytium formation

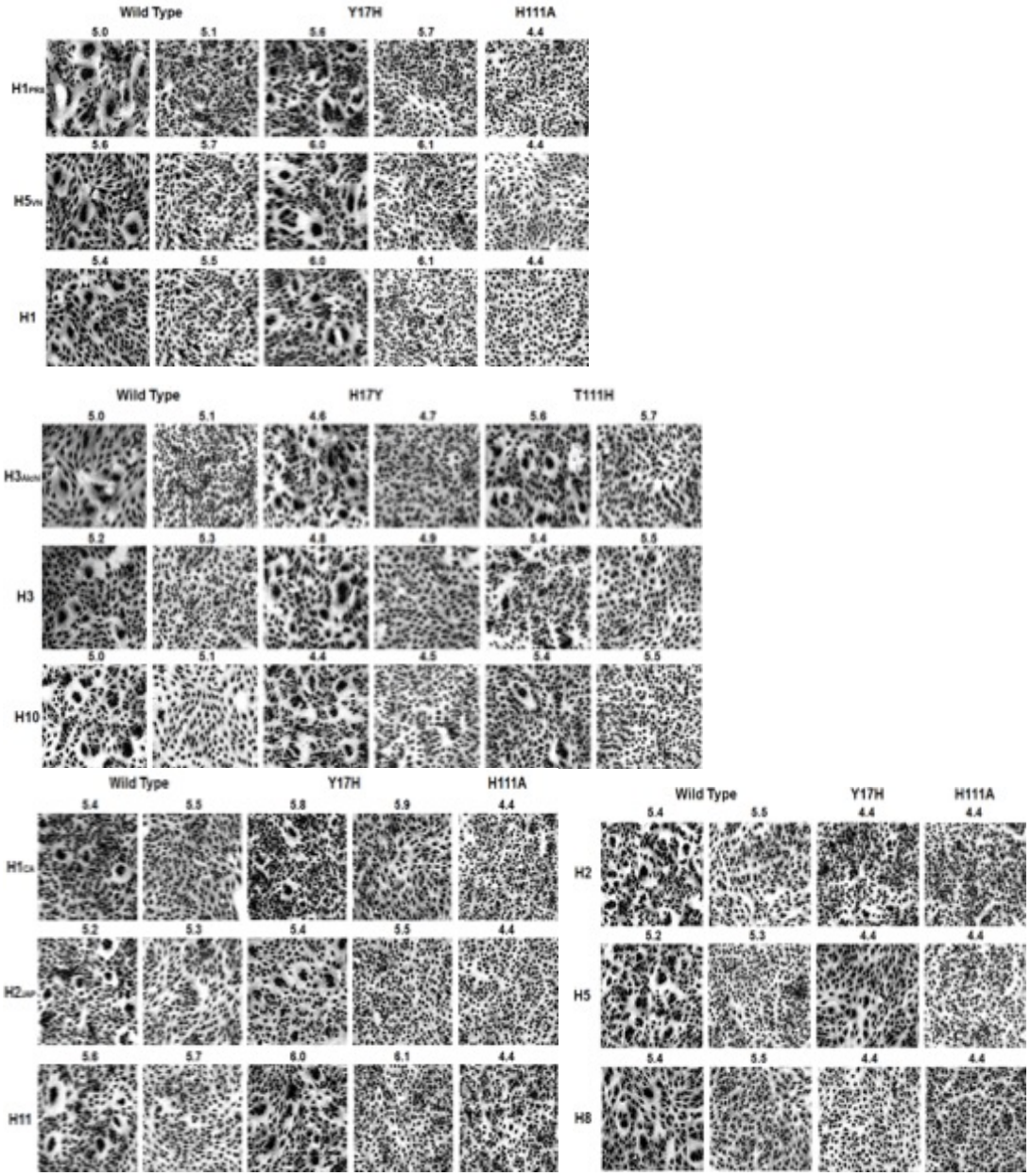

Supplemental Figure 2. Fusion pH as detected by luciferase reporter assay.

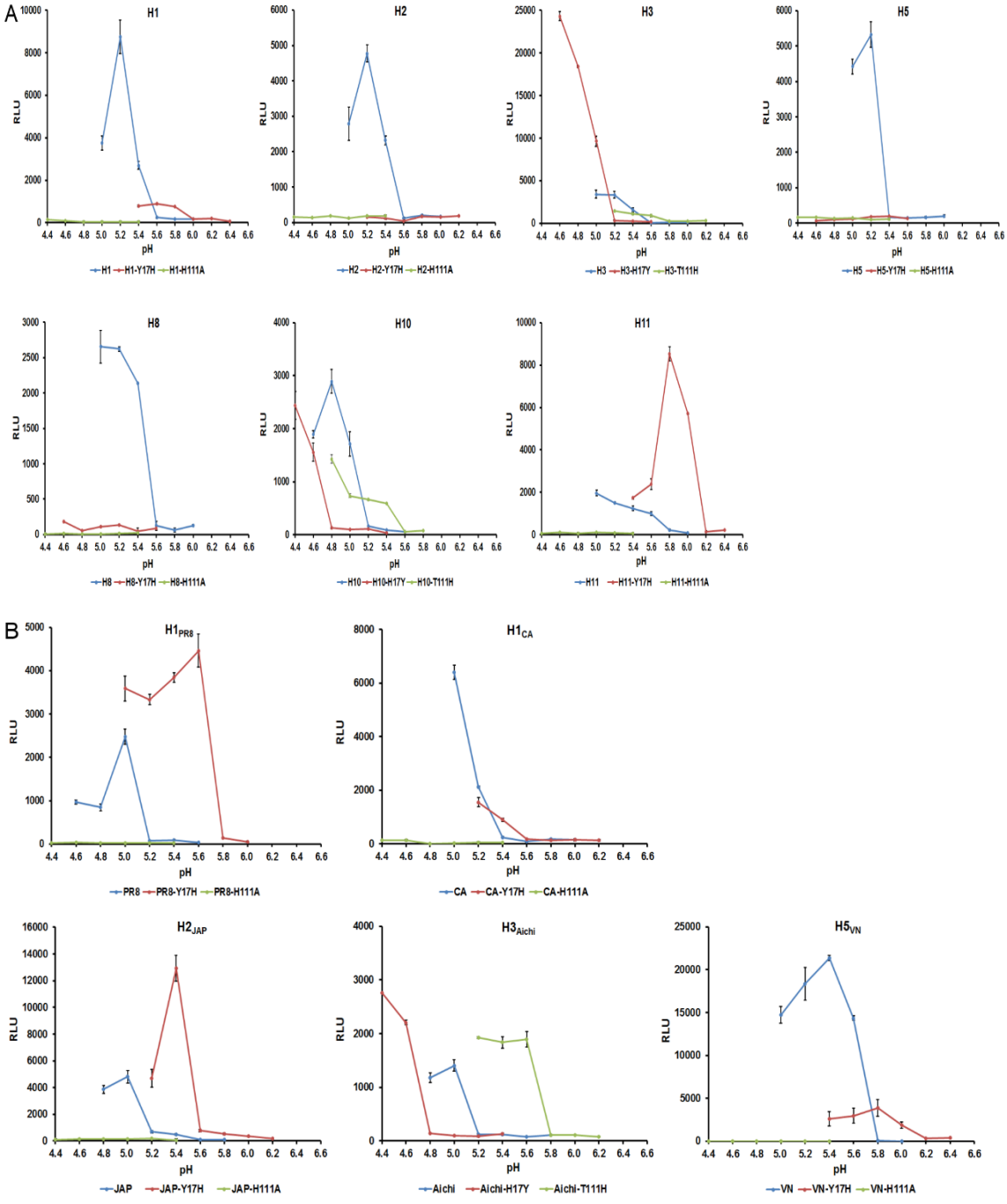

REFERENCES

1. Hause, B.M., et al., *Characterization of a novel influenza virus in cattle and Swine: proposal for a new genus in the Orthomyxoviridae family.* MBio, 2014. **5**(2): p. e00031-14.
2. Shope, R.E., *Swine Influenza : I. Experimental Transmission and Pathology.* J Exp Med, 1931. **54**(3): p. 349-59.
3. Geraci, J.R., et al., *Mass mortality of harbor seals: pneumonia associated with influenza A virus.* Science, 1982. **215**(4536): p. 1129-31.
4. Sovinova, O., et al., *Isolation of a virus causing respiratory disease in horses.* Acta Virol, 1958. **2**(1): p. 52-61.
5. Organization, W.H. *Fact sheet 211 - Influenza (Seasonal)*. 2014; Available from: http://www.who.int/mediacentre/factsheets/fs211/en/.
6. Lowen, A.C., et al., *Influenza virus transmission is dependent on relative humidity and temperature.* PLoS Pathog, 2007. **3**(10): p. 1470-6.
7. Deyle, E.R., et al., *Global environmental drivers of influenza.* Proc Natl Acad Sci U S A, 2016.
8. Claas, E.C., et al., *Human influenza A H5N1 virus related to a highly pathogenic avian influenza virus.* Lancet, 1998. **351**(9101): p. 472-7.
9. Subbarao, K., et al., *Characterization of an avian influenza A (H5N1) virus isolated from a child with a fatal respiratory illness.* Science, 1998. **279**(5349): p. 393-6.
10. Normile, D., *Avian influenza. New H5N1 strain emerges in southern China.* Science, 2006. **314**(5800): p. 742.
11. Ungchusak, K., et al., *Probable person-to-person transmission of avian influenza A (H5N1).* N Engl J Med, 2005. **352**(4): p. 333-40.
12. Wilson, I.A., J.J. Skehel, and D.C. Wiley, *Structure of the haemagglutinin membrane glycoprotein of influenza virus at 3 A resolution.* Nature, 1981. **289**(5796): p. 366-73.
13. Weis, W., et al., *Structure of the influenza virus haemagglutinin complexed with its receptor, sialic acid.* Nature, 1988. **333**(6172): p. 426-31.
14. Xu, R., et al., *Structure, receptor binding, and antigenicity of influenza virus hemagglutinins from the 1957 H2N2 pandemic.* J Virol, 2010. **84**(4): p. 1715-21.
15. Rogers, G.N., et al., *Single amino acid substitutions in influenza haemagglutinin change receptor binding specificity.* Nature, 1983. **304**(5921): p. 76-8.
16. Viswanathan, K., et al., *Determinants of glycan receptor specificity of H2N2 influenza A virus hemagglutinin.* PloS one, 2010. **5**(10): p. e13768.
17. Ha, Y., et al., *X-ray structure of the hemagglutinin of a potential H3 avian progenitor of the 1968 Hong Kong pandemic influenza virus.* Virology, 2003. **309**(2): p. 209-18.
18. Liu, J., et al., *Structures of receptor complexes formed by hemagglutinins from the Asian Influenza pandemic of 1957.* Proc Natl Acad Sci U S A, 2009. **106**(40): p. 17175-80.

19. Glaser, L., et al., *A single amino acid substitution in 1918 influenza virus hemagglutinin changes receptor binding specificity.* J Virol, 2005. **79**(17): p. 11533-6.
20. Stevens, J., et al., *Glycan microarray analysis of the hemagglutinins from modern and pandemic influenza viruses reveals different receptor specificities.* J Mol Biol, 2006. **355**(5): p. 1143-55.
21. Stevens, J., et al., *Structure and receptor specificity of the hemagglutinin from an H5N1 influenza virus.* Science, 2006. **312**(5772): p. 404-10.
22. Tumpey, T.M., et al., *A two-amino acid change in the hemagglutinin of the 1918 influenza virus abolishes transmission.* Science, 2007. **315**(5812): p. 655-9.
23. Stevens, J., et al., *Receptor specificity of influenza A H3N2 viruses isolated in mammalian cells and embryonated chicken eggs.* J Virol, 2010. **84**(16): p. 8287-99.
24. Maines, T.R., et al., *Transmission and pathogenesis of swine-origin 2009 A(H1N1) influenza viruses in ferrets and mice.* Science, 2009. **325**(5939): p. 484-7.
25. Bradley, K.C., et al., *Analysis of influenza virus hemagglutinin receptor binding mutants with limited receptor recognition properties and conditional replication characteristics.* Journal of virology, 2011. **85**(23): p. 12387-98.
26. Bulai, T., et al., *Diversity of the human erythrocyte membrane sialic acids in relation with blood groups.* FEBS Lett, 2003. **534**(1-3): p. 185-9.
27. Bradley, K.C., et al., *Comparison of the receptor binding properties of contemporary swine isolates and early human pandemic H1N1 isolates (Novel 2009 H1N1).* Virology, 2011. **413**(2): p. 169-82.
28. Chen, L.M., et al., *Receptor specificity of subtype H1 influenza A viruses isolated from swine and humans in the United States.* Virology, 2011. **412**(2): p. 401-10.
29. Connor, R.J., et al., *Receptor specificity in human, avian, and equine H2 and H3 influenza virus isolates.* Virology, 1994. **205**(1): p. 17-23.
30. Gamblin, S.J., et al., *The structure and receptor binding properties of the 1918 influenza hemagglutinin.* Science, 2004. **303**(5665): p. 1838-42.
31. Ibricevic, A., et al., *Influenza virus receptor specificity and cell tropism in mouse and human airway epithelial cells.* J Virol, 2006. **80**(15): p. 7469-80.
32. Kumari, K., et al., *Receptor binding specificity of recent human H3N2 influenza viruses.* Virol J, 2007. **4**: p. 42.
33. Maines, T.R., et al., *Effect of receptor binding domain mutations on receptor binding and transmissibility of avian influenza H5N1 viruses.* Virology, 2011. **413**(1): p. 139-47.
34. Rogers, G.N. and B.L. D'Souza, *Receptor binding properties of human and animal H1 influenza virus isolates.* Virology, 1989. **173**(1): p. 317-22.
35. Rogers, G.N. and J.C. Paulson, *Receptor determinants of human and animal influenza virus isolates: differences in receptor specificity of the H3 hemagglutinin based on species of origin.* Virology, 1983. **127**(2): p. 361-73.
36. Russell, R.J., et al., *Avian and human receptor binding by hemagglutinins of influenza A viruses.* Glycoconj J, 2006. **23**(1-2): p. 85-92.

37. Shelton, H., et al., *Receptor binding profiles of avian influenza virus hemagglutinin subtypes on human cells as a predictor of pandemic potential.* J Virol, 2011. **85**(4): p. 1875-80.
38. Yamada, S., et al., *Haemagglutinin mutations responsible for the binding of H5N1 influenza A viruses to human-type receptors.* Nature, 2006. **444**(7117): p. 378-82.
39. Yang, Z.Y., et al., *Immunization by avian H5 influenza hemagglutinin mutants with altered receptor binding specificity.* Science, 2007. **317**(5839): p. 825-8.
40. Shinya, K., et al., *Avian flu: influenza virus receptors in the human airway.* Nature, 2006. **440**(7083): p. 435-6.
41. Kimble, B., G.R. Nieto, and D.R. Perez, *Characterization of influenza virus sialic acid receptors in minor poultry species.* Virology journal, 2010. **7**: p. 365.
42. de Vries, E., et al., *Dissection of the influenza A virus endocytic routes reveals macropinocytosis as an alternative entry pathway.* PLoS Pathog, 2011. **7**(3): p. e1001329.
43. Matlin, K.S., et al., *Infectious entry pathway of influenza virus in a canine kidney cell line.* J Cell Biol, 1981. **91**(3 Pt 1): p. 601-13.
44. Patterson, S., J.S. Oxford, and R.R. Dourmashkin, *Studies on the mechanism of influenza virus entry into cells.* J Gen Virol, 1979. **43**(1): p. 223-9.
45. Sieczkarski, S.B. and G.R. Whittaker, *Influenza virus can enter and infect cells in the absence of clathrin-mediated endocytosis.* J Virol, 2002. **76**(20): p. 10455-64.
46. Rossman, J.S., G.P. Leser, and R.A. Lamb, *Filamentous influenza virus enters cells via macropinocytosis.* J Virol, 2012. **86**(20): p. 10950-60.
47. Chen, J., et al., *Structure of the hemagglutinin precursor cleavage site, a determinant of influenza pathogenicity and the origin of the labile conformation.* Cell, 1998. **95**(3): p. 409-17.
48. Bullough, P.A., et al., *Structure of influenza haemagglutinin at the pH of membrane fusion.* Nature, 1994. **371**(6492): p. 37-43.
49. Galloway, S.E., et al., *Influenza HA subtypes demonstrate divergent phenotypes for cleavage activation and pH of fusion: implications for host range and adaptation.* PLoS Pathog, 2013. **9**(2): p. e1003151.
50. Bottcher-Friebertshauser, E., et al., *Cleavage of influenza virus hemagglutinin by airway proteases TMPRSS2 and HAT differs in subcellular localization and susceptibility to protease inhibitors.* J Virol, 2010. **84**(11): p. 5605-14.
51. Bottcher, E., et al., *Proteolytic activation of influenza viruses by serine proteases TMPRSS2 and HAT from human airway epithelium.* J Virol, 2006. **80**(19): p. 9896-8.
52. Kido, H., et al., *Isolation and characterization of a novel trypsin-like protease found in rat bronchiolar epithelial Clara cells. A possible activator of the viral fusion glycoprotein.* J Biol Chem, 1992. **267**(19): p. 13573-9.
53. Carr, C.M. and P.S. Kim, *A spring-loaded mechanism for the conformational change of influenza hemagglutinin.* Cell, 1993. **73**(4): p. 823-32.
54. Harter, C., et al., *Hydrophobic binding of the ectodomain of influenza hemagglutinin to membranes occurs through the "fusion peptide".* J Biol Chem, 1989. **264**(11): p. 6459-64.

55. Brunner, J., *Testing topological models for the membrane penetration of the fusion peptide of influenza virus hemagglutinin.* FEBS Lett, 1989. **257**(2): p. 369-72.
56. Skehel, J.J., et al., *Changes in the conformation of influenza virus hemagglutinin at the pH optimum of virus-mediated membrane fusion.* Proc Natl Acad Sci U S A, 1982. **79**(4): p. 968-72.
57. Doms, R.W. and A. Helenius, *Quaternary structure of influenza virus hemagglutinin after acid treatment.* J Virol, 1986. **60**(3): p. 833-9.
58. Stegmann, T., J.M. White, and A. Helenius, *Intermediates in influenza induced membrane fusion.* EMBO J, 1990. **9**(13): p. 4231-41.
59. Steinhauer, D.A., et al., *Studies of the membrane fusion activities of fusion peptide mutants of influenza virus hemagglutinin.* J Virol, 1995. **69**(11): p. 6643-51.
60. Steinhauer, D.A., et al., *Studies using double mutants of the conformational transitions in influenza hemagglutinin required for its membrane fusion activity.* Proc Natl Acad Sci U S A, 1996. **93**(23): p. 12873-8.
61. Orlich, M. and R. Rott, *Thermolysin activation mutants with changes in the fusogenic region of an influenza virus hemagglutinin.* J Virol, 1994. **68**(11): p. 7537-9.
62. Nobusawa, E., et al., *The role of acidic residues in the "fusion segment" of influenza A virus hemagglutinin in low-pH-dependent membrane fusion.* Arch Virol, 1995. **140**(5): p. 865-75.
63. Lin, Y.P., et al., *Adaptation of egg-grown and transfectant influenza viruses for growth in mammalian cells: selection of hemagglutinin mutants with elevated pH of membrane fusion.* Virology, 1997. **233**(2): p. 402-10.
64. Lai, A.L. and L.K. Tamm, *Locking the kink in the influenza hemagglutinin fusion domain structure.* J Biol Chem, 2007. **282**(33): p. 23946-56.
65. Han, X., et al., *Interaction of mutant influenza virus hemagglutinin fusion peptides with lipid bilayers: probing the role of hydrophobic residue size in the central region of the fusion peptide.* Biochemistry, 1999. **38**(45): p. 15052-9.
66. Gething, M.J., et al., *Studies on the mechanism of membrane fusion: site-specific mutagenesis of the hemagglutinin of influenza virus.* J Cell Biol, 1986. **102**(1): p. 11-23.
67. Cross, K.J., et al., *Studies on influenza haemagglutinin fusion peptide mutants generated by reverse genetics.* EMBO J, 2001. **20**(16): p. 4432-42.
68. Byrd-Leotis, L., et al., *Influenza hemagglutinin (HA) stem region mutations that stabilize or destabilize the structure of multiple HA subtypes.* J Virol, 2015. **89**(8): p. 4504-16.
69. Bukrinskaya, A.G., et al., *Influenza virus uncoating in infected cells and effect of rimantadine.* J Gen Virol, 1982. **60**(Pt 1): p. 49-59.
70. Zebedee, S.L. and R.A. Lamb, *Influenza A virus M2 protein: monoclonal antibody restriction of virus growth and detection of M2 in virions.* J Virol, 1988. **62**(8): p. 2762-72.
71. Takeda, M., et al., *Influenza a virus M2 ion channel activity is essential for efficient replication in tissue culture.* J Virol, 2002. **76**(3): p. 1391-9.

72. Baudin, F., et al., *Structure of influenza virus RNP. I. Influenza virus nucleoprotein melts secondary structure in panhandle RNA and exposes the bases to the solvent.* EMBO J, 1994. **13**(13): p. 3158-65.
73. Murti, K.G., et al., *Composition of the helical internal components of influenza virus as revealed by immunogold labeling/electron microscopy.* Virology, 1992. **186**(1): p. 294-9.
74. Murti, K.G., R.G. Webster, and I.M. Jones, *Localization of RNA polymerases on influenza viral ribonucleoproteins by immunogold labeling.* Virology, 1988. **164**(2): p. 562-6.
75. Honda, A., et al., *Identification of the RNA polymerase-binding site on genome RNA of influenza virus.* J Biochem, 1987. **102**(5): p. 1241-9.
76. Huang, T.S., P. Palese, and M. Krystal, *Determination of influenza virus proteins required for genome replication.* J Virol, 1990. **64**(11): p. 5669-73.
77. Kimura, N., et al., *Transcription of a recombinant influenza virus RNA in cells that can express the influenza virus RNA polymerase and nucleoprotein genes.* J Gen Virol, 1992. **73 (Pt 6)**: p. 1321-8.
78. de la Luna, S., et al., *Influenza virus naked RNA can be expressed upon transfection into cells co-expressing the three subunits of the polymerase and the nucleoprotein from simian virus 40 recombinant viruses.* J Gen Virol, 1993. **74 (Pt 3)**: p. 535-9.
79. Mena, I., et al., *Synthesis of biologically active influenza virus core proteins using a vaccinia virus-T7 RNA polymerase expression system.* J Gen Virol, 1994. **75 (Pt 8)**: p. 2109-14.
80. Klumpp, K., R.W. Ruigrok, and F. Baudin, *Roles of the influenza virus polymerase and nucleoprotein in forming a functional RNP structure.* EMBO J, 1997. **16**(6): p. 1248-57.
81. Detjen, B.M., et al., *The three influenza virus polymerase (P) proteins not associated with viral nucleocapsids in the infected cell are in the form of a complex.* J Virol, 1987. **61**(1): p. 16-22.
82. Ruigrok, R.W., L.J. Calder, and S.A. Wharton, *Electron microscopy of the influenza virus submembranal structure.* Virology, 1989. **173**(1): p. 311-6.
83. Martin, K. and A. Helenius, *Nuclear transport of influenza virus ribonucleoproteins: the viral matrix protein (M1) promotes export and inhibits import.* Cell, 1991. **67**(1): p. 117-30.
84. Eisfeld, A.J., G. Neumann, and Y. Kawaoka, *At the centre: influenza A virus ribonucleoproteins.* Nat Rev Microbiol, 2015. **13**(1): p. 28-41.
85. Martin, K. and A. Helenius, *Transport of incoming influenza virus nucleocapsids into the nucleus.* J Virol, 1991. **65**(1): p. 232-44.
86. O'Neill, R.E., et al., *Nuclear import of influenza virus RNA can be mediated by viral nucleoprotein and transport factors required for protein import.* J Biol Chem, 1995. **270**(39): p. 22701-4.
87. Gabriel, G., et al., *Differential use of importin-alpha isoforms governs cell tropism and host adaptation of influenza virus.* Nat Commun, 2011. **2**: p. 156.
88. Boivin, S. and D.J. Hart, *Interaction of the influenza A virus polymerase PB2 C-terminal region with importin alpha isoforms provides insights into host adaptation and polymerase assembly.* J Biol Chem, 2011. **286**(12): p. 10439-48.

89. Hudjetz, B. and G. Gabriel, *Human-like PB2 627K influenza virus polymerase activity is regulated by importin-alpha1 and -alpha7.* PLoS Pathog, 2012. **8**(1): p. e1002488.
90. Perez, J.T., et al., *Influenza A virus-generated small RNAs regulate the switch from transcription to replication.* Proc Natl Acad Sci U S A, 2010. **107**(25): p. 11525-30.
91. Plotch, S.J., et al., *A unique cap(m7GpppXm)-dependent influenza virion endonuclease cleaves capped RNAs to generate the primers that initiate viral RNA transcription.* Cell, 1981. **23**(3): p. 847-58.
92. Dias, A., et al., *The cap-snatching endonuclease of influenza virus polymerase resides in the PA subunit.* Nature, 2009. **458**(7240): p. 914-8.
93. Li, M.L., B.C. Ramirez, and R.M. Krug, *RNA-dependent activation of primer RNA production by influenza virus polymerase: different regions of the same protein subunit constitute the two required RNA-binding sites.* EMBO J, 1998. **17**(19): p. 5844-52.
94. Gonzalez, S. and J. Ortin, *Characterization of influenza virus PB1 protein binding to viral RNA: two separate regions of the protein contribute to the interaction domain.* J Virol, 1999. **73**(1): p. 631-7.
95. Braam, J., I. Ulmanen, and R.M. Krug, *Molecular model of a eucaryotic transcription complex: functions and movements of influenza P proteins during capped RNA-primed transcription.* Cell, 1983. **34**(2): p. 609-18.
96. Biswas, S.K. and D.P. Nayak, *Mutational analysis of the conserved motifs of influenza A virus polymerase basic protein 1.* J Virol, 1994. **68**(3): p. 1819-26.
97. Poon, L.L., et al., *Direct evidence that the poly(A) tail of influenza A virus mRNA is synthesized by reiterative copying of a U track in the virion RNA template.* J Virol, 1999. **73**(4): p. 3473-6.
98. Shapiro, G.I. and R.M. Krug, *Influenza virus RNA replication in vitro: synthesis of viral template RNAs and virion RNAs in the absence of an added primer.* J Virol, 1988. **62**(7): p. 2285-90.
99. Das, K., et al., *Structural basis for suppression of a host antiviral response by influenza A virus.* Proc Natl Acad Sci U S A, 2008. **105**(35): p. 13093-8.
100. Li, S., et al., *Binding of the influenza A virus NS1 protein to PKR mediates the inhibition of its activation by either PACT or double-stranded RNA.* Virology, 2006. **349**(1): p. 13-21.
101. Noah, D.L., K.Y. Twu, and R.M. Krug, *Cellular antiviral responses against influenza A virus are countered at the posttranscriptional level by the viral NS1A protein via its binding to a cellular protein required for the 3' end processing of cellular pre-mRNAS.* Virology, 2003. **307**(2): p. 386-95.
102. Talon, J., et al., *Activation of interferon regulatory factor 3 is inhibited by the influenza A virus NS1 protein.* J Virol, 2000. **74**(17): p. 7989-96.
103. Wang, X., et al., *Influenza A virus NS1 protein prevents activation of NF-kappaB and induction of alpha/beta interferon.* J Virol, 2000. **74**(24): p. 11566-73.
104. Ye, Z.P., et al., *Functional and antigenic domains of the matrix (M1) protein of influenza A virus.* J Virol, 1987. **61**(2): p. 239-46.
105. Deng, T., et al., *Role of ran binding protein 5 in nuclear import and assembly of the influenza virus RNA polymerase complex.* J Virol, 2006. **80**(24): p. 11911-9.

106. Fodor, E. and M. Smith, *The PA subunit is required for efficient nuclear accumulation of the PB1 subunit of the influenza A virus RNA polymerase complex.* J Virol, 2004. **78**(17): p. 9144-53.
107. Beaton, A.R. and R.M. Krug, *Transcription antitermination during influenza viral template RNA synthesis requires the nucleocapsid protein and the absence of a 5' capped end.* Proc Natl Acad Sci U S A, 1986. **83**(17): p. 6282-6.
108. Iwatsuki-Horimoto, K., et al., *Generation of influenza A virus NS2 (NEP) mutants with an altered nuclear export signal sequence.* J Virol, 2004. **78**(18): p. 10149-55.
109. Neumann, G., M.T. Hughes, and Y. Kawaoka, *Influenza A virus NS2 protein mediates vRNP nuclear export through NES-independent interaction with hCRM1.* EMBO J, 2000. **19**(24): p. 6751-8.
110. O'Neill, R.E., J. Talon, and P. Palese, *The influenza virus NEP (NS2 protein) mediates the nuclear export of viral ribonucleoproteins.* EMBO J, 1998. **17**(1): p. 288-96.
111. Elton, D., et al., *Interaction of the influenza virus nucleoprotein with the cellular CRM1-mediated nuclear export pathway.* J Virol, 2001. **75**(1): p. 408-19.
112. Bancroft, C.T. and T.G. Parslow, *Evidence for segment-nonspecific packaging of the influenza a virus genome.* J Virol, 2002. **76**(14): p. 7133-9.
113. Cao, S., et al., *A nuclear export signal in the matrix protein of Influenza A virus is required for efficient virus replication.* J Virol, 2012. **86**(9): p. 4883-91.
114. Sakaguchi, A., et al., *Nuclear export of influenza viral ribonucleoprotein is temperature-dependently inhibited by dissociation of viral matrix protein.* Virology, 2003. **306**(2): p. 244-53.
115. Whittaker, G., M. Bui, and A. Helenius, *Nuclear trafficking of influenza virus ribonuleoproteins in heterokaryons.* J Virol, 1996. **70**(5): p. 2743-56.
116. Akarsu, H., et al., *Crystal structure of the M1 protein-binding domain of the influenza A virus nuclear export protein (NEP/NS2).* EMBO J, 2003. **22**(18): p. 4646-55.
117. Calder, L.J., et al., *Structural organization of a filamentous influenza A virus.* Proc Natl Acad Sci U S A, 2010. **107**(23): p. 10685-90.
118. Bruce, E.A., P. Digard, and A.D. Stuart, *The Rab11 pathway is required for influenza A virus budding and filament formation.* J Virol, 2010. **84**(12): p. 5848-59.
119. Amorim, M.J., et al., *A Rab11- and microtubule-dependent mechanism for cytoplasmic transport of influenza A virus viral RNA.* J Virol, 2011. **85**(9): p. 4143-56.
120. Copeland, C.S., et al., *Folding, trimerization, and transport are sequential events in the biogenesis of influenza virus hemagglutinin.* Cell, 1988. **53**(2): p. 197-209.
121. Veit, M., et al., *The M2 protein of influenza A virus is acylated.* J Gen Virol, 1991. **72 (Pt 6)**: p. 1461-5.
122. Veit, M., et al., *Site-specific mutagenesis identifies three cysteine residues in the cytoplasmic tail as acylation sites of influenza virus hemagglutinin.* J Virol, 1991. **65**(5): p. 2491-500.
123. Chen, B.J., M. Takeda, and R.A. Lamb, *Influenza virus hemagglutinin (H3 subtype) requires palmitoylation of its cytoplasmic tail for assembly: M1 proteins*

of two subtypes differ in their ability to support assembly. J Virol, 2005. **79**(21): p. 13673-84.
124. Roberts, P.C., W. Garten, and H.D. Klenk, *Role of conserved glycosylation sites in maturation and transport of influenza A virus hemagglutinin.* J Virol, 1993. **67**(6): p. 3048-60.
125. Ohuchi, R., et al., *Oligosaccharides in the stem region maintain the influenza virus hemagglutinin in the metastable form required for fusion activity.* J Virol, 1997. **71**(5): p. 3719-25.
126. Wiley, D.C., I.A. Wilson, and J.J. Skehel, *Structural identification of the antibody-binding sites of Hong Kong influenza haemagglutinin and their involvement in antigenic variation.* Nature, 1981. **289**(5796): p. 373-8.
127. Zhang, M., et al., *Tracking global patterns of N-linked glycosylation site variation in highly variable viral glycoproteins: HIV, SIV, and HCV envelopes and influenza hemagglutinin.* Glycobiology, 2004. **14**(12): p. 1229-46.
128. Takeda, M., et al., *Influenza virus hemagglutinin concentrates in lipid raft microdomains for efficient viral fusion.* Proc Natl Acad Sci U S A, 2003. **100**(25): p. 14610-7.
129. Leser, G.P. and R.A. Lamb, *Influenza virus assembly and budding in raft-derived microdomains: a quantitative analysis of the surface distribution of HA, NA and M2 proteins.* Virology, 2005. **342**(2): p. 215-27.
130. Chen, B.J., et al., *Influenza virus hemagglutinin and neuraminidase, but not the matrix protein, are required for assembly and budding of plasmid-derived virus-like particles.* J Virol, 2007. **81**(13): p. 7111-23.
131. Inagaki, A., et al., *Competitive incorporation of homologous gene segments of influenza A virus into virions.* J Virol, 2012. **86**(18): p. 10200-2.
132. Marshall, N., et al., *Influenza virus reassortment occurs with high frequency in the absence of segment mismatch.* PLoS Pathog, 2013. **9**(6): p. e1003421.
133. Noda, T., et al., *Architecture of ribonucleoprotein complexes in influenza A virus particles.* Nature, 2006. **439**(7075): p. 490-2.
134. Enami, M., et al., *An influenza virus containing nine different RNA segments.* Virology, 1991. **185**(1): p. 291-8.
135. Gao, Q., et al., *A nine-segment influenza a virus carrying subtype H1 and H3 hemagglutinins.* J Virol, 2010. **84**(16): p. 8062-71.
136. Moules, V., et al., *In vitro characterization of naturally occurring influenza H3NA- viruses lacking the NA gene segment: toward a new mechanism of viral resistance?* Virology, 2010. **404**(2): p. 215-24.
137. Fonville, J.M., et al., *Influenza Virus Reassortment Is Enhanced by Semi-infectious Particles but Can Be Suppressed by Defective Interfering Particles.* PLoS Pathog, 2015. **11**(10): p. e1005204.
138. Brooke, C.B., et al., *Most influenza a virions fail to express at least one essential viral protein.* J Virol, 2013. **87**(6): p. 3155-62.
139. Lai, J.C., et al., *Formation of virus-like particles from human cell lines exclusively expressing influenza neuraminidase.* J Gen Virol, 2010. **91**(Pt 9): p. 2322-30.
140. Gomez-Puertas, P., et al., *Influenza virus matrix protein is the major driving force in virus budding.* J Virol, 2000. **74**(24): p. 11538-47.

141. Rossman, J.S., et al., *Influenza virus M2 protein mediates ESCRT-independent membrane scission.* Cell, 2010. **142**(6): p. 902-13.
142. Hui, E.K. and D.P. Nayak, *Role of ATP in influenza virus budding.* Virology, 2001. **290**(2): p. 329-41.
143. Rossman, J.S. and R.A. Lamb, *Influenza virus assembly and budding.* Virology, 2011. **411**(2): p. 229-36.
144. Zebedee, S.L., C.D. Richardson, and R.A. Lamb, *Characterization of the influenza virus M2 integral membrane protein and expression at the infected-cell surface from cloned cDNA.* J Virol, 1985. **56**(2): p. 502-11.
145. Li, J., et al., *Emergence and genetic variation of neuraminidase stalk deletions in avian influenza viruses.* PLoS One, 2011. **6**(2): p. e14722.
146. Baigent, S.J. and J.W. McCauley, *Glycosylation of haemagglutinin and stalk-length of neuraminidase combine to regulate the growth of avian influenza viruses in tissue culture.* Virus Res, 2001. **79**(1-2): p. 177-85.
147. Matsuoka, Y., et al., *Neuraminidase stalk length and additional glycosylation of the hemagglutinin influence the virulence of influenza H5N1 viruses for mice.* J Virol, 2009. **83**(9): p. 4704-8.
148. Sorrell, E.M., et al., *Minimal molecular constraints for respiratory droplet transmission of an avian-human H9N2 influenza A virus.* Proc Natl Acad Sci U S A, 2009. **106**(18): p. 7565-70.
149. Castrucci, M.R. and Y. Kawaoka, *Biologic importance of neuraminidase stalk length in influenza A virus.* J Virol, 1993. **67**(2): p. 759-64.
150. Gottschalk, A., *Neuraminidase: the specific enzyme of influenza virus and Vibrio cholerae.* Biochim Biophys Acta, 1957. **23**(3): p. 645-6.
151. Taylor, N.R. and M. von Itzstein, *Molecular modeling studies on ligand binding to sialidase from influenza virus and the mechanism of catalysis.* J Med Chem, 1994. **37**(5): p. 616-24.
152. Palese, P., et al., *Characterization of temperature sensitive influenza virus mutants defective in neuraminidase.* Virology, 1974. **61**(2): p. 397-410.
153. Ohuchi, M., et al., *Neuraminidase is essential for fowl plague virus hemagglutinin to show hemagglutinating activity.* Virology, 1995. **212**(1): p. 77-83.
154. Tiffany, J.M. and H.A. Blough, *Models of structure of the envelope of influenza virus.* Proc Natl Acad Sci U S A, 1970. **65**(4): p. 1105-12.
155. Schulze, I.T., *The structure of influenza virus. II. A model based on the morphology and composition of subviral particles.* Virology, 1972. **47**(1): p. 181-96.
156. Ruigrok, R.W., et al., *Characterization of three highly purified influenza virus strains by electron microscopy.* J Gen Virol, 1984. **65 (Pt 4)**: p. 799-802.
157. Steinhauer, D.A. and J.J. Holland, *Rapid evolution of RNA viruses.* Annu Rev Microbiol, 1987. **41**: p. 409-33.
158. Buonagurio, D.A., et al., *Evolution of human influenza A viruses over 50 years: rapid, uniform rate of change in NS gene.* Science, 1986. **232**(4753): p. 980-2.
159. Chen, Z., et al., *Evaluation of live attenuated influenza a virus h6 vaccines in mice and ferrets.* J Virol, 2009. **83**(1): p. 65-72.
160. Li, S., et al., *Recombinant influenza A virus vaccines for the pathogenic human A/Hong Kong/97 (H5N1) viruses.* J Infect Dis, 1999. **179**(5): p. 1132-8.

161. Maassab, H.F., *Adaptation and growth characteristics of influenza virus at 25 degrees c.* Nature, 1967. **213**(5076): p. 612-4.
162. Pappas, C., et al., *Development and evaluation of an Influenza virus subtype H7N2 vaccine candidate for pandemic preparedness.* Clin Vaccine Immunol, 2007. **14**(11): p. 1425-32.
163. Robertson, J.S., et al., *The development of vaccine viruses against pandemic A(H1N1) influenza.* Vaccine, 2011. **29**(9): p. 1836-43.
164. Suguitan, A.L., Jr., et al., *Live, attenuated influenza A H5N1 candidate vaccines provide broad cross-protection in mice and ferrets.* PLoS Med, 2006. **3**(9): p. e360.
165. Webby, R.J., et al., *Responsiveness to a pandemic alert: use of reverse genetics for rapid development of influenza vaccines.* Lancet, 2004. **363**(9415): p. 1099-103.
166. Fulvini, A.A., et al., *Gene constellation of influenza A virus reassortants with high growth phenotype prepared as seed candidates for vaccine production.* PLoS One, 2011. **6**(6): p. e20823.
167. Zhang, H., et al., *Universal influenza vaccines, a dream to be realized soon.* Viruses, 2014. **6**(5): p. 1974-91.
168. Krammer, F., *Emerging influenza viruses and the prospect of a universal influenza virus vaccine.* Biotechnol J, 2015. **10**(5): p. 690-701.
169. Pica, N. and P. Palese, *Toward a universal influenza virus vaccine: prospects and challenges.* Annu Rev Med, 2013. **64**: p. 189-202.
170. Davies, W.L., et al., *Antiviral Activity of 1-Adamantanamine (Amantadine).* Science, 1964. **144**(3620): p. 862-3.
171. Deyde, V.M., et al., *Surveillance of resistance to adamantanes among influenza A(H3N2) and A(H1N1) viruses isolated worldwide.* J Infect Dis, 2007. **196**(2): p. 249-57.
172. Hay, A.J., et al., *The molecular basis of the specific anti-influenza action of amantadine.* EMBO J, 1985. **4**(11): p. 3021-4.
173. Sweet, C., et al., *Virulence of rimantadine-resistant human influenza A (H3N2) viruses in ferrets.* J Infect Dis, 1991. **164**(5): p. 969-72.
174. Steinhauer, D.A., et al., *Amantadine selection of a mutant influenza virus containing an acid-stable hemagglutinin glycoprotein: evidence for virus-specific regulation of the pH of glycoprotein transport vesicles.* Proc Natl Acad Sci U S A, 1991. **88**(24): p. 11525-9.
175. Daniels, R.S., et al., *Fusion mutants of the influenza virus hemagglutinin glycoprotein.* Cell, 1985. **40**(2): p. 431-9.
176. von Itzstein, M., et al., *Rational design of potent sialidase-based inhibitors of influenza virus replication.* Nature, 1993. **363**(6428): p. 418-23.
177. Collins, P.J., et al., *Crystal structures of oseltamivir-resistant influenza virus neuraminidase mutants.* Nature, 2008. **453**(7199): p. 1258-61.
178. Gubareva, L.V., et al., *Characterization of mutants of influenza A virus selected with the neuraminidase inhibitor 4-guanidino-Neu5Ac2en.* J Virol, 1996. **70**(3): p. 1818-27.
179. McKimm-Breschkin, J.L., et al., *Mutation in the influenza virus neuraminidase gene resulting in decreased sensitivity to the neuraminidase inhibitor 4-*

guanidino-Neu5Ac2en leads to instability of the enzyme. Virology, 1996. **225**(1): p. 240-2.
180. Fedson, D.S., et al., *Anti-neuraminidase antibody response in serum and nasal secretions following intranasal or subcutaneous inactivated A2-Hong Kong-68 influenza virus vaccine.* J Immunol, 1971. **107**(3): p. 730-7.
181. Sun, S., et al., *Glycosylation site alteration in the evolution of influenza A (H1N1) viruses.* PLoS One, 2011. **6**(7): p. e22844.
182. Kilbourne, E.D., *Influenza pandemics of the 20th century.* Emerg Infect Dis, 2006. **12**(1): p. 9-14.
183. *A revision of the system of nomenclature for influenza viruses: a WHO memorandum.* Bull World Health Organ, 1980. **58**(4): p. 585-91.
184. Tong, S., et al., *A distinct lineage of influenza A virus from bats.* Proc Natl Acad Sci U S A, 2012. **109**(11): p. 4269-74.
185. Ma, W., A. Garcia-Sastre, and M. Schwemmle, *Expected and Unexpected Features of the Newly Discovered Bat Influenza A-like Viruses.* PLoS Pathog, 2015. **11**(6): p. e1004819.
186. Russell, R.J., et al., *H1 and H7 influenza haemagglutinin structures extend a structural classification of haemagglutinin subtypes.* Virology, 2004. **325**(2): p. 287-96.
187. Gao, R., et al., *Human infection with a novel avian-origin influenza A (H7N9) virus.* N Engl J Med, 2013. **368**(20): p. 1888-97.
188. Peiris, M., et al., *Human infection with influenza H9N2.* Lancet, 1999. **354**(9182): p. 916-7.
189. Rambaut, A., et al., *The genomic and epidemiological dynamics of human influenza A virus.* Nature, 2008. **453**(7195): p. 615-9.
190. Nelson, M.I., et al., *Multiple reassortment events in the evolutionary history of H1N1 influenza A virus since 1918.* PLoS Pathog, 2008. **4**(2): p. e1000012.
191. Schweiger, B., L. Bruns, and K. Meixenberger, *Reassortment between human A(H3N2) viruses is an important evolutionary mechanism.* Vaccine, 2006. **24**(44-46): p. 6683-90.
192. Simonsen, L., et al., *The genesis and spread of reassortment human influenza A/H3N2 viruses conferring adamantane resistance.* Mol Biol Evol, 2007. **24**(8): p. 1811-20.
193. Li, K.S., et al., *Genesis of a highly pathogenic and potentially pandemic H5N1 influenza virus in eastern Asia.* Nature, 2004. **430**(6996): p. 209-13.
194. Baez, M., P. Palese, and E.D. Kilbourne, *Gene composition of high-yielding influenza vaccine strains obtained by recombination.* J Infect Dis, 1980. **141**(3): p. 362-5.
195. Song, M.S., et al., *Growth and Pathogenic Potential of Naturally Selected Reassortants after Coinfection with Pandemic H1N1 and Highly Pathogenic Avian Influenza H5N1 Viruses.* J Virol, 2016. **90**(1): p. 616-23.
196. Imai, M., et al., *Experimental adaptation of an influenza H5 HA confers respiratory droplet transmission to a reassortant H5 HA/H1N1 virus in ferrets.* Nature, 2012. **486**(7403): p. 420-8.
197. Morens, D.M., et al., *The 1918 influenza pandemic: lessons for 2009 and the future.* Crit Care Med, 2010. **38**(4 Suppl): p. e10-20.

198. Taubenberger, J.K., et al., *Initial genetic characterization of the 1918 "Spanish" influenza virus.* Science, 1997. **275**(5307): p. 1793-6.
199. Reid, A.H., et al., *Origin and evolution of the 1918 "Spanish" influenza virus hemagglutinin gene.* Proc Natl Acad Sci U S A, 1999. **96**(4): p. 1651-6.
200. Anhlan, D., et al., *Origin of the 1918 pandemic H1N1 influenza A virus as studied by codon usage patterns and phylogenetic analysis.* RNA, 2011. **17**(1): p. 64-73.
201. Scholtissek, C., et al., *On the origin of the human influenza virus subtypes H2N2 and H3N2.* Virology, 1978. **87**(1): p. 13-20.
202. Gething, M.J., et al., *Cloning and DNA sequence of double-stranded copies of haemagglutinin genes from H2 and H3 strains elucidates antigenic shift and drift in human influenza virus.* Nature, 1980. **287**(5780): p. 301-6.
203. Kawaoka, Y., S. Krauss, and R.G. Webster, *Avian-to-human transmission of the PB1 gene of influenza A viruses in the 1957 and 1968 pandemics.* J Virol, 1989. **63**(11): p. 4603-8.
204. Fang, R., et al., *Complete structure of A/duck/Ukraine/63 influenza hemagglutinin gene: animal virus as progenitor of human H3 Hong Kong 1968 influenza hemagglutinin.* Cell, 1981. **25**(2): p. 315-23.
205. Smith, G.J., et al., *Origins and evolutionary genomics of the 2009 swine-origin H1N1 influenza A epidemic.* Nature, 2009. **459**(7250): p. 1122-5.
206. Garten, R.J., et al., *Antigenic and genetic characteristics of swine-origin 2009 A(H1N1) influenza viruses circulating in humans.* Science, 2009. **325**(5937): p. 197-201.
207. Nelson, M.I., et al., *Introductions and evolution of human-origin seasonal influenza a viruses in multinational swine populations.* J Virol, 2014. **88**(17): p. 10110-9.
208. Hirst, G.K., *The Agglutination of Red Cells by Allantoic Fluid of Chick Embryos Infected with Influenza Virus.* Science, 1941. **94**(2427): p. 22-3.
209. Hare, R., M. Curl, and C.L. Mc, *The efficiency of the red cell adsorption and elution method for the preparation of influenza vaccine.* Can J Public Health, 1946. **37**: p. 284-91.
210. Matrosovich, M., G. Herrler, and H.D. Klenk, *Sialic Acid Receptors of Viruses.* Top Curr Chem, 2015. **367**: p. 1-28.
211. Varki, A. and R. Schauer, *Sialic Acids*, in *Essentials of Glycobiology*, A. Varki, et al., Editors. 2009: Cold Spring Harbor (NY).
212. Kelm, S. and R. Schauer, *Sialic acids in molecular and cellular interactions.* Int Rev Cytol, 1997. **175**: p. 137-240.
213. Byrd-Leotis, L., et al., *Shotgun glycomics of pig lung identifies natural endogenous receptors for influenza viruses.* Proc Natl Acad Sci U S A, 2014. **111**(22): p. E2241-50.
214. Stanley, P., H. Schachter, and N. Taniguchi, *N-Glycans*, in *Essentials of Glycobiology*, A. Varki, et al., Editors. 2009: Cold Spring Harbor (NY).
215. Helenius, A. and M. Aebi, *Roles of N-linked glycans in the endoplasmic reticulum.* Annu Rev Biochem, 2004. **73**: p. 1019-49.
216. Freeze, H.H. and H. Schachter, *Genetic Disorders of Glycosylation*, in *Essentials of Glycobiology*, A. Varki, et al., Editors. 2009: Cold Spring Harbor (NY).

217. Brockhausen, I., H. Schachter, and P. Stanley, *O-GalNAc Glycans*, in *Essentials of Glycobiology*, A. Varki, et al., Editors. 2009: Cold Spring Harbor (NY).
218. Gagneux, P., et al., *Human-specific regulation of alpha 2-6-linked sialic acids.* J Biol Chem, 2003. **278**(48): p. 48245-50.
219. Button, B., et al., *A periciliary brush promotes the lung health by separating the mucus layer from airway epithelia.* Science, 2012. **337**(6097): p. 937-41.
220. Roy, M.G., et al., *Muc5b is required for airway defence.* Nature, 2014. **505**(7483): p. 412-6.
221. Ehre, C., et al., *Overexpressing mouse model demonstrates the protective role of Muc5ac in the lungs.* Proc Natl Acad Sci U S A, 2012. **109**(41): p. 16528-33.
222. Lillehoj, E.P., et al., *Cellular and molecular biology of airway mucins.* Int Rev Cell Mol Biol, 2013. **303**: p. 139-202.
223. Campbell, P.J., et al., *The M segment of the 2009 pandemic influenza virus confers increased neuraminidase activity, filamentous morphology, and efficient contact transmissibility to A/Puerto Rico/8/1934-based reassortant viruses.* J Virol, 2014. **88**(7): p. 3802-14.
224. Lakdawala, S.S., et al., *Eurasian-origin gene segments contribute to the transmissibility, aerosol release, and morphology of the 2009 pandemic H1N1 influenza virus.* PLoS Pathog, 2011. **7**(12): p. e1002443.
225. Booy, F.P., R.W. Ruigrok, and E.F. van Bruggen, *Electron microscopy of influenza virus. A comparison of negatively stained and ice-embedded particles.* J Mol Biol, 1985. **184**(4): p. 667-76.
226. Nermut, M.V., *Further investigation on the fine structure of influenza virus.* J Gen Virol, 1972. **17**(3): p. 317-31.
227. Elleman, C.J. and W.S. Barclay, *The M1 matrix protein controls the filamentous phenotype of influenza A virus.* Virology, 2004. **321**(1): p. 144-53.
228. Roberts, P.C., R.A. Lamb, and R.W. Compans, *The M1 and M2 proteins of influenza A virus are important determinants in filamentous particle formation.* Virology, 1998. **240**(1): p. 127-37.
229. Burleigh, L.M., et al., *Influenza a viruses with mutations in the m1 helix six domain display a wide variety of morphological phenotypes.* J Virol, 2005. **79**(2): p. 1262-70.
230. Choppin, P.W. and I. Tamm, *Studies of two kinds of virus particles which comprise influenza A2 virus strains. II. Reactivity with virus inhibitors in normal sera.* J Exp Med, 1960. **112**: p. 921-44.
231. Chu, C.M., I.M. Dawson, and W.J. Elford, *Filamentous forms associated with newly isolated influenza virus.* Lancet, 1949. **1**(6554): p. 602.
232. Campbell, P.J., et al., *Residue 41 of the Eurasian avian-like swine influenza a virus matrix protein modulates virion filament length and efficiency of contact transmission.* J Virol, 2014. **88**(13): p. 7569-77.
233. Bourmakina, S.V. and A. Garcia-Sastre, *Reverse genetics studies on the filamentous morphology of influenza A virus.* J Gen Virol, 2003. **84**(Pt 3): p. 517-27.
234. Seladi-Schulman, J., et al., *Filament-producing mutants of influenza A/Puerto Rico/8/1934 (H1N1) virus have higher neuraminidase activities than the spherical wild-type.* PLoS One, 2014. **9**(11): p. e112462.

235. Seladi-Schulman, J., J. Steel, and A.C. Lowen, *Spherical influenza viruses have a fitness advantage in embryonated eggs, while filament-producing strains are selected in vivo.* J Virol, 2013. **87**(24): p. 13343-53.
236. Harris, A., et al., *Influenza virus pleiomorphy characterized by cryoelectron tomography.* Proc Natl Acad Sci U S A, 2006. **103**(50): p. 19123-7.
237. Burnet, F.M., *Enzymic action of influenza viruses on glandular mucin and on purified blood group substances.* Aust J Sci, 1947. **10**(1): p. 21.
238. Gottschalk, A. and P.E. Lind, *Product of interaction between influenza virus enzyme and ovomucin.* Nature, 1949. **164**(4162): p. 232.
239. Matrosovich, M.N., et al., *Neuraminidase is important for the initiation of influenza virus infection in human airway epithelium.* J Virol, 2004. **78**(22): p. 12665-7.
240. Ohuchi, M., et al., *Roles of neuraminidase in the initial stage of influenza virus infection.* Microbes Infect, 2006. **8**(5): p. 1287-93.
241. Cohen, M., et al., *Influenza A penetrates host mucus by cleaving sialic acids with neuraminidase.* Virol J, 2013. **10**: p. 321.
242. Zanin, M., et al., *Pandemic Swine H1N1 Influenza Viruses with Almost Undetectable Neuraminidase Activity Are Not Transmitted via Aerosols in Ferrets and Are Inhibited by Human Mucus but Not Swine Mucus.* J Virol, 2015. **89**(11): p. 5935-48.
243. Ito, T., et al., *Molecular basis for the generation in pigs of influenza A viruses with pandemic potential.* J Virol, 1998. **72**(9): p. 7367-73.
244. Webster, R.G., et al., *Evolution and ecology of influenza A viruses.* Microbiol Rev, 1992. **56**(1): p. 152-79.
245. Shibuya, N., et al., *The elderberry (Sambucus nigra L.) bark lectin recognizes the Neu5Ac(alpha 2-6)Gal/GalNAc sequence.* The Journal of biological chemistry, 1987. **262**(4): p. 1596-601.
246. Wang, W.C. and R.D. Cummings, *The immobilized leukoagglutinin from the seeds of Maackia amurensis binds with high affinity to complex-type Asn-linked oligosaccharides containing terminal sialic acid-linked alpha-2,3 to penultimate galactose residues.* The Journal of biological chemistry, 1988. **263**(10): p. 4576-85.
247. Konami, Y., et al., *Strong affinity of Maackia amurensis hemagglutinin (MAH) for sialic acid-containing Ser/Thr-linked carbohydrate chains of N-terminal octapeptides from human glycophorin A.* FEBS Lett, 1994. **342**(3): p. 334-8.
248. Geisler, C. and D.L. Jarvis, *Effective glycoanalysis with Maackia amurensis lectins requires a clear understanding of their binding specificities.* Glycobiology, 2011. **21**(8): p. 988-93.
249. Franca, M., D.E. Stallknecht, and E.W. Howerth, *Expression and distribution of sialic acid influenza virus receptors in wild birds.* Avian Pathol, 2013. **42**(1): p. 60-71.
250. Wan, H. and D.R. Perez, *Quail carry sialic acid receptors compatible with binding of avian and human influenza viruses.* Virology, 2006. **346**(2): p. 278-86.
251. Costa, T., et al., *Distribution patterns of influenza virus receptors and viral attachment patterns in the respiratory and intestinal tracts of seven avian species.* Vet Res, 2012. **43**: p. 28.

252. Gambaryan, A., R. Webster, and M. Matrosovich, *Differences between influenza virus receptors on target cells of duck and chicken.* Arch Virol, 2002. **147**(6): p. 1197-208.
253. Kuchipudi, S.V., et al., *Differences in influenza virus receptors in chickens and ducks: Implications for interspecies transmission.* J Mol Genet Med, 2009. **3**(1): p. 143-51.
254. Nicholls, J.M., et al., *Sialic acid receptor detection in the human respiratory tract: evidence for widespread distribution of potential binding sites for human and avian influenza viruses.* Respiratory research, 2007. **8**: p. 73.
255. Nelli, R.K., et al., *Comparative distribution of human and avian type sialic acid influenza receptors in the pig.* BMC veterinary research, 2010. **6**: p. 4.
256. Scholtissek, C., *Molecular evolution of influenza viruses.* Virus Genes, 1995. **11**(2-3): p. 209-15.
257. Punyadarsaniya, D., et al., *Infection of differentiated porcine airway epithelial cells by influenza virus: differential susceptibility to infection by porcine and avian viruses.* PLoS One, 2011. **6**(12): p. e28429.
258. Van Poucke, S.G., et al., *Replication of avian, human and swine influenza viruses in porcine respiratory explants and association with sialic acid distribution.* Virology journal, 2010. **7**: p. 38.
259. Bateman, A.C., et al., *Glycan analysis and influenza A virus infection of primary swine respiratory epithelial cells: the importance of NeuAc{alpha}2-6 glycans.* The Journal of biological chemistry, 2010. **285**(44): p. 34016-26.
260. Gambaryan, A.S., et al., *Receptor-binding properties of swine influenza viruses isolated and propagated in MDCK cells.* Virus Res, 2005. **114**(1-2): p. 15-22.
261. Takemae, N., et al., *Alterations in receptor-binding properties of swine influenza viruses of the H1 subtype after isolation in embryonated chicken eggs.* J Gen Virol, 2010. **91**(Pt 4): p. 938-48.
262. Chou, H.H., et al., *A mutation in human CMP-sialic acid hydroxylase occurred after the Homo-Pan divergence.* Proc Natl Acad Sci U S A, 1998. **95**(20): p. 11751-6.
263. Irie, A., et al., *The molecular basis for the absence of N-glycolylneuraminic acid in humans.* J Biol Chem, 1998. **273**(25): p. 15866-71.
264. Sillanaukee, P., M. Ponnio, and I.P. Jaaskelainen, *Occurrence of sialic acids in healthy humans and different disorders.* Eur J Clin Invest, 1999. **29**(5): p. 413-25.
265. Sriwilaijaroen, N., et al., *N-glycans from porcine trachea and lung: predominant NeuAcalpha2-6Gal could be a selective pressure for influenza variants in favor of human-type receptor.* PLoS One, 2011. **6**(2): p. e16302.
266. Suzuki, T., et al., *Swine influenza virus strains recognize sialylsugar chains containing the molecular species of sialic acid predominantly present in the swine tracheal epithelium.* FEBS Lett, 1997. **404**(2-3): p. 192-6.
267. Karasin, A.I., et al., *Genetic characterization of H3N2 influenza viruses isolated from pigs in North America, 1977-1999: evidence for wholly human and reassortant virus genotypes.* Virus Res, 2000. **68**(1): p. 71-85.
268. Couceiro, J.N., J.C. Paulson, and L.G. Baum, *Influenza virus strains selectively recognize sialyloligosaccharides on human respiratory epithelium; the role of the*

host cell in selection of hemagglutinin receptor specificity. Virus Res, 1993. **29**(2): p. 155-65.
269. Matrosovich, M.N., et al., *Human and avian influenza viruses target different cell types in cultures of human airway epithelium.* Proc Natl Acad Sci U S A, 2004. **101**(13): p. 4620-4.
270. Barkhordari, A., et al., *Lectin histochemistry of normal human lung.* J Mol Histol, 2004. **35**(2): p. 147-56.
271. van Riel, D., et al., *Human and avian influenza viruses target different cells in the lower respiratory tract of humans and other mammals.* Am J Pathol, 2007. **171**(4): p. 1215-23.
272. van Riel, D., et al., *H5N1 Virus Attachment to Lower Respiratory Tract.* Science, 2006. **312**(5772): p. 399.
273. Eisen, M.B., et al., *Binding of the influenza A virus to cell-surface receptors: structures of five hemagglutinin-sialyloligosaccharide complexes determined by X-ray crystallography.* Virology, 1997. **232**(1): p. 19-31.
274. Chutinimitkul, S., et al., *Virulence-associated substitution D222G in the hemagglutinin of 2009 pandemic influenza A(H1N1) virus affects receptor binding.* J Virol, 2010. **84**(22): p. 11802-13.
275. Liu, Y., et al., *Altered receptor specificity and cell tropism of D222G hemagglutinin mutants isolated from fatal cases of pandemic A(H1N1) 2009 influenza virus.* J Virol, 2010. **84**(22): p. 12069-74.
276. Matrosovich, M., et al., *Early alterations of the receptor-binding properties of H1, H2, and H3 avian influenza virus hemagglutinins after their introduction into mammals.* J Virol, 2000. **74**(18): p. 8502-12.
277. Watanabe, Y., et al., *Acquisition of human-type receptor binding specificity by new H5N1 influenza virus sublineages during their emergence in birds in Egypt.* PLoS Pathog, 2011. **7**(5): p. e1002068.
278. Shi, Y., et al., *Structures and receptor binding of hemagglutinins from human-infecting H7N9 influenza viruses.* Science, 2013. **342**(6155): p. 243-7.
279. Herfst, S., et al., *Airborne transmission of influenza A/H5N1 virus between ferrets.* Science, 2012. **336**(6088): p. 1534-41.
280. Yassine, H.M., et al., *Interspecies and intraspecies transmission of influenza A viruses: viral, host and environmental factors.* Anim Health Res Rev, 2010. **11**(1): p. 53-72.
281. Long, J.S., et al., *Species difference in ANP32A underlies influenza A virus polymerase host restriction.* Nature, 2016. **529**(7584): p. 101-4.
282. McFadden, E.R., Jr., et al., *Thermal mapping of the airways in humans.* J Appl Physiol (1985), 1985. **58**(2): p. 564-70.
283. Massin, P., S. van der Werf, and N. Naffakh, *Residue 627 of PB2 is a determinant of cold sensitivity in RNA replication of avian influenza viruses.* J Virol, 2001. **75**(11): p. 5398-404.
284. Lindemann, J., et al., *Nasal mucosal temperature during respiration.* Clin Otolaryngol Allied Sci, 2002. **27**(3): p. 135-9.
285. Steel, J., et al., *Transmission of influenza virus in a mammalian host is increased by PB2 amino acids 627K or 627E/701N.* PLoS Pathog, 2009. **5**(1): p. e1000252.

286. Subbarao, E.K., Y. Kawaoka, and B.R. Murphy, *Rescue of an influenza A virus wild-type PB2 gene and a mutant derivative bearing a site-specific temperature-sensitive and attenuating mutation.* J Virol, 1993. **67**(12): p. 7223-8.
287. Zaraket, H., et al., *Increased acid stability of the hemagglutinin protein enhances H5N1 influenza virus growth in the upper respiratory tract but is insufficient for transmission in ferrets.* J Virol, 2013. **87**(17): p. 9911-22.
288. Shortridge, K.F., *Poultry and the influenza H5N1 outbreak in Hong Kong, 1997: abridged chronology and virus isolation.* Vaccine, 1999. **17 Suppl 1**: p. S26-9.
289. Donatelli, I., et al., *Human-Animal Interface: The Case for Influenza Interspecies Transmission.* Adv Exp Med Biol, 2016.
290. Swayne, D.E. and D.L. Suarez, *Highly pathogenic avian influenza.* Rev Sci Tech, 2000. **19**(2): p. 463-82.
291. Rohm, C., et al., *Do hemagglutinin genes of highly pathogenic avian influenza viruses constitute unique phylogenetic lineages?* Virology, 1995. **209**(2): p. 664-70.
292. Capua, I. and S. Marangon, *The avian influenza epidemic in Italy, 1999-2000: a review.* Avian Pathol, 2000. **29**(4): p. 289-94.
293. Li, F.C., et al., *Finding the real case-fatality rate of H5N1 avian influenza.* J Epidemiol Community Health, 2008. **62**(6): p. 555-9.
294. Wood, G.W., et al., *Deduced amino acid sequences at the haemagglutinin cleavage site of avian influenza A viruses of H5 and H7 subtypes.* Arch Virol, 1993. **130**(1-2): p. 209-17.
295. Horimoto, T., et al., *Proprotein-processing endoproteases PC6 and furin both activate hemagglutinin of virulent avian influenza viruses.* J Virol, 1994. **68**(9): p. 6074-8.
296. Rott, R., et al., *Influenza viruses, cell enzymes, and pathogenicity.* Am J Respir Crit Care Med, 1995. **152**(4 Pt 2): p. S16-9.
297. Bosch, F.X., et al., *Proteolytic cleavage of influenza virus hemagglutinins: primary structure of the connecting peptide between HA1 and HA2 determines proteolytic cleavability and pathogenicity of Avian influenza viruses.* Virology, 1981. **113**(2): p. 725-35.
298. Gao, P., et al., *Biological heterogeneity, including systemic replication in mice, of H5N1 influenza A virus isolates from humans in Hong Kong.* J Virol, 1999. **73**(4): p. 3184-9.
299. Horimoto, T. and Y. Kawaoka, *The hemagglutinin cleavability of a virulent avian influenza virus by subtilisin-like endoproteases is influenced by the amino acid immediately downstream of the cleavage site.* Virology, 1995. **210**(2): p. 466-70.
300. Kawaoka, Y. and R.G. Webster, *Sequence requirements for cleavage activation of influenza virus hemagglutinin expressed in mammalian cells.* Proc Natl Acad Sci U S A, 1988. **85**(2): p. 324-8.
301. Stieneke-Grober, A., et al., *Influenza virus hemagglutinin with multibasic cleavage site is activated by furin, a subtilisin-like endoprotease.* EMBO J, 1992. **11**(7): p. 2407-14.
302. Walker, J.A., et al., *Sequence specificity of furin, a proprotein-processing endoprotease, for the hemagglutinin of a virulent avian influenza virus.* J Virol, 1994. **68**(2): p. 1213-8.

303. Yen, H.L., et al., *Changes in H5N1 influenza virus hemagglutinin receptor binding domain affect systemic spread.* Proc Natl Acad Sci U S A, 2009. **106**(1): p. 286-91.
304. Taubenberger, J.K., et al., *Characterization of the 1918 influenza virus polymerase genes.* Nature, 2005. **437**(7060): p. 889-93.
305. Shinya, K., et al., *Adaptation of an H7N7 equine influenza A virus in mice.* J Gen Virol, 2007. **88**(Pt 2): p. 547-53.
306. Baum, L.G. and J.C. Paulson, *The N2 neuraminidase of human influenza virus has acquired a substrate specificity complementary to the hemagglutinin receptor specificity.* Virology, 1991. **180**(1): p. 10-5.
307. Xu, R., et al., *Functional balance of the hemagglutinin and neuraminidase activities accompanies the emergence of the 2009 H1N1 influenza pandemic.* J Virol, 2012. **86**(17): p. 9221-32.
308. Ginting, T.E., et al., *Amino acid changes in hemagglutinin contribute to the replication of oseltamivir-resistant H1N1 influenza viruses.* J Virol, 2012. **86**(1): p. 121-7.
309. Blick, T.J., et al., *The interaction of neuraminidase and hemagglutinin mutations in influenza virus in resistance to 4-guanidino-Neu5Ac2en.* Virology, 1998. **246**(1): p. 95-103.
310. Kaverin, N.V., et al., *Postreassortment changes in influenza A virus hemagglutinin restoring HA-NA functional match.* Virology, 1998. **244**(2): p. 315-21.
311. Hughes, M.T., et al., *Influenza A viruses lacking sialidase activity can undergo multiple cycles of replication in cell culture, eggs, or mice.* J Virol, 2000. **74**(11): p. 5206-12.
312. Richard, M., et al., *Rescue of a H3N2 influenza virus containing a deficient neuraminidase protein by a hemagglutinin with a low receptor-binding affinity.* PLoS One, 2012. **7**(5): p. e33880.
313. Mitnaul, L.J., et al., *Balanced hemagglutinin and neuraminidase activities are critical for efficient replication of influenza A virus.* J Virol, 2000. **74**(13): p. 6015-20.
314. Yen, H.L., et al., *Hemagglutinin-neuraminidase balance confers respiratory-droplet transmissibility of the pandemic H1N1 influenza virus in ferrets.* Proc Natl Acad Sci U S A, 2011. **108**(34): p. 14264-9.
315. Diederich, S., et al., *Hemagglutinin-Neuraminidase Balance Influences the Virulence Phenotype of a Recombinant H5N3 Influenza A Virus Possessing a Polybasic HA0 Cleavage Site.* J Virol, 2015. **89**(21): p. 10724-34.
316. de Vries, E., et al., *Influenza A virus entry into cells lacking sialylated N-glycans.* Proc Natl Acad Sci U S A, 2012. **109**(19): p. 7457-62.
317. Benton, D.J., et al., *Biophysical measurement of the balance of influenza a hemagglutinin and neuraminidase activities.* J Biol Chem, 2015. **290**(10): p. 6516-21.
318. Herfst, S., et al., *Avian influenza virus transmission to mammals.* Curr Top Microbiol Immunol, 2014. **385**: p. 137-55.
319. de Jong, J.C., et al., *A pandemic warning?* Nature, 1997. **389**(6651): p. 554.

320. Hien, T.T., M. de Jong, and J. Farrar, *Avian influenza--a challenge to global health care structures.* N Engl J Med, 2004. **351**(23): p. 2363-5.
321. Beigel, J.H., et al., *Avian influenza A (H5N1) infection in humans.* N Engl J Med, 2005. **353**(13): p. 1374-85.
322. Almond, J.W., *A single gene determines the host range of influenza virus.* Nature, 1977. **270**(5638): p. 617-8.
323. Oxford, J.S., et al., *Analysis of virion RNA segments and polypeptides of influenza A virus recombinants of defined virulence.* Nature, 1978. **273**(5665): p. 778-9.
324. Scholtissek, C., et al., *The nucleoprotein as a possible major factor in determining host specificity of influenza H3N2 viruses.* Virology, 1985. **147**(2): p. 287-94.
325. Scholtissek, C., I. Koennecke, and R. Rott, *Host range recombinants of fowl plague (influenza A) virus.* Virology, 1978. **91**(1): p. 79-85.
326. Scholtissek, C. and B.R. Murphy, *Host range mutants of an influenza A virus.* Arch Virol, 1978. **58**(4): p. 323-33.
327. Snyder, M.H., et al., *The avian influenza virus nucleoprotein gene and a specific constellation of avian and human virus polymerase genes each specify attenuation of avian-human influenza A/Pintail/79 reassortant viruses for monkeys.* J Virol, 1987. **61**(9): p. 2857-63.
328. Snyder, M.H., et al., *Attenuation of wild-type human influenza A virus by acquisition of the PA polymerase and matrix protein genes of influenza A/Ann Arbor/6/60 cold-adapted donor virus.* J Clin Microbiol, 1985. **22**(5): p. 719-25.
329. Snyder, M.H., et al., *Four viral genes independently contribute to attenuation of live influenza A/Ann Arbor/6/60 (H2N2) cold-adapted reassortant virus vaccines.* J Virol, 1988. **62**(2): p. 488-95.
330. Chanock, R.M., et al., *Live viral vaccines for respiratory and enteric tract diseases.* Vaccine, 1988. **6**(2): p. 129-33.
331. de Wit, E., et al., *Pathogenicity of highly pathogenic avian influenza virus in mammals.* Vaccine, 2008. **26 Suppl 4**: p. D54-8.
332. Steinhauer, D.A. and J.J. Skehel, *Genetics of influenza viruses.* Annu Rev Genet, 2002. **36**: p. 305-32.
333. Russell, C.A., et al., *The potential for respiratory droplet-transmissible A/H5N1 influenza virus to evolve in a mammalian host.* Science, 2012. **336**(6088): p. 1541-7.
334. Brown, E.G., et al., *Pattern of mutation in the genome of influenza A virus on adaptation to increased virulence in the mouse lung: identification of functional themes.* Proc Natl Acad Sci U S A, 2001. **98**(12): p. 6883-8.
335. de Graaf, M. and R.A. Fouchier, *Role of receptor binding specificity in influenza A virus transmission and pathogenesis.* EMBO J, 2014. **33**(8): p. 823-41.
336. Wilks, S., et al., *A review of influenza haemagglutinin receptor binding as it relates to pandemic properties.* Vaccine, 2012. **30**(29): p. 4369-76.
337. Mair, C.M., et al., *Receptor binding and pH stability - how influenza A virus hemagglutinin affects host-specific virus infection.* Biochim Biophys Acta, 2014. **1838**(4): p. 1153-68.

338. Xiong, X., J.W. McCauley, and D.A. Steinhauer, *Receptor binding properties of the influenza virus hemagglutinin as a determinant of host range.* Curr Top Microbiol Immunol, 2014. **385**: p. 63-91.
339. Reed, M.L., et al., *The pH of activation of the hemagglutinin protein regulates H5N1 influenza virus pathogenicity and transmissibility in ducks.* J Virol, 2010. **84**(3): p. 1527-35.
340. DuBois, R.M., et al., *Acid stability of the hemagglutinin protein regulates H5N1 influenza virus pathogenicity.* PLoS Pathog, 2011. **7**(12): p. e1002398.
341. Shelton, H., et al., *Mutations in haemagglutinin that affect receptor binding and pH stability increase replication of a PR8 influenza virus with H5 HA in the upper respiratory tract of ferrets and may contribute to transmissibility.* J Gen Virol, 2013. **94**(Pt 6): p. 1220-9.
342. Collins, P.J., et al., *Recent evolution of equine influenza and the origin of canine influenza.* Proc Natl Acad Sci U S A, 2014. **111**(30): p. 11175-80.
343. Koerner, I., et al., *Altered receptor specificity and fusion activity of the haemagglutinin contribute to high virulence of a mouse-adapted influenza A virus.* J Gen Virol, 2012. **93**(Pt 5): p. 970-9.
344. Bottcher-Friebertshauser, E., et al., *The hemagglutinin: a determinant of pathogenicity.* Curr Top Microbiol Immunol, 2014. **385**: p. 3-34.
345. Belser, J.A., et al., *Pathogenesis and transmission of avian influenza A (H7N9) virus in ferrets and mice.* Nature, 2013. **501**(7468): p. 556-9.
346. Klenk, H.D., et al., *Activation of influenza A viruses by trypsin treatment.* Virology, 1975. **68**(2): p. 426-39.
347. Lazarowitz, S.G. and P.W. Choppin, *Enhancement of the infectivity of influenza A and B viruses by proteolytic cleavage of the hemagglutinin polypeptide.* Virology, 1975. **68**(2): p. 440-54.
348. Appleyard, G. and H.B. Maber, *Plaque formation by influenza viruses in the presence of trypsin.* J Gen Virol, 1974. **25**(3): p. 351-7.
349. Scholtissek, C., *Stability of infectious influenza A viruses to treatment at low pH and heating.* Arch Virol, 1985. **85**(1-2): p. 1-11.
350. Scholtissek, C., *Stability of infectious influenza A viruses at low pH and at elevated temperature.* Vaccine, 1985. **3**(3 Suppl): p. 215-8.
351. Ruigrok, R.W., et al., *Conformational changes in the hemagglutinin of influenza virus which accompany heat-induced fusion of virus with liposomes.* Virology, 1986. **155**(2): p. 484-97.
352. Carr, C.M., C. Chaudhry, and P.S. Kim, *Influenza hemagglutinin is spring-loaded by a metastable native conformation.* Proc Natl Acad Sci U S A, 1997. **94**(26): p. 14306-13.
353. Haywood, A.M. and B.P. Boyer, *Time and temperature dependence of influenza virus membrane fusion at neutral pH.* J Gen Virol, 1986. **67 (Pt 12)**: p. 2813-7.
354. Fischer, H. and J.H. Widdicombe, *Mechanisms of acid and base secretion by the airway epithelium.* J Membr Biol, 2006. **211**(3): p. 139-50.
355. Fischer, H., J.H. Widdicombe, and B. Illek, *Acid secretion and proton conductance in human airway epithelium.* Am J Physiol Cell Physiol, 2002. **282**(4): p. C736-43.

356. O'Donnell, C.D., et al., *The matrix gene segment destabilizes the Acid and thermal stability of the hemagglutinin of pandemic live attenuated influenza virus vaccines.* J Virol, 2014. **88**(21): p. 12374-84.
357. Weis, W.I., et al., *The structure of a membrane fusion mutant of the influenza virus haemagglutinin.* EMBO J, 1990. **9**(1): p. 17-24.
358. Thoennes, S., et al., *Analysis of residues near the fusion peptide in the influenza hemagglutinin structure for roles in triggering membrane fusion.* Virology, 2008. **370**(2): p. 403-14.
359. Reed, M.L., et al., *Amino acid residues in the fusion peptide pocket regulate the pH of activation of the H5N1 influenza virus hemagglutinin protein.* J Virol, 2009. **83**(8): p. 3568-80.
360. Zaraket, H., O.A. Bridges, and C.J. Russell, *The pH of activation of the hemagglutinin protein regulates H5N1 influenza virus replication and pathogenesis in mice.* J Virol, 2013. **87**(9): p. 4826-34.
361. Ha, Y., et al., *H5 avian and H9 swine influenza virus haemagglutinin structures: possible origin of influenza subtypes.* EMBO J, 2002. **21**(5): p. 865-75.
362. Wiley, D.C. and J.J. Skehel, *The structure and function of the hemagglutinin membrane glycoprotein of influenza virus.* Annu Rev Biochem, 1987. **56**: p. 365-94.
363. Skehel, J.J. and D.C. Wiley, *Receptor binding and membrane fusion in virus entry: the influenza hemagglutinin.* Annu Rev Biochem, 2000. **69**: p. 531-69.
364. Russell, R.J., et al., *Structure of influenza hemagglutinin in complex with an inhibitor of membrane fusion.* Proc Natl Acad Sci U S A, 2008. **105**(46): p. 17736-41.
365. Bodian, D.L., et al., *Inhibition of the fusion-inducing conformational change of influenza hemagglutinin by benzoquinones and hydroquinones.* Biochemistry, 1993. **32**(12): p. 2967-78.
366. Kumru, O.S., et al., *Vaccine instability in the cold chain: mechanisms, analysis and formulation strategies.* Biologicals, 2014. **42**(5): p. 237-59.
367. Wang, W., et al., *Glycosylation at 158N of the hemagglutinin protein and receptor binding specificity synergistically affect the antigenicity and immunogenicity of a live attenuated H5N1 A/Vietnam/1203/2004 vaccine virus in ferrets.* J Virol, 2010. **84**(13): p. 6570-7.
368. Krenn, B.M., et al., *Single HA2 mutation increases the infectivity and immunogenicity of a live attenuated H5N1 intranasal influenza vaccine candidate lacking NS1.* PLoS One, 2011. **6**(4): p. e18577.
369. Cotter, C.R., H. Jin, and Z. Chen, *A single amino acid in the stalk region of the H1N1pdm influenza virus HA protein affects viral fusion, stability and infectivity.* PLoS Pathog, 2014. **10**(1): p. e1003831.
370. Coenen, F., J.T. Tolboom, and H.W. Frijlink, *Stability of influenza sub-unit vaccine. Does a couple of days outside the refrigerator matter?* Vaccine, 2006. **24**(4): p. 525-31.
371. Hickey, J.M., et al., *Mechanism of a decrease in potency for the recombinant influenza a virus hemagglutinin H3 antigen during storage.* J Pharm Sci, 2014. **103**(3): p. 821-7.

372. Wang, W., et al., *Generation of recombinant pandemic H1N1 influenza virus with the HA cleavable by bromelain and identification of the residues influencing HA bromelain cleavage.* Vaccine, 2012. **30**(5): p. 872-8.
373. Yen, H.L. and R.G. Webster, *Pandemic influenza as a current threat.* Curr Top Microbiol Immunol, 2009. **333**: p. 3-24.
374. Klenk, E., H. Faillard, and H. Lempfrid, *[Enzymatic effect of the influenza virus].* Hoppe-Seyler's Zeitschrift fur physiologische Chemie, 1955. **301**(4-6): p. 235-46.
375. Matrosovich, M.N., et al., *Avian influenza A viruses differ from human viruses by recognition of sialyloligosaccharides and gangliosides and by a higher conservation of the HA receptor-binding site.* Virology, 1997. **233**(1): p. 224-34.
376. Glaser, L., et al., *A single amino acid substitution in 1918 influenza virus hemagglutinin changes receptor binding specificity.* Journal of virology, 2005. **79**(17): p. 11533-6.
377. Sauter, N.K., et al., *Hemagglutinins from two influenza virus variants bind to sialic acid derivatives with millimolar dissociation constants: a 500-MHz proton nuclear magnetic resonance study.* Biochemistry, 1989. **28**(21): p. 8388-96.
378. Sauter, N.K., et al., *Binding of influenza virus hemagglutinin to analogs of its cell-surface receptor, sialic acid: analysis by proton nuclear magnetic resonance spectroscopy and X-ray crystallography.* Biochemistry, 1992. **31**(40): p. 9609-21.
379. Nicholls, J.M., et al., *Evolving complexities of influenza virus and its receptors.* Trends Microbiol, 2008. **16**(4): p. 149-57.
380. Walther, T., et al., *Glycomic analysis of human respiratory tract tissues and correlation with influenza virus infection.* PLoS pathogens, 2013. **9**(3): p. e1003223.
381. Blixt, O., et al., *Printed covalent glycan array for ligand profiling of diverse glycan binding proteins.* Proceedings of the National Academy of Sciences of the United States of America, 2004. **101**(49): p. 17033-8.
382. Smith, D.F., X. Song, and R.D. Cummings, *Use of glycan microarrays to explore specificity of glycan-binding proteins.* Methods in enzymology, 2010. **480**: p. 417-44.
383. Song, X., et al., *Preparation of a mannose-6-phosphate glycan microarray through fluorescent derivatization, phosphorylation, and immobilization of natural high-mannose N-glycans and application in ligand identification of P-type lectins.* Methods in molecular biology, 2012. **808**: p. 137-48.
384. Song, X., et al., *Derivatization of free natural glycans for incorporation onto glycan arrays: derivatizing glycans on the microscale for microarray and other applications (ms# CP-10-0194).* Current protocols in chemical biology, 2011. **3**(2): p. 53-63.
385. Song, X., et al., *Quantifiable fluorescent glycan microarrays.* Glycoconjugate journal, 2008. **25**(1): p. 15-25.
386. Stevens, J., et al., *Glycan microarray technologies: tools to survey host specificity of influenza viruses.* Nat Rev Microbiol, 2006. **4**(11): p. 857-64.
387. Gulati, S., et al., *Human H3N2 Influenza Viruses Isolated from 1968 To 2012 Show Varying Preference for Receptor Substructures with No Apparent Consequences for Disease or Spread.* PLoS One, 2013. **8**(6): p. e66325.

388. Song, X., et al., *Shotgun glycomics: a microarray strategy for functional glycomics.* Nature methods, 2011. **8**(1): p. 85-90.
389. Jang-Lee, J., et al., *Glycomic profiling of cells and tissues by mass spectrometry: fingerprinting and sequencing methodologies.* Methods in enzymology, 2006. **415**: p. 59-86.
390. North, S.J., et al., *Mass spectrometry in the analysis of N-linked and O-linked glycans.* Current opinion in structural biology, 2009. **19**(5): p. 498-506.
391. Song, X., et al., *Novel fluorescent glycan microarray strategy reveals ligands for galectins.* Chem Biol, 2009. **16**(1): p. 36-47.
392. Shibuya, N., et al., *Fractionation of sialylated oligosaccharides, glycopeptides, and glycoproteins on immobilized elderberry (Sambucus nigra L.) bark lectin.* Archives of biochemistry and biophysics, 1987. **254**(1): p. 1-8.
393. Bai, X., et al., *Enhanced 3-O-sulfation of galactose in Asn-linked glycans and Maackia amurensis lectin binding in a new Chinese hamster ovary cell line.* Glycobiology, 2001. **11**(8): p. 621-32.
394. Seko, A., et al., *Novel O-linked glycans containing 6'-sulfo-Gal/GalNAc of MUC1 secreted from human breast cancer YMB-S cells: possible carbohydrate epitopes of KL-6(MUC1) monoclonal antibody.* Glycobiology, 2012. **22**(2): p. 181-95.
395. Kochibe, N. and K. Furukawa, *Purification and properties of a novel fucose-specific hemagglutinin of Aleuria aurantia.* Biochemistry, 1980. **19**(13): p. 2841-6.
396. Baenziger, J.U. and D. Fiete, *Structural determinants of concanavalin A specificity for oligosaccharides.* The Journal of biological chemistry, 1979. **254**(7): p. 2400-7.
397. Kornfeld, R. and C. Ferris, *Interaction of immunoglobulin glycopeptides with concanavalin A.* The Journal of biological chemistry, 1975. **250**(7): p. 2614-9.
398. Ogata, S., T. Muramatsu, and A. Kobata, *Fractionation of glycopeptides by affinity column chromatography on concanavalin A-sepharose.* Journal of biochemistry, 1975. **78**(4): p. 687-96.
399. Itakura, Y., et al., *Systematic comparison of oligosaccharide specificity of Ricinus communis agglutinin I and Erythrina lectins: a search by frontal affinity chromatography.* Journal of biochemistry, 2007. **142**(4): p. 459-69.
400. Baenziger, J.U. and D. Fiete, *Structural determinants of Ricinus communis agglutinin and toxin specificity for oligosaccharides.* The Journal of biological chemistry, 1979. **254**(19): p. 9795-9.
401. Wang, M.L., J.M. Katz, and R.G. Webster, *Extensive heterogeneity in the hemagglutinin of egg-grown influenza viruses from different patients.* Virology, 1989. **171**(1): p. 275-9.
402. Yu, Y., et al., *Functional glycomic analysis of human milk glycans reveals the presence of virus receptors and embryonic stem cell biomarkers.* J Biol Chem, 2012. **287**(53): p. 44784-99.
403. Andersen, D.C. and C.F. Goochee, *The effect of ammonia on the O-linked glycosylation of granulocyte colony-stimulating factor produced by chinese hamster ovary cells.* Biotechnol Bioeng, 1995. **47**(1): p. 96-105.

404. Gawlitzek, M., et al., *Characterization of changes in the glycosylation pattern of recombinant proteins from BHK-21 cells due to different culture conditions.* J Biotechnol, 1995. **42**(2): p. 117-31.
405. Chandrasekaran, A., et al., *Glycan topology determines human adaptation of avian H5N1 virus hemagglutinin.* Nature biotechnology, 2008. **26**(1): p. 107-13.
406. Viswanathan, K., et al., *Glycans as receptors for influenza pathogenesis.* Glycoconj J, 2010. **27**(6): p. 561-70.
407. Suzuki, Y., et al., *Sialic acid species as a determinant of the host range of influenza A viruses.* J Virol, 2000. **74**(24): p. 11825-31.
408. Huang, Y., Y. Mechref, and M.V. Novotny, *Microscale nonreductive release of O-linked glycans for subsequent analysis through MALDI mass spectrometry and capillary electrophoresis.* Anal Chem, 2001. **73**(24): p. 6063-9.
409. Song, X., D.F. Smith, and R.D. Cummings, *Nonenzymatic release of free reducing glycans from glycosphingolipids.* Anal. Biochem., 2012. **429**(Copyright (C) 2013 American Chemical Society (ACS). All Rights Reserved.): p. 82-87.
410. Heimburg-Molinaro, J., et al., *Probing virus-glycan interactions using glycan microarrays.* Methods Mol Biol, 2012. **808**: p. 251-67.
411. Amonsen, M., et al., *Human parainfluenza viruses hPIV1 and hPIV3 bind oligosaccharides with alpha2-3-linked sialic acids that are distinct from those bound by H5 avian influenza virus hemagglutinin.* J Virol, 2007. **81**(15): p. 8341-5.
412. Heimburg-Molinaro, J., et al., *Preparation and analysis of glycan microarrays.* Current protocols in protein science / editorial board, John E. Coligan ... [et al.], 2011. **Chapter 12**: p. Unit12 10.
413. Giannecchini, S., et al., *Comparison of in vitro replication features of H7N3 influenza viruses from wild ducks and turkeys: potential implications for interspecies transmission.* J Gen Virol, 2006. **87**(Pt 1): p. 171-5.
414. Baumann, J., et al., *H1N1 Swine Influenza Viruses Differ from Avian Precursors by a Higher pH Optimum of Membrane Fusion.* J Virol, 2016. **90**(3): p. 1569-77.
415. Song, X., et al., *Oxidative release of natural glycans for functional glycomics.* Nat Methods, 2016. **13**(6): p. 528-34.
416. Seko, A., et al., *Occurence of a sialylglycopeptide and free sialylglycans in hen's egg yolk.* Biochim Biophys Acta, 1997. **1335**(1-2): p. 23-32.
417. Xia, B., et al., *Glycan reductive isotope labeling for quantitative glycomics.* Anal Biochem, 2009. **387**(2): p. 162-70.
418. Rohm, C., et al., *Characterization of a novel influenza hemagglutinin, H15: criteria for determination of influenza A subtypes.* Virology, 1996. **217**(2): p. 508-16.
419. Fouchier, R.A., et al., *Characterization of a novel influenza A virus hemagglutinin subtype (H16) obtained from black-headed gulls.* J Virol, 2005. **79**(5): p. 2814-22.
420. Kawaoka, Y., et al., *Molecular characterization of a new hemagglutinin, subtype H14, of influenza A virus.* Virology, 1990. **179**(2): p. 759-67.
421. Rohm, C., et al., *Different hemagglutinin cleavage site variants of H7N7 in an influenza outbreak in chickens in Leipzig, Germany.* Virology, 1996. **218**(1): p. 253-7.

422. Nobusawa, E., et al., *Comparison of complete amino acid sequences and receptor-binding properties among 13 serotypes of hemagglutinins of influenza A viruses.* Virology, 1991. **182**(2): p. 475-85.
423. Daniels, R.S., et al., *Antigenic analyses of influenza virus haemagglutinins with different receptor-binding specificities.* Virology, 1984. **138**(1): p. 174-7.
424. Wharton, S.A., J.J. Skehel, and D.C. Wiley, *Studies of influenza haemagglutinin-mediated membrane fusion.* Virology, 1986. **149**(1): p. 27-35.
425. Rott, R., et al., *Studies on the adaptation of influenza viruses to MDCK cells.* EMBO J, 1984. **3**(13): p. 3329-32.